Dynamic Remodeling of Central Amygdala Glutamatergic Circuits Across Fear States: A Mechanism for Experience-Dependent Modification of Behavioral Selection

By

Nolan D. Hartley

Dissertation
Submitted to the Faculty of the
Graduate School of Vanderbilt University
in partial fulfillment of the requirements
for the degree of

DOCTOR OF PHILOSOPHY
in
Neuroscience
September 30th, 2019
Nashville, Tennessee

Approved:

Danny Winder, Ph.D.

Brad Grueter, Ph.D.

Terunaga Nakagawa, Ph.D.

Sachin Patel, M.D., Ph.D.

Dedicated to my parents, Sharon and Gordon Hartley,

whose love, wisdom, and enduring support have given me the opportunity

to pursue all of my passions in life.

ACKNOWLEDGEMENTS

Firstly, I would like to acknowledge my funding sources that have made this work possible. My training was supported by the National Institutes of Health (NIH) Ruth L. Kirschstein National Research Service Award of Institutional Predoctoral Training Program in the Neurosciences (*T32 MH064913),* my individual Predoctoral Ruth L. Kirschstein National Research Service Award (*F31 MH111103),* and Dr. Sachin Patel's AA26186 and DA042475 grants. Furthermore, this work was also supported in part by Dr. Danny Winder's AA019455 grant.

Next, I would like to thank my family for always expressing interest in my career, and supporting my intellectual endeavors. I would like to thank my Mom and Dad for being my biggest fans, and always rooting for my success. They have given me every opportunity to follow my passion for science, and without them this would not have been possible. I also want to thank Connor and Sara for being such great role models and friends, and pushing me to "hurry up and graduate already!" Moreover, I want to thank my wife Lex, for being my rock, grounding me, keeping me sane, supporting me, encouraging me, loving me, and being by my side through every step of this long journey. I hope she realizes the completion of this work is an accomplishment on her part as well.

I would also like to acknowledge my committee members and peers, who have guided and challenged me over the years. They have all been excellent educators both in the classroom and out, and I am grateful to have had the opportunity to learn from what I consider to be some of the best scientists in their fields. Furthermore, I would like to thank every member of the Patel lab (current and past) for being passionate, determined, cooperative, collaborative, and an overall

fun group of people. The positive energy, comradery, and culture in the lab was fundamental to what made graduate school such a rewarding experience. Additionally, I would like to specifically thank Dr. Teniel Ramikie. She has been an incredible mentor to me, has trained me (both with lessons in the lab and in life), and most importantly inspired me to be a hard worker and a diligent scientist. She will always be like an older sister to me, and I am indebted by her devotion to my development as a young researcher.

Lastly, I would like to thank Dr. Sachin Patel. He is an amazing mentor who has made me the best scientist I can be. He continuously leads by example, inspires excellence, and is always available for his students. His devotion to my training, and his trust in my abilities has made my graduate tenure one of the most intellectually stimulating, challenging, and rewarding undertakings of my life. I will certainly miss having him as a boss and a teacher, and will always approach my life and research career with the blunt advice he gave me the very first day we met: "You get out what you put in."

TABLE OF CONTENTS

Page

LIST OF FIGURES

LIST OF ABBREVIATIONS

ACTH..... adrenocorticotropic hormone

AMPAR..... α-amino-3-hydroxy-5-methyl-4-isoxazoleproprionate receptor

AVP..... arginine vasopressin

BA..... basal amygdala

BL ..... basolateral nucleus

BLA..... basolateral amygdala complex

BM .....basomedial nucleus

CBT.....cognitive behavioral therapy

CeA .....central nucleus of the amygdala

CeC ..... central capsular division

CeL..... central lateral division

CeM.....central medial division

CGRPR.....calcitonin gene-related peptide receptor

ChR2 .....channel rhodopsin

CNO ..... clozapine-*N*-oxide

CNS.....central nervous system

CR ..... conditioned response

CREB .....cyclic adenosine monophosphate response element binding protein

CRF .....corticotropin-releasing factor

CRFR ..... corticotropin-releasing factor receptor

CS.....conditioned stimulus

DG ..... dentate gyrus

DREADD ..... designer receptor exclusively activated by designer drug

*dm*ICM ..... dorsomedial intercalated cell masses

DVC ..... dorsal vagal complex

GPCR ..... g-protein coupled receptor

GR ..... glucocorticoid receptor

HFS ..... high-frequency stimulation

HPA ..... hypothalamic-pituitary-adrenal axis

Htr2A ..... 5-hydroxytryptamine receptor 2A

ICM ..... intercalated cell masses

INS ..... insular cortex

LA ..... lateral amygdala

*l*ICM ..... lateral intercalated cell masses

LTP ..... long-term potentiation

mGluR1 ..... metabotropic glutamate receptor type 1

mPFC ..... medial prefrontal cortex

NOC ..... nociceptin

NMDAR ..... N-methyl-D-aspartate receptor

NTRS2 ..... neurotensin receptor 2

oEPSC ..... optically-evoked excitatory post-synaptic current

OXTR ..... oxytocin receptor

PAG ..... periaqueductal gray

PBN ..... parabrachial nucleus

PKCδ ..... protein kinase C delta

PNOC ..... prepronociceptin

Ppp1r1b ..... protein phosphatase 1 regulatory inhibitory subunit B

PTSD ..... post-traumatic stress disorder

PVN ..... paraventricular nucleus of the hypothalamus

Rspo2 ..... r-spondin-2

sEPSC ..... spontaneous excitatory postsynaptic current

Serotonin 5-HT

sIPSC ..... spontaneous inhibitory postsynaptic current

SOM ..... somatostatin

UR ..... unconditioned response

US ..... unconditioned stimulus

*vm*ICM ..... ventromedial intercalated cell masses

CHAPTER I

INTRODUCTION

Fear As An Adaptive Response

Physiological and psychological well-being require an ability to react to, attend, assess, and cope with bombardment by any number of predictable or unpredictable environmental stressors. These stressors come in many forms, producing potential psychological or physical harm. Whether it's the fear of public speaking, financial insecurity, sexual abuse or assault, losing a loved one, or dodging an oncoming car on the highway, the emotional response and decisions made that follow determine the capacity to face adversity and effectively resume everyday life. In the latter case, the momentary decision one makes could be the difference between life and death, and such scenarios often give rise to the phenomenological expression of fear. Although humans demonstrate subjective emotional responses to a diverse range of stressors, rapid and innate fear responses to immediate threats (i.e. fight or flight) are evolutionarily conserved across species (LeDoux, 1996; Pereira and Moita, 2016; Phelps and LeDoux, 2005; Vuilleumier, 2005). Whether by reflex or conscious intent, fear is a defensive reaction that provides organisms with the adaptive means to avoid danger or discomfort, and by circumstance is necessary for survival. From this evolutionary perspective, fear expression across the animal kingdom can be considered an inborn reaction, involving conserved neural circuitry that drive rapid or autonomic physiological and behavioral responses.

One of the most evolutionarily conserved fear behaviors across vertebrate species is the passive freezing response, a rapid transition to immobility or ceasing of any detectable

movement other than respiration (Blanchard and Blanchard, 1969a; Fanselow, 1980). In cases of highly salient threat exposure, animals will often freeze so as to quickly assess their surroundings for the imminence of the perceived threat (LeDoux, 1996). For example, this response can often occur in scenarios in which changes in the intensity of a stimulus immediately demands attentional resources, such as when sensory stimuli signal the presence of potential predation (Pereira and Moita, 2016), or following profound alterations in the magnitude of sensory stimuli associated with a wide-array of naturalistic dangers (i.e. chemoreception from olfactory cues indicating spread of disease, bright flashes of light or looming visual cues, warning vocalizations from conspecifics, loud noises reflecting brontides, or even multi-modal changes such as that which would result from combat related explosions (Frese et al., 2014; Gold and Soter, 1979; Pereira and Moita, 2016; van de Weyer et al., 2011)). However, in scenarios of forthcoming danger and imminent proximity to threat, animals may transition to more active fear responses involving escape or flight, which require neural motor programs that rapidly initiate movement away from harm (Blanchard and Blanchard, 1969b; LeDoux, 1996). Notably, although these passive and active responses are sculpted by evolution and typically instinctive, the experience of fear throughout the life-span may further facilitate these same responses during exposure to new contexts, demonstrating that animals can instrumentally learn to avoid similar environments and sensory cues by performing the same behavioral responses that afforded successful mitigation of harm during a previous encounter. Thus, the same neural circuitry that governs rapid fear responses may drive associative memory formation and enhance fear-related physiological responses. Fear learning may then confer an advantage by creating a threat-memory, and allowing an organism to adequately respond to future scenarios that similarly predict peril.

In coordination with the motor responses meant to deter a threat, ongoing fear is most commonly expressed through initiation of the hypothalamic-pituitary-adrenal (HPA) stress axis. The HPA axis mediates both brisk and sustained hormonal responses to external and internal stress cues. Afferents relaying signals from limbic, endocrine, and visceral brainstem sources converge onto parvocellular secretory neurons of the paraventricular nucleus of the hypothalamus (PVN) (Bale and Vale, 2004). Upon excitation, these neurons release the hormones corticotropin-releasing factor (CRF) and arginine vasopressin (AVP) into the portal vessels of the median eminence bordering the anterior pituitary gland. These neuropeptide signals can act synergistically to enhance the speed of HPA axis activation (Dunlop and Wong, 2019). However, the capacity of CRF release and signaling within this hypothalamic-pituitary projection serves as the main determinant of generating the stress response within the central nervous system (CNS) (Dunlop and Wong, 2019). CRF receptor binding on anterior pituitary gland corticotropes then stimulates the release of adrenocorticotropic hormone (ACTH) into the circulating blood stream. Once in circulation, ACTH promotes the synthesis and release of glucocorticoids from the adrenal cortex (primarily cortisol in humans and corticosterone in rodents), which can then interact with glucocorticoid receptors (GRs) widely distributed throughout organs and bodily tissues. GRs are ubiquitous cytosolic receptors that upon activation serve to produce the large range of physiological symptoms associated with fear expression, including elevated heart rate, blood pressure, pupil dilation, and enhanced respiration (Thau and Sharma, 2019). Activation of GRs is also responsible for producing some of the behavioral advantages of fear responses, including increased arousal, enhanced cognition and awareness, increased analgesia, and improved memory consolidation (Smith and Vale, 2006). Thus, the recruitment of the HPA stress axis allows animals to appropriately respond to fearful stimuli and

to successfully mitigate dangerous encounters. Importantly, the HPA stress axis serves as a homeostatic feedback mechanism. GR activation in the CNS, in particular at the level of the PVN and the pituitary gland, can quickly dampen further CRF and ACTH release and allow restoration of circulating glucocorticoids to baseline levels (Smith and Vale, 2006). This feedback regulation is imperative for homeostasis following stress exposure as it serves to restore bodily functions to resting levels, dissipates fear expression, and allows for behavioral normalization.

When Fear Responses Become Maladaptive

Although acute fear responses grant a survival advantage in the moment, persistent fear responses can become maladaptive in the long-term. Indeed, the unremittent experience of fear through chronic stress exposure or intense trauma can produce sustained levels of general malaise or anxiety and further sensitize subjects to fear-evoking stimuli, resulting in predisposition to disease. In particular, prolonged activation of the HPA stress axis can result in impairments in its negative feedback modulation and lead to immune deficiency, metabolic dysfunction, persistent anxiety, heart attack, and stroke (DeMorrow, 2018; Hackett et al., 2016; Schnall et al., 1994; Whitworth et al., 2005). Similarly, prolonged HPA stress axis activation has been positively correlated with the development of affective mood disorders and neuropsychiatric anxiety disorders, including major depressive disorder, generalized anxiety disorder, panic disorder, social anxiety disorder, and post-traumatic stress disorder (PTSD) (DeMorrow, 2018; Dunlop and Wong, 2019; Faravelli et al., 2012; Juruena, 2014).

Notably, PTSD has been extensively characterized as a neuropsychiatric condition that stems from alterations in the processing, expression, and memory of fearful experiences

(Pattwell and Bath, 2017), and has been implicated in HPA axis dysfunction (Dunlop and Wong, 2019). Moreover, it is described as one of the only neuropsychiatric conditions with a specific known environmental cause (traumatic stress exposure) (Lissek and van Meurs, 2015). Although about 70% of the population may experience a traumatic episode at some point in life, PTSD only develops in a subset of these individuals (in some cases as high as 15%), and within at-risk populations, such as combat and military personnel, lifetime prevalence can be as high as 20-30% (Karam et al., 2014; Kessler et al., 1995; Koenen et al., 2008; Ramchand et al., 2010; Zuj and Norrholm, 2019). Given the prevalence and severity of PTSD, significant resources have been devoted to researching the etiology of this disease. Over several decades, extensive preclinical and clinical data have provided evidence for abnormalities in sensory processing of fear-inducing stimuli and aversive learning that are fundamental to the pathophysiology of PTSD (Etkin, 2010; Fani et al., 2012; Garfinkel et al., 2014; Packard et al., 2014; Parsons and Ressler, 2013; VanElzakker et al., 2014). The findings that most consistently emerge from these data are evidence for enhanced fear learning, heightened arousal to fearful stimuli, generalization of fear to otherwise neutral stimuli, and impairments in the diminishment of fear responses (Fani et al., 2012; Lissek and van Meurs, 2015; Parsons and Ressler, 2013; Rauch et al., 2006).

Perhaps the most relevant to the persistence of PTSD symptomatology and lack of effective treatments is the impairments found in extinction learning. Extinction learning is a natural process in which the continued presentation of fear-provoking stimuli in the absence of explicit danger causes a reduction in fear expression. This form of learning occurs in most subjects who have acquired memory of a fearful event and is adaptive as it facilitates behavioral homeostasis. However, impairment of extinction learning in certain subjects becomes maladaptive in that fear expression will persist when no longer appropriate. Clinical strategies

have aimed at attempting to facilitate extinction learning in patients through the use of exposure therapy, a form of cognitive behavioral therapy (CBT), which has held some promise (Yue et al., 2018). However, exaggerated fear expression and impairments in extinction continue to be hallmark symptoms of PTSD, and are difficult to treat throughout a patient's lifetime without combinations of behavioral and pharmacological interventions (de Kleine et al., 2013). Therefore, there is a significant need in understanding the biological basis and mechanisms of fear memory formation, expression, and extinction, in order to find new therapeutic interventions and to improve patient outcomes. Profound advances have been made in this regard over the years, which highlight critical brain structures, but much more work is needed to understand the complexity of emotional learning and memory in the CNS. As such, the remainder of this chapter will discuss common preclinical strategies used in rodents that model these processes, the neurocircuitry most relevant to these phenomena, and recent advances that suggest the amygdala as an essential brain region for both fear and extinction learning.

Models of Fear Learning and Fear Extinction in Rodents

Rodents have long been used in preclinical biomedical research due to their genetic, physiological, and anatomical similarities to humans (Bryda, 2013). Of the approximately 30,000 genes found in humans, rats, and mice, up to 95% of this genetic material is believed to be homologous (Bryda, 2013; Waterston et al., 2002). Despite their stark contrast in size to humans, rats and mice have been favored for studying models of human disease due to the minimal resources needed to maintain them in the laboratory, the ease in which they can be handled and bred, their relatively short gestation times, large numbers of offspring, rapid development, and short life-span (Bryda, 2013; Perlman, 2016). Thus, large quantities of rodents can be quickly

acquired for increasing statistical power during experimentation, and allowing for exploration of physiology throughout development, saving researchers significant time and effort. Additionally, the wealth of genetic information from mice along with the advent of genetic engineering technologies have enabled researchers to efficiently model human disease phenotypes on the molecular, cellular, and systems levels through the generation of mutant, transgenic, knockout, or knock-in mouse lines. Combined with cutting-edge viral mediated gene transfer, molecular biological, pharmacological, electrophysiological, imaging, and behavioral techniques these benefits have made mice and rats the go-to model organisms for neuroscientists wishing to dissect the biological underpinnings of fear in the brain.

Given the genetic and anatomical similarities between rodents and humans, it is not surprising that many of the fear responses noted in human subjects have significant face validity in rodents and can be reproduced under analogous experimental conditions. One of the most commonly used behavioral techniques for studying fear learning in rodents is Pavlovian fear conditioning. Pavlovian fear conditioning explores the strong associative memories that form when a sensory stimulus from the environment serves to predict exposure to a threat. In most fear conditioning paradigms, an initially neutral stimulus (i.e. a tone), known as the conditioned stimulus (CS) is presented in temporal coincidence with a noxious (i.e. foot-shock) unconditioned stimulus (US). The US by nature is aversive and produces an unconditioned fear response (UR), most notably freezing, escape, or avoidance, as described above. However, the pairing of the CS and the US produces a conditioned fear response (CR) to continued presentations of the CS. Consequently, much like humans, rodents learn the predictive quality of the CS which can serve as a cue to the presentation of danger or discomfort, and will subsequently mount a CR (i.e. freezing or autonomic arousal) to future presentations of the CS in

the absence of the US, resulting in a fear memory to the cued CS. This form of cued associative learning is powerful, occurs for stimuli across all sensory modalities, and the resulting memory formation long-lasting, often being retained throughout the entirety of a subject's life (Gale et al., 2004; Ledoux and Muller, 1997). Furthermore, this experimental approach can be modified to instead explore contextual fear conditioning, where in the absence of any discrete sensory cues animals will form multimodal associations with a large range of stimuli from their environmental context in relation to their subjective internal state. Although both cued (discrete CS) and contextual fear conditioning are immensely useful for studying the basis of fear memory, cued fear learning can be most valuable for modeling the strong associations seen in PTSD patients between salient stimulus triggers and heightened arousal, fear, or anxiety.

Equally important to characterizing fear learning is the need to understand the mechanisms of resilience, restoration of behavior, and reductions in fear expression following traumatic experience. To this end, rodent models of fear extinction have served as an efficient and beneficial extension of conditioned fear paradigms, allowing researchers to gauge how fear is acquired and then subsequently diminished within the same subjects. In most fear extinction experiments, animals are fear conditioned with CS-US pairings, and then the CR is typically monitored (several hours or often days later) during continuous non-reinforced presentations of the CS (absence of the US) in a novel or 'safe' context *per se*. Fear extinction learning then takes place under sliding and scalable phases. In the first phase, multiple presentations of the CS (typically anywhere between 1-5 trials) will induce a robust CR reflecting the retrieval and expression of a fear memory, since the animal had previously learned that the contingency between the CS and US is high. However, in the second descending phase, the contingency between the CS and US degrades due to large prediction error, as the animal begins to learn that

the CS no longer predicts presentation of the US. Therefore, following the initial fear-expression phase, the time in which the animal mounts a CR will begin to decrease during consecutive CS presentations. The parameters of single or multiple extinction training sessions can then be maximized so that animals eventually reach their pre-fear conditioning levels (to the point where the CR is almost entirely absent).

Although extinction learning allows experimenters to examine reductions in fear expression, it is important to note that CRs are often never fully abolished, with some residual CRs still occurring following even the most extensive training regimes (Hartley et al., 2016; Steenkamp et al., 2015). In addition, episodes of spontaneous recovery may occur, in which lapses in time following extinction training can result in the reemergence of CRs during further testing (Baum, 1988). Similarly, fear renewal may also occur, in which re-exposure to the conditioning context causes the reemergence of the CR, indicating that fear extinction is very much a context-dependent process (Bouton and King, 1983). Since fear expression can spontaneously recover or renew outside of the extinction context, it was quickly recognized that fear memories in rodents are not likely erased following extinction learning but rather retained in the brain, which is further supported by anecdotes and post experiment questionnaires in human participants (Steenkamp et al., 2015; Yue et al., 2018). Indeed, the ability of humans to communicate their subjective experiences to investigators has confirmed that although their acute fear response may have subsided immediately following exposure therapy, they do not episodically forget the fact they experienced trauma or the cues and environmental factors that exacerbated their conditioned fear reactions (Yue et al., 2018). This raises questions about whether extinction training truly reflects an erasure of fear memory in the brain, or instead a form of new safety-learning that promotes inhibition of the existing fear memory. These findings

have led to converging hypotheses theorizing extinction training as a form of new learning and fear memory inhibition, as some degree of retention of the original fear memory may still afford an adaptive advantage if an animal is re-exposed to the exact same environment in which a CS originally predicted danger.

Although some elegant experiments provide evidence for fear memory erasure if extinction training occurs closely following fear conditioning (minutes to an hour) (Myers et al., 2006), it stands to reason that naturally occurring extinction processes in healthy individuals would happen well after an initial traumatic episode has occurred, as non-reinforced CSs would not likely be present when the traumatic episode has directly ended. In line with this, extinction training that occurs well after fear conditioning (>72 hours) can still result in spontaneous recovery and fear renewal within the same subjects, suggesting extinction training forms a competing memory trace that interferes with the retrieval of the original fear memory (Myers et al., 2006). However, some studies have provided evidence that signatures of fear inhibition in brain circuitries critical for fear memory storage only occur within the early phases of extinction training, whereas this inhibition is absent following repeated extinction sessions, all the while molecular and cellular determinants of fear erasure, such as the depotentiation of excitatory synapses thought to encode the memory, may simultaneously occur (An et al., 2017; Dalton et al., 2008; Kim et al., 2007; Lin et al., 2003). Therefore, mechanisms of both fear inhibition and fear erasure may still be at play in the brain when animals undergo acute or prolonged fear extinction training, suggesting that the timing and degree of extinction learning following trauma is an important consideration when developing strategies to temper the life-long prevalence, and often recurrence, of fear memories in patients suffering from PTSD or related disorders. Undoubtedly, continued in-depth examination of the neurobiological mechanisms necessary for

fear memory formation, retention, expression, and extinction in rodents is needed to find new avenues of treatment for neuropsychiatric patient populations.

Neural Substrates of Fear Learning

The profound need of new treatment strategies for patients suffering from PTSD or stress related anxiety disorders has led to extensive research into the neurobiology of fear learning. For the past few decades, multiple limbic brain structures and neural circuits have emerged that are each critical to the acquisition and expression of learned fear responses. Although a plethora of forebrain, midbrain, and hindbrain areas continue to be identified as important components of the limbic system and fear responsiveness, the most notable brain structures crucial for associative learning consist of an interconnected network involving the amygdala, hippocampus, and prefrontal cortex. Although the intricacies of microcircuits, cell-types, neurotransmitters, neuromodulators, and afferent or efferent projections from these structures are the basis of many thorough reviews, a more general overview of the functionality of these brain regions in the context of fear learning will be described below.

Early in the field of neuropsychology, the hippocampus was identified as a center of explicit long-term memory formation and storage, as lesions to this area in humans and rodents has been shown to cause forms of anterograde or retrograde amnesia (Cipolotti and Bird, 2006; Eichenbaum, 2013; Hassabis et al., 2007; Leal and Yassa, 2015; Scoville and Milner, 2000; Zemla and Basu, 2017). Not long after discovering the functional importance of this structure, researchers began to explore the cellular and molecular determinants of how memories are formed and stored within this region. The hippocampus primarily consists of a glutamatergic trisynaptic loop consisting of the perforant pathway, the mossy fiber pathway, and the Schaffer

collateral pathway (Knierim, 2015). The perforant pathway begins with excitatory inputs from the entorhinal cortex to the dentate gyrus region (DG) of the hippocampus. The DG granule cells then send mossy fiber projections to the CA3 region, which then in turn sends Schaffer collateral projections to the CA1 region. Pyramidal neurons of the CA1 region then project back to the entorhinal cortex to complete the trisynaptic loop (Knierim, 2015). It is well supported that the signaling within these pathways and cell classes generates a spatiotemporal representation of memory, allowing subjects to form, retrieve, or recall memories based on the location and timing of external sensory cues (Kentros, 2006; Kitamura et al., 2014; Suh et al., 2011; Zilleruelo and Beca, 1975). These external stimuli can serve to instruct contextual memory formation of an environment, allowing an animal to generate a representation of space and efficiently navigate its surroundings (Dragoi and Tonegawa, 2013, 2014; Sun et al., 2015).

The primary basis for the formation and storage of these memories within the hippocampus is synaptic long-term potentiation (LTP). LTP is a form of synaptic plasticity that strengthens the signaling capacity between neurons at chemical synapses, and is most often measured in excitatory glutamatergic circuits of the CNS (Abraham et al., 2019). Hence, this enriched synaptic communication between neurons facilitates information transfer by increasing the likelihood of neuronal activity and serves as a potential substrate for the consolidation and retrieval of memories within distributed neural networks. The very first demonstrations of LTP in the hippocampus came from electrophysiological experiments involving the stimulation of presynaptic terminals of the perforant pathway while recording the evoked potentials from neurons in the DG (Bliss and Lomo, 1973; Lomo, 2018). High frequency stimulation (HFS) of this pathway caused a robust and prolonged increase in the magnitude of potentials recorded in the DG, which was shown in both *in vitro* and *in vivo* preparations (Abraham et al., 1985; Blaise,

2013; Bliss and Lomo, 1973; Do et al., 2002). Over several decades, LTP within each pathway of the trisynaptic loop and the direct relation of LTP to memory formation in living subjects was established, providing a prototypical model for memory formation in the brain, which could be extended to many other central synapses throughout the CNS (Jaffe and Johnston, 1990; Lin et al., 2008; Pastalkova et al., 2006). Interestingly, the molecular and cellular determinants of LTP are ubiquitous at many central synapses, but the mechanisms are diverse, with some synapses undergoing postsynaptic alterations, presynaptic alterations, or both. Postsynaptic LTP is most often dependent on NMDA receptors, involves intracellular kinase signaling cascades, receptor trafficking, protein synthesis, and structural changes in spine density (Nicoll, 2017). Presynaptic LTP most often involves increases in neurotransmitter release probability, which can occur via presynaptic receptors activated by retrograde neurotransmitters released from the postsynaptic cell or intracellular signaling cascades in the presynaptic terminals mediated by calcium channel activation (Castillo, 2012; Nicoll, 2017).

Consequently, it is not surprising that the discovery of LTP and the general role of the hippocampus in overall spatial memory formation has led to the discovery of its importance in contextual fear memory allocation (Kitamura et al., 2014; Liu et al., 2012; Liu et al., 2014; Ramirez et al., 2013a; Roy et al., 2017a; Roy et al., 2017b). Individual hippocampal neurons demonstrate increases in activity to the presentation of a CS following fear conditioning, and astonishingly, recent manipulations of these genetically tagged neurons in the hippocampus that anatomically represent a fear memory trace (engram) have allowed researchers to artificially create and eliminate traumatic memories in rodents. These findings may provide some proof-of-concept technological approaches for future potential therapeutic interventions in trauma patients (Liu et al., 2014; Ramirez et al., 2013a; Ramirez et al., 2013b; Yoshii et al., 2017). Moreover, the

hippocampus reciprocally and extensively signals to the prefrontal cortex and the amygdala, and the synaptic communication and strength of signaling between these structures also plays a large role in the contextual acquisition and expression of fear (Arruda-Carvalho and Clem, 2014; Chaaya et al., 2018; Farinelli et al., 2006; Kitamura et al., 2017; Orsini et al., 2011; Ryan et al., 2015). Furthermore, the synchronization in synaptic activity of the hippocampus, prefrontal cortex, and amygdala serves as a strong correlate for the consolidation or retrieval of fear memories (Jin and Maren, 2015; Knapska and Maren, 2009; Lesting et al., 2013; Lesting et al., 2011; Likhtik et al., 2014; Popa et al., 2010; Senn et al., 2014; Sotres-Bayon et al., 2012; Stujenske et al., 2014).

In addition to memory acquisition and storage, the retrieval and expression of fear memories is important for behavioral selection during re-exposure to threat predictive cues or environments. The medial prefrontal cortex (mPFC) in rodents has been described as the key top-down cortical structure responsible for regulating behavioral responsiveness to stress exposure and threat, and plays an essential role in decision-making during aversive encounters (Giustino and Maren, 2015). Unlike the human cortex, lower level mammalian species lack a granular layer IV of the mPFC. However, the mPFC of rodents still demonstrates key features and homology to that of the human cortex in terms of the cytoarchitecture, connectivity, electrophysiological properties, gene expression profile, and phenotypic changes following lesions (Giustino and Maren, 2015). Accordingly, much like its human counterpart, the rodent mPFC has emerged as a principal structure in regulating fear expression. Congruent with this description, *in vivo* recordings from the prelimbic mPFC of rodents have shown neuronal response profiles that strongly correlate with and predict the emergence of acute fear responses, including time spent freezing or movement during presentation of a CS (Baeg et al., 2001;

Burgos-Robles et al., 2009; Halladay and Blair, 2015). Additionally, reversible inactivation of the prelimbic mPFC have been shown to impair fear expression, but not acquisition, supporting the view that top-down cortical control regulates the responsiveness to threat via the retrieval of cued fear memories, but is not necessary for fear memory formation (Corcoran and Quirk, 2007; Sierra-Mercado et al., 2006). However, other findings suggest that more cognitively demanding forms of associative fear learning from complex stimuli presentations may require the mPFC for acquisition (Gilmartin and Helmstetter, 2010; Gilmartin et al., 2013a; Gilmartin et al., 2013b; Guimarais et al., 2011; Runyan et al., 2004).

Lastly, the amygdala is believed to be the final point of convergence for all processes associated with cued fear learning, as this region is absolutely necessary for the acquisition, retrieval, and expression of fear memories. Although the amygdala consists of a heterogenous complex of anatomically distinct and functionally segregated nuclei, early studies using large lesions of the entire amygdala demonstrated its necessity in associative fear memory acquisition (Blanchard and Blanchard, 1972; Maren, 2005; Schwartzbaum et al., 1964). Additionally, more directed lesions or reversible inactivation of individual nuclei within the amygdaloid complex also demonstrated its central role in cued auditory fear acquisition (Campeau and Davis, 1995; Ciocchi et al., 2010; Fendt, 2001; Goosens and Maren, 2001, 2003; Lee and Kim, 1998; Lindquist and Brown, 2004; Maren et al., 1996a; Maren et al., 1996b; Miserendino et al., 1990). Consistent with these findings, short-latency neural responses in the amygdala correspond to presentations of an auditory CS after conditioning, and the percentage of CS responsive neurons increases following fear learning, suggesting neurons within the amygdala encode fear memory (Herry et al., 2008; Herry et al., 2010; Pare and Collins, 2000; Quirk et al., 1995; Repa et al., 2001). However, neurotoxic lesioning within individual nuclei weeks or even months after fear

learning revealed the amygdala is critical for not only the acquisition but also the retrieval and expression of old fear memories (Gale et al., 2004; Lee et al., 1996; Maren, 1999, 2000, 2005; Maren et al., 1996a). Importantly, these specific findings were not the result of deficits in motor control, emotionality, or sensory processing, as the same animals retained the ability to express forms of innate fear responses (Wallace and Rosen, 2001), could express unconditioned anxiety behaviors (McHugh et al., 2004; Treit and Menard, 1997), and were able to attain newly acquired fear responses with further training (Maren, 1999, 2005). Moreover, the neural circuitry that relays sensory information regarding the CS and the US converge in the amygdala, and it is well-established that canonical forms of NMDAR-dependent LTP in the amygdala contribute to the CS-US association that occurs during fear conditioning (Bauer and LeDoux, 2004; Mahanty and Sah, 1998). Therefore, whereas the hippocampus may instruct contextual fear memory formation, the amygdala is more attune to fear memory formation between discrete sensory stimuli and aversive outcomes. A more extensive overview of the amygdala nuclei and intra-amygdalar circuitry in relation to these functions will be presented in the sections that follow.

Neural Substrates of Fear Extinction

A remarkable emergent property of brain region functionality and connectivity is that many of the same regions that are indispensable for fear learning also play an obligatory role in fear extinction. In addition to the critical role in fear learning, the hippocampus-mPFC-amygdala network is heavily implicated in the acquisition, retrieval, and expression of extinction memories. For instance, site-directed antagonism of NMDARs or metabotropic glutamate receptor type 1 (mGluR1) in the amygdala has been shown to prevent the acquisition of fear extinction, suggesting mechanisms of synaptic plasticity and new learning in this region may

contribute to fear extinction (Falls et al., 1992; Kim et al., 2007; Sotres-Bayon et al., 2007). As previously mentioned, neural responses in the amygdala tightly correspond to presentations of the CS after conditioning. Importantly, a proportion of these responses are maintained after extinction training, reflecting some retention of the original CS-US association (Herry et al., 2008; Herry et al., 2010; Pare and Collins, 2000; Quirk et al., 1995; Repa et al., 2001). However, the activity of some of these CS responsive neurons are significantly reduced during extinction learning, which may represent either the presence of inhibitory action on the original fear memory trace or reductions in excitatory signaling to these neurons (Herry et al., 2008; Herry et al., 2010; Repa et al., 2001). In the latter case, there is evidence for some forms of fear erasure occurring in the amygdala via synaptic depotentiation onto CS responsive neurons during extinction training (Mao et al., 2006), though the behavioral evidence for spontaneous recovery of fear, fear renewal, or fear reinstatement challenge this notion, and suggest mechanisms of inhibitory control over the original fear memory may also be at play, or that the storage of long-term cued fear memory becomes displaced to another location or network in the brain (Herry et al., 2010). Glutamatergic synaptic potentiation onto distinct classes of GABAergic neurons has also been measured in the amygdala, and provides a hypothesis by which feed-forward inhibition onto CS-responsive amygdala neurons can suppress fear responses following extinction training, all the while excitatory synapses to CS responsive neurons may remain intact or unchanged (Chhatwal et al., 2005; Heldt and Ressler, 2007; Rosenkranz, 2011; Royer and Pare, 2002, 2003). Interestingly, different neuronal populations demonstrating increases or decreases in activity to presentations of the CS are seen within multiple nuclei of the amygdala, indicating a conserved property of fear-promoting and fear-inhibiting cells being located within the same

microstructures (Ciocchi et al., 2010; Duvarci et al., 2011; Grewe et al., 2017; Herry et al., 2008).

Although a population of amygdala neurons increase in activity to presentation of the CS during fear conditioning, a separate subpopulation of amygdala neurons was instead found to increase in activity to the CS during extinction training, suggesting the presence of a competing population of neurons that may encode extinction learning (Herry et al., 2008). Further work has suggested these neurons may be characterized by their expression of the cell surface antigen Thy1 or the neurotensin receptor 2 (NTRS2), as stimulation of these pyramidal neurons enhances the acquisition of extinction memory, while inhibition impairs it (Jasnow et al., 2013; McCullough et al., 2016). Since a population of extinction responsive neurons emerge following extinction training, and a subset of genetically distinguishable amygdala neurons are necessary for extinction learning, it is most likely that a fear extinction memory is formed within the amygdala along-side the original fear memory, resulting in the presence of competing populations of fear-promoting ("fear on") and fear inhibiting ("fear off") cells, along with neurons whose activity is negatively correlated with the CS (also potentially "fear off" cells) (McCullough et al., 2016). However, other parts of the hippocampus-mPFC-amygdala network may allow for fear retention in the face of competing extinction memory formation.

Surprisingly, most of the identifiable "fear on" and "fear off"/extinction neurons in the amygdala project to the mPFC, suggesting fear memory encoding and extinction memory encoding may occur via differential synaptic connectivity of these neurons within regions of the mPFC (Herry et al., 2008). In support of this concept, amygdala neurons that are active during states of high fear project to the prelimbic mPFC, whereas neurons that are recruited during extinction learning project to the infralimbic mPFC (Senn et al., 2014). Moreover, unlike "fear

off"/extinction neurons, "fear on" neurons receive inputs from the ventral hippocampus (Herry et al., 2008), and ventral hippocampus inputs to the amygdala can undergo LTP (Maren and Fanselow, 1995). This would suggest that the hardwired connections, or the timing and directional flow of neural activity between these structures may also be important for the expression versus the inhibition of fear, an idea that is supported by simultaneous *in vivo* recordings from each of these brain regions and the contextual dependence of extinction learning (Lesting et al., 2011; Narayanan et al., 2007; Pape et al., 2005). In particular, theta frequency synchronization of the hippocampus, mPFC, and the amygdala promotes the expression of fear responses following conditioning, whereas uncoupling of synchronization within this frequency range between the hippocampus and amygdala is associated with extinction learning. These results provide a framework for how signaling within this network can serve to promote or suppress fear behaviors, but still lacks a thorough explanation for how extinction memory is consolidated, expressed, or retrieved to drive behavioral selection and reduce fear responses in real-time.

Early studies pointed to the infralimbic mPFC as a critical node for the expression of extinction memory. Unlike the top-down control that the prelimbic mPFC provides for fear expression, the infralimbic mPFC instructs behavioral selection by inhibiting fear CRs, but is not necessary for the acquisition of extinction memory (Herry et al., 2010). For example, although microstimulation and increasing activity of the infralimbic mPFC can enhance extinction learning (Halladay and Blair, 2015; Vidal-Gonzalez et al., 2006), lesions or directed inactivation of the infralimbic mPFC prior to fear extinction impair extinction memory recall, but not the within-session extinction of CRs, signifying that infralimbic mPFC activity is important for the consolidation and retrieval of extinction memory (Laurent and Westbrook, 2009; Quirk et al.,

2000). In line with these findings, a population of infralimbic mPFC neurons demonstrate CS responsiveness during extinction memory retrieval, but not during extinction acquisition (Milad and Quirk, 2002), and LTP at excitatory synapses in the infralimbic mPFC correlate with the behavioral expression of extinction memory (Herry and Garcia, 2002). Similarly, post-extinction training infusions of an NMDAR antagonist into the infralimbic mPFC impair the recall of extinction memory (Burgos-Robles et al., 2007). Overall, these studies converge on the functional importance of the infralimbic mPFC in fear memory inhibition following extinction learning, and suggest that the amygdala may be critical for extinction memory acquisition and retrieval, whereas the mPFC is more strictly involved with the consolidation and retrieval of extinction memory.

With the amygdala being a major source for the generation and extinction of discrete cued fear memory between a CS and US (especially from auditory cues), a major question remains as to the relative role the amygdala, mPFC, and hippocampus play in regulating the contextual contribution to fear extinction. Because the hippocampus has long been implicated in regulating contextual memory representations, much work has been devoted to dissecting its role in the context dependency of extinction learning. Reversible inactivation of the dorsal hippocampus prior to extinction learning in a cued fear conditioning paradigm impairs the rate in which extinction is acquired, and impairs the retrieval of extinction memory in the same or a different context the following day (Corcoran and Quirk, 2007). Similarly, post-extinction training lesions of the hippocampus also impair the context-dependency of extinguished fear responses (Ji and Maren, 2008). These studies provide some evidence that the hippocampus is critical for the contextual specificity of extinction learning, and the context-dependent retrieval of extinction memory, but not necessarily the encoding of extinction (Herry et al., 2010).

However, more recent evidence suggests that fear extinction neurons emerge in the hippocampus (i.e. extinction engram cells), are separate from fear engram neurons, and antagonize fear expression, retrieval, and renewal (Lacagnina et al., 2019), indicating that contextual fear extinction memory may be distinctly stored in the hippocampus. Furthermore, the hippocampus plays an important role in the context dependent retention of fear memories following extinction training, as inactivation of the dorsal or ventral hippocampus prior to an extinction retention test or prior to extinction training causes impairments in fear renewal (Corcoran and Maren, 2001, 2004; Hobin et al., 2006), and renewal of these fear memories likely involves hippocampus signaling with the amygdala, as CS responsive cells in the amygdala during renewal disappear with dorsal hippocampus inactivation (Maren and Hobin, 2007). Nevertheless, since the hippocampus plays an important role in contextual encoding and retrieval of extinction memory, it is possible that the flow of information between the hippocampus and the mPFC is more important for regulating the context dependency of extinction learning. In support of this idea, human functional magnetic resonance imaging has shown concerted activity of the mPFC and the hippocampus during extinction memory retrieval (Kalisch et al., 2006; Milad et al., 2007). In conclusion, the dual roles that the amygdala, mPFC, and hippocampus all play in regulating fear and extinction learning draw attention to the concept of how opposing memories may compete in the brain, even within the same brain structures. Thus, a general principle of these interactions could be that old memories become more contextualized by the presence of new learning and memory formation within the same brain regions (Bouton, 2004).

The Amygdala as a Nexus of Fear Circuitry and Behavioral Selection

Since the amygdala is required for the acquisition and extinction of fear memories, significant efforts have been made over the years to dissect and elucidate the microcircuits and physiological mechanisms within this structure that regulate fear. The amygdala consists of a number of heterogenous nuclei of differing developmental origins. Firstly, the basolateral amygdala complex (BLA), which is positioned between the external and intermediate capsules, is a cortical-like structure consisting of a large percentage of principal pyramidal neurons (~80%) and a smaller population of dispersed GABAergic interneurons (~20%) (Duvarci and Pare, 2014; Spampanato et al., 2011). Although the BLA is not layered like the majority of cortical structures, it demonstrates both local and long-range glutamatergic projections and receives thalamic, intercortical, and neuromodulatory inputs similar to higher order cortex. The BLA can be divided into the lateral amygdala (LA) and the basal amygdala (BA), with the BA being further divided into the basolateral (BL) and basomedial nuclei (BM). For simplicity, the basal nuclei will be considered within their larger nomenclature and be collectively referred to here as the BA (Fig. 1a). It is well supported that the LA and BA receive extensive input from regions relaying internal and external sensory stimuli and that these inputs demonstrate LTP following fear learning, making the BLA a region of immense polymodal sensory integration and emotional processing. Of note, the LA receives inputs from the medial geniculate thalamic nucleus and higher order somatosensory and association cortices, which serve to relay US and CS information during Pavlovian fear conditioning (Duvarci and Pare, 2014; Kwon et al., 2014; LeDoux, 2000).

As noted previously, a small percentage of LA and BA neurons (~20%) will become CS responsive and increase in activity with fear conditioning, with LA neurons having fleeting short

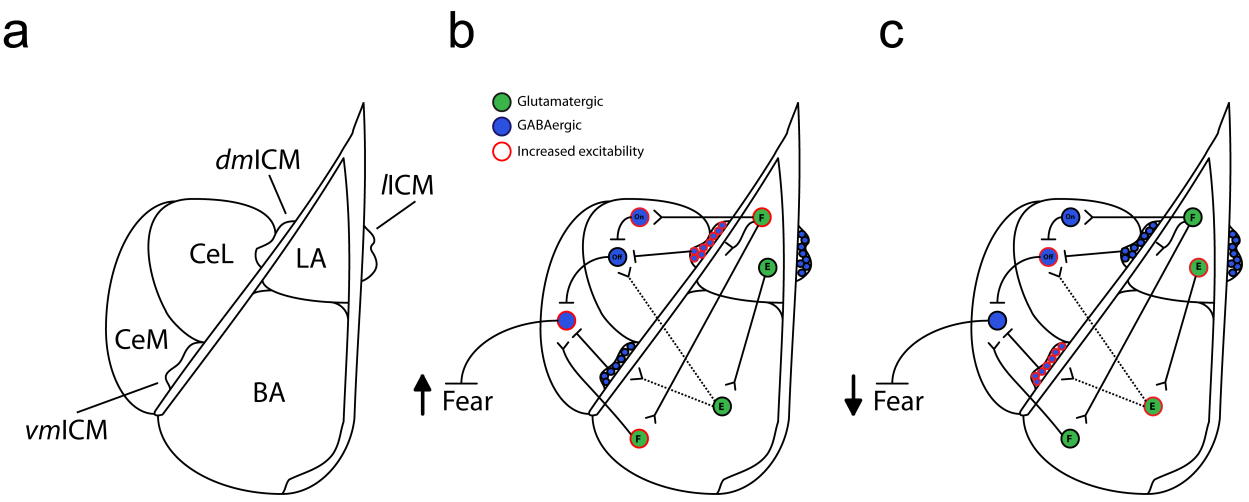

Fig. 1. Summary of the Amygdala Circuitry Regulating Fear Expression and Inhibition. **a,** Major nuclei of the amygdala (LA, lateral amygdala, BA, basal amygdala, CeL, central lateral amygdala, CeM, central medial amygdala, dmICM, dorsomedial intercalated cell masses, vmICM, ventromedial intercalated cell masses, lICM, lateral intercalated cell masses). **b,** Summary and model of the circuitry regulating fear acquisition and expression. **c,** Summary and model of circuitry regulating fear inhibition and extinction (F, "fear on" neurons, E, "fear off"/extinction neurons). Dashed lines indicate hypothetical projections expected to play a role in regulating fear. Depictions of interneurons in the BLA have been removed for simplicity.

latency responses to the CS, and BA neurons having more delayed and prolonged responses throughout the presentation of the CS (Amano et al., 2011; Quirk et al., 1995; Repa et al., 2001). The apparent difference in latency and firing properties to the CS between LA and BA neurons is believed to be due to the intranuclear connectivity of the BLA. The BLA follows a general dorsoventral to lateromedial form of serial processing, where pyramidal LA neurons synapse onto anatomically segregated pyramidal neurons of the BA across large distances, but rarely ever onto closely neighboring pyramidal neurons (Samson et al., 2003; Samson and Pare, 2006). This organization of synaptic connectivity, in addition to forms of feedback and feedforward inhibition from local interneurons, prevents runaway excitation and promotes the flow of information between areas that may receive different degrees or distributions of incoming sensory inputs (Duvarci and Pare, 2014). Interestingly, the LA is necessary for the acquisition of

cued fear conditioning, but the number of CS responsive neurons recruited into the memory trace is believed to be constrained by the degree of these internuclear synaptic interactions (Duvarci and Pare, 2014). Enhancing or decreasing the intrinsic excitability of BLA neurons by over-expressing or downregulating the transcription regulator cyclic adenosine monophosphate response element binding protein (CREB) promotes or prevents their recruitment into the memory trace, respectively, but does not change the overall number of neurons that become reactive to the CS following fear conditioning (Han et al., 2007; Viosca et al., 2009; Zhou et al., 2009). This suggests that competitive interactions between pyramidal neurons in the BLA through their synaptic connectivity determines which neurons become the anatomical substrate for fear memory storage, with neurons demonstrating higher internal excitability being more likely to be recruited into the fear memory trace.

In addition, the BLA also projects to the central nucleus of the amygdala (CeA) where the expression of defensive fear responses is most tightly regulated. The CeA consists of three subdivisions, which may have distinct functions in regulating fear responses: the central capsular division (CeC), the central lateral division (CeL), and the central medial division (CeM). Because there is no definitive anatomical delineation or morphological distinction of cell types between the CeC and CeL, these structures are most often considered a single subdivision and, unless otherwise noted, will be referred to collectively as the CeL herein (Fig. 1a). As a whole, the CeA is of striatal origin and consists almost entirely of GABAergic medium spiny-like neurons (McDonald and Augustine, 1993; Pare and Smith, 1993a). The CeM neurons tend to have larger somata and less spines than that of CeL neurons, and are considered the primary output neurons of amygdalar fear circuitry due to their dense efferent projections to hindbrain fear effector nuclei. In line with this, CeM neurons demonstrate significantly increased and

sustained activity patterns in response to the CS after conditioning, and are activated when an animal is mounting defensive behavioral responses such as freezing (Ciocchi et al., 2010; Duvarci et al., 2011). As such, reversible inactivation of the CeM leads to impairments in the expression of CS induced freezing following conditioning, whereas ectopic stimulation of the CeM neurons elicits unconditioned freezing responses. Similarly, inactivation of the CeM following conditioning impairs the expression of freezing, cumulatively suggesting that neurons in the CeM are responsive to fear associated stimuli and are required for fear expression.

Although the CeM is necessary for fear expression, and the LA for fear acquisition, the LA does not directly project to the CeM, calling into question how associative learning in the LA drives defensive freezing responses through recruitment of the CeM. As mentioned above, one possible route is through an intermediary structure such as the BA. Pyramidal neurons of the LA can project ventrally to the BA, and then BA neurons project medially to the CeM (Fig. 1b) (Duvarci and Pare, 2014). The BA is known to project heavily to the CeM, and is hypothesized to relay signals from LA neurons to the CeM neurons in order to drive fear responses during retrieval of fear memories (Fig. 1b). Despite this projection pattern, lesions or reversible inactivation of the BA does not often impair acquisition of fear memory when performed prior to or during conditioning, but will impair expression/retrieval when performed after conditioning, suggesting a separate route exists from LA to CeM to allow for fear acquisition. CeL neurons, with their medium to small somata and dense distribution of dendritic spines, are believed to fulfill this role. The LA (but also BA) sends robust projections to the CeL, and LA-CeL synapses have been shown to undergo LTP following fear conditioning (Li et al., 2013). Moreover, some CeL neurons send projections to the CeM (Fig. 1b). In line with this, reversible inactivation of the CeL impairs fear acquisition, but not the expression of fear when inactivated following

conditioning (Ciocchi et al., 2010), suggesting the CeL may relay information to the CeM during fear acquisition. However, unlike the BA, the CeL is GABAergic, and cannot directly excite the CeM (Fig. 1b). Thus, one manner in which the CeL achieves a relay of associative fear information to the CeM is through a mechanism of disinhibition. Two physiologically distinct populations of neurons exist in the CeL that differentially respond to the presentation of the CS. One population of neurons increases their firing rate to presentation of the CS (CeL-On), whereas another population decreases their firing rate in response to the CS (CeL-Off) (Fig. 1b). These responses may behaviorally correspond to the "fear on" and "fear off" neurons previously described in the BLA, but this concept has yet to be directly tested. CeL-On neurons are believed to synapse onto CeL-Off neurons, and CeL-Off neurons onto CeM neurons, providing a mechanism of disinhibition that gates freezing responses by increasing the activity of the CeM (Fig. 1b). Therefore, a hypothetical framework for fear acquisition and expression emerges; starting with the LA, glutamatergic projection neurons encode the CS-US association, these neurons then project to the CeL or the BA, which in turn project to the CeM, ultimately increasing the excitability of CeM neurons and promoting freezing responses (Fig. 1b).

Another route by which the LA may regulate activity of the CeM is through the recruitment of the intercalated cell masses (ICMs). The ICMs are three interspaced clusters of small somata GABAergic neurons that are localized along the intermediate and external capsules. Although the function of the lateral ICM (*l*ICM) is poorly understood, the dorsomedial ICM (*dm*ICM) and ventromedial ICM (*vm*ICM) play a significant role in regulating fear behaviors. The *dm*ICM neurons receive input from the LA and provide feedforward inhibition into the CeL (Geracitano et al., 2007; Pare and Smith, 1993b; Royer et al., 1999, 2000). Hence, one way in which the LA can relieve inhibition on CeM neurons and gate fear is through

*dm*ICM-mediated feedforward inhibition onto CeL-Off neurons (Fig. 1b) (Duvarci and Pare, 2014).

Despite the potential role of *dm*ICM neurons in regulating fear responses, the *vm*ICM may play a larger role in inhibiting fear responses during extinction training. Neurons of the *vm*ICM project heavily to the CeM, and genetic ablation of these cells interferes with fear extinction (Jungling et al., 2008; Likhtik et al., 2008). Additionally, LTP of BA synapses onto *vm*ICM neurons occurs with extinction training, leading to feed-forward inhibition onto CeM neurons (Amano et al., 2010). These findings are consistent with the fact that CeM neuronal activity decreases with extinction training and closely parallels the behavioral decrease seen in the CR (Duvarci et al., 2011), suggesting CeM neurons are under some form of inhibitory control. As previously described, "fear-off"/extinction cells emerge in the amygdala with extinction training, in particular in the BLA, and these neurons may be the likely candidates for providing feedforward inhibition to the CeM via the *vm*ICM (Fig. 1c). However, because the BLA projects heavily to the CeL as well, it remains to be determined which classes of functionally defined BLA neurons ("fear-on" or "fear-off"/extinction) signal to functionally defined neurons in the CeL to further regulate the acquisition or extinction of fear responses (Fig. 1b and 1c).

Genetic Enrichment Markers for Studying the CeL

The presence of two populations of neurons that respond differentially during presentation of the CS suggests some competitive interactions may take place within the CeL. These competitive interactions may ultimately affect CeM output and define the behavioral strategy an animal chooses in the face of adversity (i.e. freezing, flight, exploration). Given the

paucity of knowledge in understanding whether individual CeL neurons may promote or inhibit fear expression, many studies in recent years have heavily focused on identifying what properties make CeL-On and CeL-Off neurons unique. Interestingly, the CeA contains a plethora of genetically distinct or semi-overlapping enrichment markers for neuropeptides, intracellular enzymes, and membrane receptors that are specifically localized to the individual subdivisions of the CeA or are uniquely distributed along its axes. The CeL has a particularly large and restricted set of genetic markers that can be used to delineate its anatomical borders, and with the advent of recent neuroscience techniques in rodents, these enrichment markers can be used to gain genetic access to the CeL and dissect its function with great precision. Not surprisingly, these approaches have allowed researchers to manipulate individual populations of genetically defined neurons in the CeL to explore their role in regulating animal behavior. As a result, the CeL has recently emerged as a structure that regulates a diverse range of survival-oriented behaviors not strictly limited to defensive fear responses, suggesting the CeL may be a significant amygdalar nucleus for instructing the selection of behavioral repertoires. Below, all of the major genetically-defined classes of neurons in the CeL that have been functionally characterized by their regulation of positive and negative emotional states will be highlighted, with emphasis on how these neurons may fit into a model of action selection in the presence or absence of danger.

Oxytocin Receptor (OXTR) Neurons

OXTRs are g-protein coupled receptors (GPCRs, coupled to Gαq) whose endogenous ligand is the anti-stress and prosocial neuropeptide hormone oxytocin. Early studies examining oxytocin administration in the CNS demonstrated reductions in anxiety and fear responses, suggesting that the CeA may be an important locus for the pharmacological effects of oxytocin

in the brain (Viviani et al., 2011; Windle et al., 1997). Histoautoradiogrpahy was first used to identify OXTR-expressing (OXTR+) neurons in the CeA, which were found to be localized to the CeL (Huber et al., 2005). OXTR+ neurons of the CeL synapse specifically onto CeM neurons that project to the hindbrain periaqueductal gray (PAG), a brain region critical for generating the defensive responses to threat. Conversely, OXTR-lacking (OXTR-) neurons synapse onto a separate population of CeM neurons that project to the dorsal vagal complex (DVC), which is a region responsible for regulating cardiovascular responses to stress (Viviani et al., 2011). In line with these findings, an OXTR agonist increases the firing rate of a subset of neurons in the CeL, while increasing the frequency of spontaneous inhibitory postsynaptic currents (sIPSCs) onto CeM-PAG projecting neurons, but not CeM-DVC projecting neurons (Huber et al., 2005; Viviani et al., 2011). These studies provided the first evidence of a potential mechanism by which CeM neurons regulating autonomic control (DVC projecting) versus behavioral control (PAG projecting neurons) over fear responses may be differentially regulated by distinct CeL populations (Gozzi et al., 2010; LeDoux et al., 1988; Viviani et al., 2011). Whereas OXTR- neurons are expected to control cardiovascular responses to fearful stimuli by regulating the activity of CeM-DVC projecting neurons, OXTR+ neurons have been shown to reduce the spontaneous firing rate of CeM-PAG projecting neurons, which would be expected to decrease the generation of conditioned freezing responses. In support of this model, microinfusion of oxytocin into the CeA in fear-conditioned rodents causes a reduction in conditioned freezing without affecting cardiovascular responses . Taken together, these results indirectly suggest that OXTR+ neurons could comprise the major population of predicted "fear off" neurons in the CeL that suppress conditioned fear responses (Fig. 1b,c).

Protein Kinase C delta (PKCδ) Neurons

PKCδ is a calcium-independent PKC isoform that is involved in diverse cellular signaling pathways (Kikkawa et al., 2002). Although the role of this enzyme in neuronal physiology is not well understood, it is highly expressed in the CeL, and serves as one of the primary genetic enrichment markers that can be used to define the anatomical borders of the CeL (Haubensak et al., 2010). PKCδ+ neurons consist of ~50% of all GABAergic CeL neurons and synapse onto CeM-PAG projecting neurons (Haubensak et al., 2010). Consistent with this finding, ~65% of PKCδ+ neurons in the CeL are also OXTR+. Chemogenetic inhibition of PKCδ+ neurons decreases the tonic activity of identified CeL-Off neurons after fear conditioning, increases activity of CeM neurons, and is capable of increasing conditioned freezing responses, supporting the notion that PKCδ+ neurons are likely CeL-Off neurons (Fig. 1b) (Haubensak et al., 2010). Moreover, PKCδ+ neurons have been shown to form reciprocal inhibitory synapses with PKCδ- neurons in the CeL providing a potential neural substrate for "fear on" and "fear off" interactions. Cumulatively, these findings lend credence to the concept that PKCδ+/CeL-Off neurons compete with CeL-On neurons to inhibit freezing behavior. However, more recent studies challenge this concept by demonstrating diverse and seemingly conflicting functions of the PKCδ+ cell population. Although activity of PKCδ+/CeL-Off neurons would be expected to decrease fear responses (Fig. 1b), optogenetic stimulation of this population has been shown to produce anxiety, fear generalization, aversion, and anorexia (Botta et al., 2015; Cai et al., 2014; Cui et al., 2017). Conversely, optogenetic inhibition reduces these same measures. Furthermore, PKCδ+ neurons are indispensable for fear learning, as silencing the activity of these neurons during conditioning prevents both acquired freezing responses to the CS and associative plasticity within the LA, suggesting PKCδ+ neurons exert a strong degree of control over fear memory

formation and expression (Yu et al., 2017). Moreover, a fraction of PKCδ+ neurons demonstrate responses to the US and acquire CS responsiveness following conditioning, signifying this population cannot strictly be identified as CeL-Off neurons (Yu et al., 2017). Interestingly, the discrepancy between some of these studies may be explained by further anatomical segregation and heterogeneity of PKCδ+ neurons along the rostrocaudal and mediolateral axes. While PKCδ+ neurons in the more caudal portions of the CeL are believed to inhibit conditioned fear responses and anxiety (Griessner et al., 2018), PKCδ+ neurons in the more rostral portions of the CeL are heavily localized to the capsular border and are believed to promote aversive learning (Kim et al., 2017). Studies examining the function of neurons primarily residing in the CeC support this notion and will be discussed in further detail below.

Somatostatin (SOM) Neurons

SOM is a neuropeptide hormone that produces anxiolytic and consummatory behaviors throughout the CNS (Stengel and Tache, 2019). Central administration of SOM or its receptor agonists have been shown to increase locomotion, increase orexigenic behavior, and decrease anxiety (Danguir, 1988; Scheich et al., 2016; Van Wimersma Greidanus et al., 1987; Vecsei et al., 1989; Vecsei and Widerlov, 1990). Similarly, direct microinfusion of SOM into the amygdala decreases anxiety and fear behaviors (Kahl and Fendt, 2014; Yeung et al., 2011; Yeung and Treit, 2012). Consistent with these pharmacological findings, SOM has been shown to inhibit CeM-PAG projecting neurons, supporting an overall role of this neuropeptide in negatively regulating fear responses (Chieng and Christie, 2010). These effects may be due to local SOM release in the CeA, as SOM+ neurons are largely expressed in the CeL, with a smaller percentage also present in the CeM. Interestingly, SOM+ neurons are primarily distinct

from PKCδ+ neurons (Li et al., 2013), and form mutually reciprocal inhibitory synapses with various other cell-types in the CeL (Fadok et al., 2017; Hunt et al., 2017). SOM+ neurons also do not send significant inhibitory synapses to the CeM, and do not specifically provide inhibition onto the CeM-PAG projecting neurons. Given the small genetic overlap between SOM+ neurons and PKCδ+ neurons, and their differing extent of connectivity with the CeM, researchers initially hypothesized that these populations of cells may be functionally segregated. Notably, SOM+ neuron firing rates increase when animals are freezing in response to the CS, and optogenetic stimulation of SOM+ neurons in the CeL produces unconditioned freezing behavior, whereas inhibition of these neurons impairs the acquisition and expression of conditioned freezing, indicating SOM+ neurons are absolutely necessary for producing passive fear responses during aversive learning (Fadok et al., 2017; Li et al., 2013; Yu et al., 2016). Furthermore, a small degree of SOM+ neurons in the CeL send direct projections to the PAG, and demonstrate potentiated excitatory synapses from the LA following fear conditioning. Cumulatively, these results suggest that SOM+ neurons are likely CeL-On neurons, which could be further supported as "fear on" neurons due to their necessity in fear learning and potentiation of input from the upstream LA (Fig. 1b). However, the dichotomy between the apparent function of these cells and the neuropeptide they express is ripe for further exploration.

Calcitonin Gene-Related Peptide Receptor (CGRPR) Neurons

CGRPRs are GPCRs (coupled to Gαs) whose endogenous ligand is the vasodilatory and pain-transmitting neuropeptide CGRP. CGRP is expressed in pain fibers of sensory nerves and is highly enriched in the parabrachial nucleus (PBN) (Han et al., 2015; Russell et al., 2014). Together, sensory neurons of the superficial spinal cord and PBN neurons make up the spino-

parabrachial pathway that transmits nociceptive information in the CNS (Han and Palmiter). Unlike the spino-thalamic pathway, which relays US information via projections to the LA, the spino-parabrachial pathway circumvents the LA and provides direct input to the CeL. Consistent with this organization, CGRP+ neurons of the PBN provide strong glutamatergic input to CeL neurons (particularly in the capsular portion) and are necessary for the acquisition of conditioned fear (Han et al., 2015). Moreover, inhibition of this projection impairs pain-processing specific to the US (foot-shock), but not overall processing of other painful stimuli, suggesting the PBN input to the CeL is a major source of affective information regarding the US during fear learning. In support of these findings, CGRPR+ neurons are highly expressed in the CeL and are in quantities that greatly exceed PKCδ+ and SOM+ neurons. Much like the function of the spino-parabrachial pathway, CGRPR+ neurons in the CeL are necessary for processing the US information during fear learning and are necessary for fear acquisition. Additionally, optogenetic stimulation of these neurons drives unconditioned freezing responses along with subsequent contextual and cue-specific fear responses, suggesting CGRPR+ neurons likely encode CS-US associations and the affective components of pain processing. Interestingly, these neurons demonstrate a high degree of overlap with PKCδ+ neurons (~50%) throughout the CeL, and are most heavily localized to the CeC (Han et al., 2015). Since PKCδ+ neurons are paradoxically required for fear learning as well as being identified as CeL-Off neurons, the function of either of these populations may be due to where they overlap within the CeL/CeC. Thus, the location of neurons within the CeL and their afferent input may be more important to the regulation of fear responses than how they are genetically defined.

5-Hydroxytryptamine Receptor 2A (Htr2A) Neurons

Htr2A is a GPCR (coupled to Gαq) whose endogenous ligand is serotonin (5-HT). Htr2As regulate diverse functions in the brain and are highly expressed within the CeA. Htr2A+ neurons are most heavily localized to the CeL, but also are expressed to a smaller degree within the CeM (Douglass et al., 2017). Although these neurons have partial co-expression with other genetic markers, they are completely distinct from PKCδ+ cells, indicating they may have segregated function. Whereas PKCδ+ neurons are anorexigenic, Htr2A+ neurons are likely orexigenic as their optogenetic or chemogenetic stimulation is capable of increasing food consumption (Douglass et al., 2017). Similarly, Htr2A+ neuron activity is increased during the early phase of food consumption, and inhibition of this population decreases food consumption. However, Htr2A+ neuronal activity can also drive real time place preference and appetitive responding without affecting the latency to consume palatable foods, suggesting these neurons influence consummatory behavior through a positive-valence mechanism rather than affecting the motivation to feed. Surprisingly, much like the diversity of function seen in other CeL neuron populations, Htr2A+ neurons also positively regulate fear behaviors. Htr2A+ neurons have been shown to control the hierarchy between innate and learned fear responses to distinct olfactory cues (Isosaka et al., 2015). Inhibition of Htr2A+ neurons decreases conditioned freezing responses while simultaneously enhancing innate freezing responses. Alternatively, activation of Htr2A+ neurons only decreases innate freezing responses. Intriguingly, innately fearful stimuli are preferentially avoided over fear-conditioned stimuli in tasks where the desire to seek out food is high (food-deprived animals) and is presented in proximity to either of these cues. Also, animals that have been previously exposed to innately fearful cues freeze less when subsequently exposed to conditioned cues, but not *vice versa*. These results indicate that Htr2A+ neurons in

the CeL promote pro-consummatory behaviors while also being able to regulate the hierarchy of fear responses in the presence of both innate and conditioned fear-provoking stimuli. Therefore, the specific function of this population in regulating real-time decision-making may be highly dependent on the internal state of the animal and its environmental context.

Prepronociceptin (PNOC) Neurons

PNOC is precursor for the orexigenic neuropeptide nociceptin (NOC), which can promote feeding behavior in the CNS. PNOC+ neurons are expressed throughout the CeA, with the highest expression in the CeL and a lesser degree of expression in the CeM (Hardaway et al., 2019). These neurons demonstrate a weak but notable degree of overlap with CRF+, SOM+, PKCδ+, CGRPR+, and Htr2A+ neurons. Given the relatively low overlap with other CeL enrichment markers, PNOC+ neurons are generally believed to be a unique genetically-defined population of CeA neurons. Similar to Htr2A+ neurons, PNOC+ neurons are activated during feeding of highly palatable foods. Additionally, activity of PNOC+ neurons appears to promote high-fat diet-induced metabolic dysfunction, as ablation or chemogenetic inhibition of these neurons decreases palatable food consumption and the development of obesity (Hardaway et al., 2019). Interestingly, downstream optogenetic stimulation of a number of efferent projections from PNOC+ neurons does not specifically drive feeding behavior but is capable of enhancing reward, suggesting these neurons may also promote consummatory behaviors through a positive-valence mechanism.

CRF Neurons

Despite the essential role of CRF in activation of the HPA axis, this hormone also serves as a neuropeptide capable of positively regulating stress responsivity within extrahypothalamic brain regions. CRF is enriched along the extended amygdala, and its signaling throughout various limbic structures has been shown to promote anxiety and fear behaviors (Marcinkiewcz et al., 2016; McCall et al., 2015; Nijsen et al., 2001; Pliota et al., 2018; Pomrenze et al., 2019; Thoeringer et al., 2012). Specifically, direct microinfusion of CRF or CRF receptor (CRFR) agonists into the CeA promotes certain anxiety and fear responses (Wiersma et al., 1998), whereas CRFR antagonism in the CeA has been shown to reduce fear and anxiety expression (Swiergiel et al., 1993). Similarly, genetic overexpression or knockdown of CRF in the CeA has been shown to increase fear, anxiety, and recruitment of the HPA axis, or decrease HPA axis activation, respectively (Callahan et al., 2013; Flandreau et al., 2012; Keen-Rhinehart et al., 2009; Pitts and Takahashi, 2011; Pitts et al., 2009). Although these data generally support CRF as a pro-stress hormone, many studies using similar approaches have either found no effect of CRF manipulations in the CeA, or in some cases, opposing effects (i.e. anxiolysis and decreased freezing responses) (Callahan et al., 2013; Dedic et al., 2018; Gafford and Ressler, 2015; Hubbard et al., 2007; Isogawa et al., 2013; Roozendaal et al., 2002; Wiersma et al., 1995; Wiersma et al., 1997).

Since CRF+ neurons are densely clustered within the CeA, recent studies have sought to examine how activity of this extrahypothalamic population of neurons is capable of regulating fear responses. CRF+ neurons are heavily localized within the CeL, with evidence for a small quantity of CRF+ neurons also present in the CeM (Sanford et al., 2017). Optogenetic inhibition of CRF+ neurons in the CeA during fear conditioning has been shown to reduce sustained

freezing responses during a contextual fear recall test, suggesting CRF+ neurons may be responsible for the maintenance or retention of fear over time (Asok et al., 2018). This finding is consistent with another study demonstrating how chemogenetic inhibition or complete silencing of CRF+ neurons prevents conditioned freezing responses to the CS, which is also dependent on the CRF expression in these cells (Sanford et al., 2017). Indirectly, these data suggest activity of CRF+ neurons and their release of CRF are important for acquiring fear memory. However, after fear conditioning, inhibition of CRF+ neurons during memory recall does not impair fear memory expression in either of these studies, and the effects of CRF signaling on fear responses are only produced under conditions of low US intensity (i.e. low foot-shock intensity). Taken together, these results suggest that CRF+ neurons may facilitate acquisition of passive fear responses under conditions of low threat exposure via CRF release, but may not be necessary for continued fear expression once fear memory has been acquired.

Although previous studies support a general role of CeA-CRF+ neurons in promoting passive fear responses, a more recent study has demonstrated opposing results for the role of CRF+ neurons in regulating fear responses. For instance, in animals conditioned to mount freezing or flight responses to discrete sensory cues, optogenetic stimulation of CRF+ neurons facilitates conditioned flight responses, while optogenetic inhibition reduces these conditioned flight responses (Fadok et al., 2017). Furthermore, CRF+ neuronal activity is only increased when animals are performing conditioned flight responses or presented with the CS that elicits conditioned flight responses. Therefore, these findings strongly suggest CRF+ neurons are necessary for the selection of active fear responses such as conditioned flight and escape behaviors, rather than the passive fear responses like freezing, which rely on activation of SOM+ neurons. Therefore, CRF+ neurons in the CeA appear to control a diverse range of behavioral

responses. Whereas CRF peptide release from this population may contribute to fear learning by promoting passive freezing to an inescapable CS, the real-time activity of these neurons appears to be critical for driving active motivational behaviors aimed at avoiding imminent threats, such as conditioned flight and escape responses. Interestingly, these active motivational responses may rely on an animal's internal state and environmental setting, as optogenetic activation of CRF+ neurons in non-threatening contexts also drives appetitive and rewarding/consummatory behaviors (Kim et al., 2017). Taken together, these findings signify that CRF+ neurons drive different forms of fear expression or appetitive behaviors that are reliant on the animal's contextual experience.

Research Aims and Hypothesis

Many of the above mentioned cell-types in the CeL appear to control negative emotional states (fear behavior) and positive emotional states (consummatory and reward-related behavior), suggesting that an animal's experience may shape how these neuronal populations cooperate with other brain regions to regulate behavioral output and promote survival. Currently, it is not well understood how individual populations of CeL neurons are recruited by afferent inputs to drive the selection of distinct behavioral strategies. It also is not well understood whether the afferent and efferent circuitry of CeL neurons is remodeled by experience, internal state, and environmental context to alter behavior. As such, a remaining question is how changes in the phenomenological expression of fear are mediated by excitatory synaptic inputs to the CeL.

Provided that CRF signaling in the CNS also plays a large role in appetitive or reward related behaviors such as feeding and drug use (Lemos et al., 2012; Roberto et al., 2017), further work is needed to elucidate the behaviors imposed by CRF+ neuron activity when an animal is in

a high-fear (threatening context) or low-fear state (non-threatening context). CeA-CRF+ neurons appear unique in that they comprise a population of cells that can drive functionally divergent behavioral states in different environmental contexts, and thus may be a cellular substrate for the regulation of experience-dependent changes in fear expression following fear learning and extinction. In this dissertation, we hypothesize that excitatory transmission onto CRF+ neurons will change following the acquisition and extinction of fear relative to other classes of genetically-defined CeL neurons. Specifically, we hypothesize that the relative excitatory drive to CRF+ neurons over other cell-types in the CeL will reflect the functional regulation of these neurons on conditioned fear behaviors. Thus, our aim is to establish how excitatory plasticity onto CRF+ neurons corresponds to the behavioral regulation these neurons impart on learned and extinguished fear responses. Considering these are still rather unexplored questions, we aim to provide novel insight into the neural circuitry of CeA-CRF+ neurons, the circuit-specific plasticity of glutamatergic synapses onto these neurons following fear acquisition and extinction, and the direct role these neurons play in regulating conditioned fear responses. In the following chapter, my colleagues and I present the first evidence to date of bidirectional plasticity within a single glutamatergic circuit to the CeL that is remodeled by the animals' experience and how this plasticity may serve as biological substrate for both fear memory acquisition and extinction. Furthermore, we expand upon the current knowledge of CeL neuronal function by demonstrating how CRF+ neurons regulate conditioned freezing behavior and provide a model by which circuit-specific remodeling of distinct afferents to the CeL shape the acquisition and extinction of passive fear responses by biasing input between CRF+ and CRF- neurons.

CHAPTER II

DYNAMIC REMODELING OF CENTRAL AMYGDALA GLUTAMATERGIC CIRCUITS ACROSS FEAR STATES

Nolan D. Hartley[1,4], Andrew D. Gaulden[1], Rita Baldi[1], Nathan Winters[1,4], Gregory J. Salimando[2,4], Luis Eduardo Rosas-Vidal[1], Alexis Jameson[1,4], Danny G. Winder[1,2,3,4], and Sachin Patel[1,2,3,4]*

[1]Department of Psychiatry and Behavioral Sciences, Vanderbilt University Medical Center, Nashville TN USA

[2]Department of Molecular Physiology & Biophysics, Vanderbilt University School of Medicine, Nashville TN USA

[3]Department of Pharmacology, Vanderbilt University School of Medicine, Nashville TN USA

[4]Vanderbilt Brain Institute, Vanderbilt University, Nashville TN USA

Abstract

Acquisition and extinction of learned fear responses utilize flexible yet conserved neural circuits that promote or suppress fear expression, respectively. Here we show that acquisition of passive fear behavior is associated with dynamic remodeling of synaptic excitatory drive from the basolateral amygdala (BLA) away from corticotropin releasing factor-expressing (CRF+) central lateral amygdala (CeL) neurons, while fear extinction training remodels this circuit back toward favoring CRF+ neurons. Importantly, BLA activity is required for this experience-dependent remodeling, while directed inhibition of the BLA-CeL circuit impairs both fear memory acquisition and extinction memory retrieval. Additionally, ectopic excitation of CRF+ neurons impairs memory acquisition and facilities extinction, whereas CRF+ neuron inhibition impairs extinction memory retrieval, supporting the notion that CRF+ neurons serve to inhibit learned freezing behavior. These data suggest afferent-specific dynamic remodeling of relative excitatory drive to functionally distinct subcortical neuronal-output populations represent an important mechanism underlying experience-dependent modification of behavioral selection.

Adapted from: Hartley et. al. 2019, Nature Neuroscience (accepted in principle).

Introduction

The CeA is a nodal structure at the limbic-motor interface critical for rapid action selection in response to changing environmental and homeostatic needs. Functionally distinct CeA neuron subpopulations have been found to coordinate conserved survival-oriented behaviors including freezing, flight, feeding, foraging, and hunting in mice (Amir et al., 2015; Douglass et al., 2017; Fadok et al., 2017; Han et al., 2017; Li et al., 2013). Importantly, these diverse CeA-mediated behavioral responses can be guided by previous experience to ensure optimal behavioral selection during future environmental challenges (Do Monte et al., 2016). One example of experience-dependent learning that has been extensively shown to recruit CeA neurocircuitry is Pavlovian fear conditioning, in which animals can form lasting associative memories between conditioned stimuli (CSs) and temporally coinciding aversive unconditioned stimuli (US) (Maren, 2001). Importantly, these conditioned stimuli are reinforced during learning to serve as strong predictors of threat and are adaptive in the short-term. However, the proper extinction of fear responses to CSs when they no longer predict threat is an adaptive learning process as well, and is imperative for the normalization of behavior following traumatic stress exposure.

The CeA, containing almost entirely GABAergic medium-spiny like neurons, was previously thought to function as a passive output relay of conditioned stimulus information that would drive rapid and evolutionarily conserved fear responses, such as freezing behavior (Duvarci and Pare, 2014). However, recent studies have provided evidence for the CeL as an essential regulator of fear memory formation and storage (Li et al., 2013; Penzo et al., 2015), suggesting it may also serve as an important nexus of synaptic plasticity for competing circuits that either promote the acquisition of conditioned fear responses or serve to suppress conditioned

fear expression (Haubensak et al., 2010). Indeed, genetically or functionally distinguishable CeL neurons have been shown to have corresponding increases or decreases in activity to fear-promoting CSs (Ciocchi et al., 2010), or extinction training (Duvarci et al., 2011), respectively, most commonly referred to as "fear on" and "fear off" neurons (Duvarci and Pare, 2014). However, a mechanistic understanding of how excitatory afferent signals are capable of selecting distinct CeL cell types to drive the expression and extinction of fear responses is lacking.

CeA neurons that express the neuropeptide CRF have recently emerged as key determinants of both passive and active forms of fear expression in response to threat-predictive cues (Asok et al., 2018; Fadok et al., 2017; McCall et al., 2015; Sanford et al., 2017), as well as appetitive behavior under non-threatening conditions (Kim et al., 2017), suggesting CeA-CRF neurons control diverse survival-related behaviors depending on an animal's context and previous experience. Here, we examined top-down and bottom-up excitatory afferents to CeL-CRF+ neurons following bipartite experiential learning and reveal how plasticity in the BLA-CeL circuit preferentially selects distinct neurons via changes in relative excitatory input strength between neighboring CRF+ and CRF- neurons. We provide evidence that BLA-CeL glutamatergic projections dynamically remodel in response to fear acquisition and extinction and suggest that this remodeling may serve as a synaptic correlate of fear and extinction learning. Lastly, our work also highlights an unexpected role for CeA CRF+ neurons in the regulation of fear extinction. Whereas CRF peptide release has long been implicated in positively regulating fear and anxiety behaviors (Gafford and Ressler, 2015; McCall et al., 2015), we find that CRF+ neuron activity also serves to reduce passive conditioned fear responses.

Results

Distribution, membrane properties and molecular phenotype of CeA CRF+ neurons.

Using a *CRF-IRES-Cre::Ai14* mouse reporter line, we found that CRF+ neurons are largely localized to the CeL (Fig. 1a,b), the primary input nucleus of the CeA (Duvarci and Pare, 2014). CRF+ neurons in the CeL consist primarily of late firing neurons (Fig. 1c) and exhibit slight differences in basal membrane properties compared to CRF- neurons (Supplementary Fig. 1). CRF+ neurons have been described as being largely segregated from other genetically defined populations of neurons in the CeA (Fadok et al., 2017; Sanford et al., 2017). Consistent with these previous studies, we find that CRF+ neurons in the CeL have minimal overlap with neurons expressing protein kinase Cδ (PKCδ+) (Botta et al., 2015; Haubensak et al., 2010; Kim et al., 2017; Yu et al., 2017). We also find that CRF+ neurons demonstrate a detectable but low level of overlap with the neuropeptide marker somatostatin (SOM+) (Supplementary Fig. 1), which labels neurons necessary for the acquisition and expression of conditioned freezing (Fadok et al., 2017; Li et al., 2013; Penzo et al., 2015). Overlap with SOM+ neurons was assessed using two methods, *in situ* hybridization and dual reporter mice, yielding different quantities of co-labeled neurons but consistent results in distribution within the CeL (Supplementary Fig. 1). These data suggest that CRF+ neurons overlap to a small degree with SOM+ neurons but are primarily genetically segregated from these functionally distinct CeA cell-types, indicating CRF+ neurons may regulate conditioned fear in ways unique to that of SOM+ and PKCδ+ neurons.

Fear conditioning and extinction training bidirectionally remodel relative glutamatergic input strength onto CeL CRF+ and CRF- neurons.

To begin to elucidate experience-dependent plasticity at excitatory glutamatergic inputs to CeL-CRF+ neurons, we performed *ex vivo* whole-cell patch-clamp recordings from naïve (basal), fear-conditioned, and fear-extinguished mice (Fig. 1d, and Supplementary Fig. 2). We alternated recordings of spontaneous excitatory post-synaptic currents (sEPSCs) from samples of closely neighboring CRF+ and CRF- neurons within the same plane of coronal brain slices (Fig. 1d,e). Using this approach, we found that average sEPSC frequency, but not amplitude, was significantly greater onto CRF+ neurons than CRF- neurons in naïve mice (Fig. 1f). However, following fear conditioning, average sEPSC frequency was not significantly different between CRF+ and CRF- neurons (Fig. 1g), but following extinction training, the average sEPSC frequency was again significantly greater onto CRF+ neurons than CRF- neurons (Fig. 1h).

To assess the relative influence of excitatory neurotransmission onto CRF+ neurons compared to neighboring CRF- neurons, we plotted the sEPSC frequency and amplitude ratios of neighboring cell-types, a method of analysis that is sensitive to differences in input bias onto anatomically adjacent neurons (MacAskill et al., 2014). We found that the CRF+/CRF- sEPSC frequency ratio was high in naïve mice, but significantly lower and close to 1:1 in fear-conditioned animals, and then was significantly higher again in mice that underwent extinction training (Fig. 1i). Analysis of average sEPSC frequency and amplitude for each cell-type across fear states revealed a shift in input bias away from CRF+ neurons that was driven by increased glutamatergic drive to CRF- cells (Fig. 1j), while the shift in relative input bias back onto CRF+ neurons following extinction training was driven in part by an enhancement of excitatory neurotransmission onto CRF+ neurons as well as a concomitant reduction in excitatory

neurotransmission onto CRF- neurons (Fig. 1j). These changes across fear states were reflected in sEPSC frequency, but not amplitude, suggesting a presynaptic locus of plasticity that contributes to shifts in input bias following fear conditioning and extinction training. Cumulatively, these results demonstrate that excitatory drive is biased toward CRF+ neurons under basal conditions, that this bias disappears with the acquisition of conditioned freezing, and then reemerges after extinction training.

Since the expression of conditioned freezing behavior requires a presynaptic strengthening of excitatory input onto SOM+ neurons (Li et al., 2013), we wanted to confirm whether the increase in the sEPSC frequency onto CRF- neurons following fear conditioning is also occurring onto SOM+ neurons. Using *SOM-IRES-Cre::Ai14* reporter mice, we found significantly greater average sEPSC frequency onto SOM+ neurons in the CeL following fear conditioning relative to naïve mice (Supplementary Fig. 3). Furthermore, we found that the average sEPSC frequency was significantly reduced following extinction training, while there were no significant changes in average sEPSC amplitude across conditions, suggesting a population of CRF- neurons in this study likely consists of SOM+ neurons (Supplementary Fig. 3).

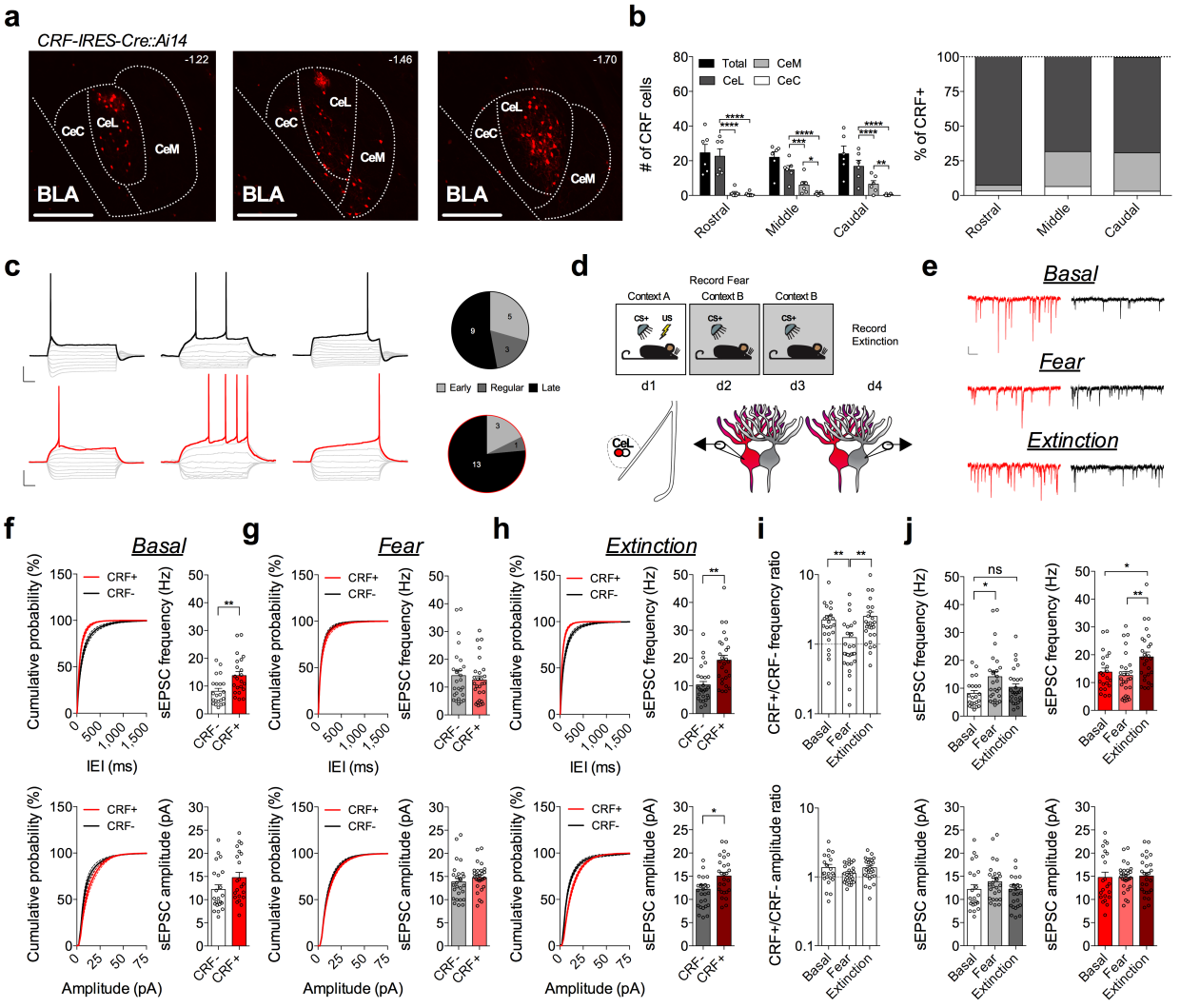

Fig. 1. Fear conditioning and extinction training bidirectionally remodel excitatory input bias onto CRF+ and CRF- CeL neurons. a, Images depicting CRF+ neuronal distribution across the rostrocaudal axis of the CeA (numbers in top right corner depict distance from bregma; scale bars 250µm). **b,** Number and percentage of CRF+ neurons within each subdivision of the CeA along the rostrocaudal axis (n=6 mice; two-way ANOVA, $F(3,15)=31.72$, $P=0.000000974496$ for CeA subdivisions; post-hoc Holm-Sidak's multiple comparisons, Rostral CeL vs. CeM $P=0.000000000016557$, CeL vs. Cec $P=0.00000000000556646$, Middle CeL vs. CeM $P=0.0004$, CeL vs. CeC $P=0.000000157542$, CeM vs. CeC $P=0.0228$, Caudal CeL vs. CeM $P=0.0000160055$, CeL vs. CeM $P=0.00000000467613$, CeM vs. CeC $P=0.0057$). **c,** Left: traces of early, regular, and late firing CRF+ and CRF- neurons. CRF- neuronal traces are depicted with a black outline, and CRF+ with a red outline (scale bars 100ms, and 20mV). Right: total number of early, regular and late firing CRF+ and neighboring CRF- neurons plotted as parts of whole graph (n=17 cells per group, 4 mice). **d,** Experimental paradigm for recording from fear conditioned or fear extinguished mice using alternating patch-clamp technique of neighboring CRF+ and CRF- neurons. **e,** Traces of sEPSC recordings from neighboring CRF+ and CRF- neurons across behavioral conditions (scale bar 100ms, and 10pA). **f,** Cumulative probability

distribution and average sEPSC frequency and amplitude for neighboring CRF+ and CRF- neurons in naïve mice (basal condition) (n=22 cells per group, 5 mice, two-tailed unpaired t-tests, P=0.0031 for sEPSC frequency). **g,** Cumulative probability distribution and average sEPSC frequency and amplitude for neighboring CRF+ and CRF- neurons following fear conditioning (n=27 cells per group, 5 mice, two-tailed unpaired t-tests, not significant). **h,** Cumulative probability distribution and average sEPSC frequency and amplitude for neighboring CRF+ and CRF- neurons following fear extinction (n=27 cells per group, 5 mice, two-tailed unpaired t-tests, P=0.0001 for sEPSC frequency and P=0.0304 for sEPSC amplitude). **i,** CRF+/CRF- frequency and amplitude ratios from neighboring CRF+ and CRF- neurons during sEPSC recordings (log scale; n=22 basal, n=27 fear, n=27 extinction cells for each group; Kruskal-Wallis tests, P=0.0134; post-hoc Dunn's multiple comparisons, basal vs. fear P=0.0049, fear vs. extinction P=0.0011). **j,** Average sEPSC frequency and amplitude for CRF+ neurons or CRF- neurons across behavioral conditions (n=22 basal, n=27 fear, n=27 extinction cells for each group, one-way ANOVAs, F(2,73)=4.295 and P=0.0172 for CRF-, F(2,73)=5.316 and P=0.0070 for CRF+; post-hoc Holm-Sidak's multiple comparisons, CRF- basal vs. fear frequency P=0.0109, CRF- basal vs. extinction frequency ns=not significant, CRF+ basal vs. extinction frequency P=0.0196, CRF+ fear vs. extinction frequency P=0.0057). IEI=inter-event interval, ns=non-significant. Cumulative probability distributions are plotted as mean ± S.E.M., and bar graphs are presented as mean + S.E.M.*P<0.05, **P<0.01, ***P<0.001, ****P<0.0001.

Fear conditioning produces circuit-specific remodeling of relative input strength onto CeL CRF+ and CRF- neurons.

Although our sEPSC recordings demonstrate the presence of experience-dependent shifts in relative excitatory drive to CRF+ and CRF- neurons, they do not provide information regarding which specific afferent inputs may be remodeled during fear acquisition and extinction. We therefore utilized optogenetic projection-targeting approaches to determine which afferent circuits to the CeL may contribute to experience-dependent shifts in relative input strength onto CRF+ and CRF- neurons and the potential expression mechanisms underlying observed circuit-specific plasticity. We bilaterally injected *CRF-IRES-Cre::Ai14* mice with an adeno-associated virus that drives the expression of channel rhodopsin (AAV-CamKIIα-ChR2-eYFP) into three brain regions known to send prominent glutamatergic projections to the CeL, all of which are necessary for intact fear learning (Fig. 2a, Fig. 3a): the BLA, which is responsible for relaying polymodal sensory information to the CeL regarding the CS (Duvarci

and Pare, 2014), the insular cortex (INS), which relays interospective and visceral information to the CeL (Berret et al., 2019; Nieuwenhuys, 2012), and the parabrachial nucleus (PBN), which is a hindbrain projection largely responsible for conveying nociceptive and affective pain signals associated with the US (foot-shock) to the CeL (Han et al., 2017). Whole-cell recordings from CRF+ neurons in the CeL revealed TTX-sensitive fast optically-evoked excitatory post-synaptic currents (oEPSCs) from each afferent input, consistent with action potential dependent monosynaptic responses (Supplementary Fig. 4) (Cai et al., 2014; Han et al., 2015; Tye et al., 2011). Interestingly, CRF+ neurons received significantly greater input from cortical-like descending afferents of the BLA and INS, than ascending input from the PBN, suggesting a greater capacity for top-down than bottom-up regulation of CRF+ cellular excitability (Supplementary Fig. 4).

We next performed simultaneous dual whole-cell patch-clamp recordings from CRF+ and proximally adjacent CRF- neurons from naïve and fear-conditioned mice (Fig. 2a) and examined the relative input strength onto both populations (Supplementary Fig. 5). The power of this approach is that it allows for a measure of bias in the relative input strength by comparing maximal oEPSC amplitude from anatomically-localized neuronal pairs, which controls for differences in light penetration and ChR2 expression between mice. Using this technique, we first sought to determine which afferent inputs could be regulating the overall change in relative glutamatergic neurotransmission onto CRF+ and CRF- neurons following the acquisition of conditioned fear. Notably, the BLA-CeL circuit demonstrated an endogenous input bias characterized by greater relative input strength onto CRF+ neurons compared to CRF- neurons in naïve mice, which was quantified as a significant deviation from 1 in the slope of the linear regression of paired maximal oEPSC amplitude measures, and a high CRF+/CRF- maximal

amplitude ratio (Fig. 2b-d). Importantly, this basal input bias was unaffected by exposure to the conditioning context or the CS+ in the absence of foot-shock (Supplementary Fig. 6). However, following fear conditioning, this input bias shifted away from CRF+ neurons, resulting in equal relative input strength between CRF+ and CRF- neurons (Fig. 2b-d).

In contrast to the to the BLA-CeL circuit, we found that the INS and PBN inputs to the CeL demonstrate a lack of input bias in naïve mice but following fear conditioning demonstrate a shift toward significantly greater relative input strength onto CRF+ neurons (Fig. 2e-l). Interestingly, traumatic stress exposure in the form of over-conditioning reproduced a similar pattern of changes in relative input strength in each of these circuitries as single-day conditioning, supporting the reliability of these observations (Supplementary Fig. 7). Cumulatively, these results indicate that each afferent projection examined dynamically remodels the weight of its synaptic input onto CRF+ and CRF- neurons following fear conditioning, but that plasticity within the BLA-CeL circuit is most closely associated with the overall changes in relative excitatory input between CRF+ and CRF- neurons observed via measurement of sEPSCs (see Fig. 1).

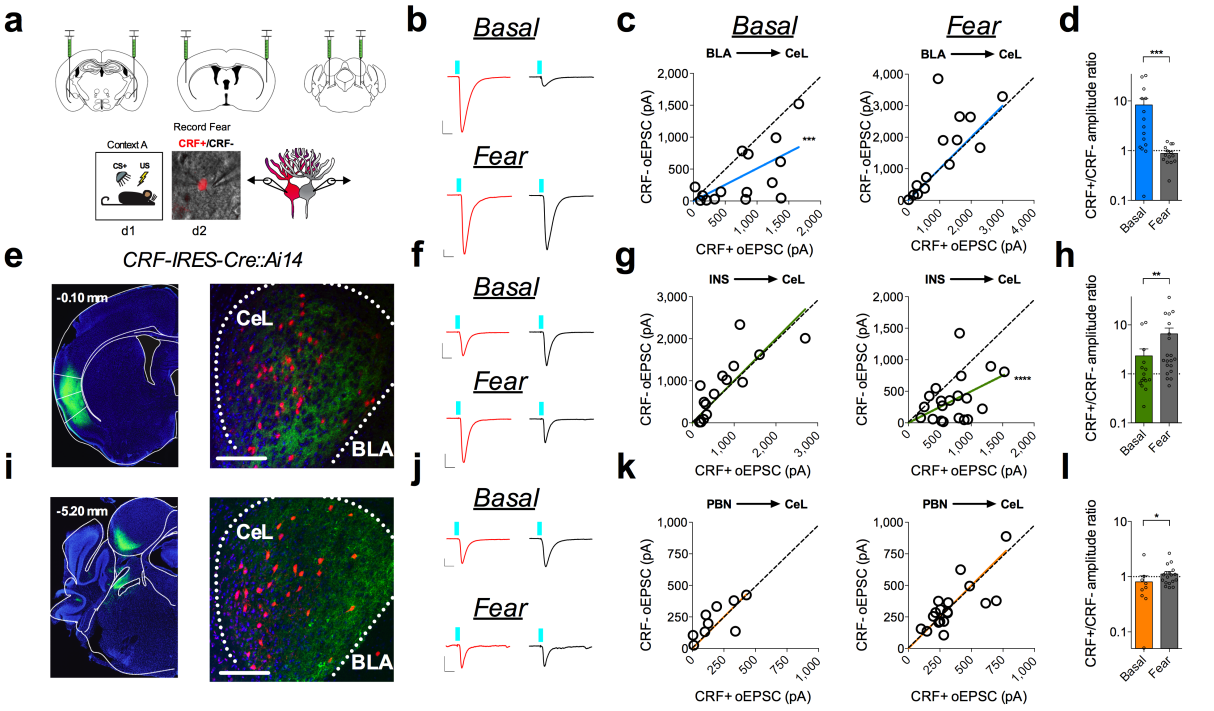

Fig. 2. Fear conditioning remodels circuit specific input bias onto CRF+ and CRF- neurons in the CeL. a, Optogenetic circuit-mapping approach with viral injections into the BLA, INS, and PBN. Bottom-right: DIC and fluorescent overlay of dual-patch clamp recording from CRF+ and CRF- pair. **b,** Traces of maximal oEPSC amplitude from CRF+ (red) and CRF- (black) neuronal pairs across behavioral conditions for stimulation of the BLA-CeL circuit (scale bars 10ms, 200pA). **c,** XY graphs depicting skew-plot of maximal oEPSC amplitude from each CRF+ and CRF- neuronal pair for behavioral conditions (n=15 basal pairs, 5 mice, n=14 fear pairs, 5 mice, extra sum-of-squares F test, F(1,14)=25.61, P=0.0002 for basal). **d,** CRF+/CRF- maximal oEPSC amplitude ratio (log scale; n=15 basal pairs, n=14 fear pairs, Mann-Whitney test, P=0.0005). **e,** Image of ChR2-eYFP expression in the INS (number in top left corner depicts distance from bregma), and eYFP-positive terminals in the CeL (scale bar 150µm). **f,** Traces of maximal oEPSC amplitude from CRF+ (red) and CRF- (black) neuronal pairs across behavioral conditions for stimulation of the INS-CeL circuit (scale bars 10ms, 200pA). **g,** XY graphs depicting skew-plot of maximal oEPSC amplitude from each CRF+ and CRF- neuronal pair for behavioral conditions (n=15 basal, 5 mice, n=20 fear pairs, 5 mice, extra sum-of-squares F test, F(1,19)=28.72, P=0.00003588). **h,** CRF+/CRF- maximal oEPSC amplitude ratio (log scale; n=15 basal pairs, n=20 fear pairs, Mann-Whitney test, P=0.0076). **i,** Image of ChR2-eYFP expression in the PBN (number in top left corner depicts distance from bregma), and eYFP-positive terminals in the CeL (scale bar 150µm). **j,** Traces of maximal oEPSC amplitude from CRF+ (red) and CRF- (black) neuronal pairs across behavioral conditions for stimulation of the PBN-CeL circuit (scale bars 10ms, 100pA). **k,** XY graphs depicting skew-plot of maximal oEPSC amplitude from each CRF+ and CRF- neuronal pair for behavioral conditions (n=9 basal pairs, 5 mice, n=19 fear pairs, 4 mice, extra sum-of-squares F test, not significant). **l,** CRF+/CRF- maximal oEPSC amplitude ratio (log scale; n=9 basal pairs, n=19 fear pairs, Mann-Whitney test, P=0.0196). XY skew-plots are presented as absolute value with line through origin. Bars graphs are presented as mean + S.E.M. *P<0.05, **P<0.01, ***P<0.001, ****P<0.0001.

The BLA-CeL circuit bidirectionally remodels following fear conditioning and extinction training.

Given that the BLA-CeL circuit most closely reflects the global changes in excitatory input bias seen in afferent-indiscriminate neurotransmission following fear conditioning (see Fig. 1), we next tested whether the BLA bias away from CRF+ neurons observed after conditioning normalizes following fear extinction. Fear-conditioned littermate mice were separated into two groups, one group that remained in their home cage for two days, and one group that received two days of extinction training (Fig. 3b), allowing a comparison between time-matched control and experimental groups while simultaneously testing for a persistence of synaptic changes and fear expression following fear memory formation. Importantly, mice that did not undergo extinction training, and remain in their home cage for two days, show elevated freezing behavior to the CS (Supplementary Fig. 2), marking a persistent retention of fear memory. In naïve mice, maximal oEPSC amplitudes from the BLA again showed a significant deviation from a linear regression of 1, indicating a bias in input strength favoring CRF+ neurons (Fig. 3c, d). As shown above, this bias disappeared following fear conditioning but reemerged after extinction training (Fig. 3d), an effect that was mirrored by changes in the CRF+/CRF- oEPSC amplitude ratios (Fig. 3e). These data suggest that the BLA-CeL circuit is bidirectionally remodeled by the acquisition and extinction of conditioned fear to alter relative input strength onto neighboring populations of CRF+ and CRF- neurons across fear states.

Next, we sought to determine whether the BLA-CeL circuit contributes to the presynaptically-mediated alterations in input bias onto CRF+ and CRF- neurons as reflected in our analysis of afferent indiscriminate sEPSCs. Since sEPSC analysis only provides information regarding the net excitation from various inputs, individual input changes may go unnoticed due

to counterbalancing or opposing plasticity changes at other afferents. Therefore, to gain further mechanistic insight as to how the balance of excitatory input strength between CRF+ and CRF- neurons is remodeled by fear acquisition and extinction, we examined BLA-CeL synapses via analysis of strontium-induced asynchronous EPSCs (aEPSCs) using *ex vivo* optogenetics (Fig. 4a-d). The advantage of this method is that it allows for a concurrent assessment of presynaptic and postsynaptic changes within an optogenetically isolated circuit (Biane et al., 2016; Geddes et al., 2016; MacAskill et al., 2014), where optically evoked aEPSC amplitude provides a direct estimate of postsynaptic efficacy, while aEPSC frequency indirectly estimates number of synaptic release sites or release probability (Kaeser and Regehr, 2014; MacAskill et al., 2014; McGarry and Carter, 2017). Using this method, we alternated recordings from closely neighboring pairs of CRF+ and CRF- neurons in the CeL and found that optically evoked aEPSCs from BLA-CeL synapses mirrored the previous experience-dependent changes in input-bias we observed after analysis of maximally evoked oEPSC amplitudes (Fig. 4e-i). Specifically, the CRF+/CRF- aEPSC frequency and amplitude measures were biased towards CRF+ neurons in the naive and fear-extinguished states, relative to the fear-conditioned state (Fig. 4f-i), suggesting the occurrence of both presynaptic and postsynaptic alterations in the BLA-CeL circuit contributing to the bidirectional change in input bias across fear states.

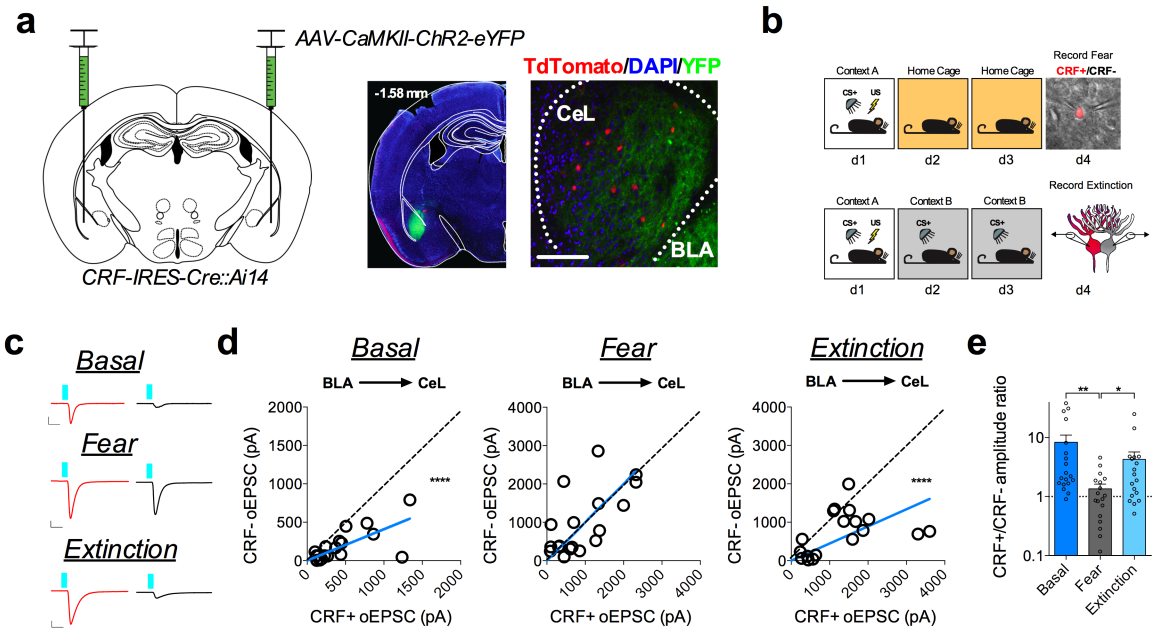

Fig. 3. Fear conditioning and extinction training bidirectionally remodel the BLA-CeL circuit input bias onto CRF+ and CRF- neurons. a, Left: optogenetic circuit mapping approach with viral injection. Right: image of ChR2-eYFP expression in the BLA (number in top left corner depicts distance from bregma) and adjacent eYFP-positive terminals in the CeL (scale bar 150μm). **b,** Experimental paradigm for dual patch-clamp recordings from neighboring CRF+ and CRF- neurons in fear conditioned and fear extinguished mice. Bottom-right: DIC and fluorescent overlay image of dual-patch clamp recording from CRF+ and CRF- pair. **c,** Traces of maximal oEPSC amplitude from CRF+ (red) and CRF- (black) neuronal pairs across behavioral conditions for stimulation of the BLA-CeL circuit (scale bars 10ms, 100pA for basal, and 10ms, 400pA for fear and extinction). **d,** XY graphs depicting skew-plot of maximal oEPSC amplitude from each CRF+ and CRF- neuronal pair for behavioral conditions (n=19 basal pairs, 5 mice, n=18 fear pairs, 5 mice, and n=18 extinction pairs, 5 mice, extra sum-of-squares F test, $F(1,18)=92.68$, $P=0.00000002$ for basal, and $F(1,17)=45.08$, $P=0.00000363$ for extinction). **e,** CRF+/CRF- maximal oEPSC amplitude ratio (log scale; n=19 basal pairs, n=18 fear pairs, and n=18 extinction pairs, Kruskal-Wallis test, $P=0.0021$; post-hoc Dunn's multiple comparisons, basal vs. fear $P=0.0011$, fear vs. extinction $P=0.0442$). XY skew-plots are presented as absolute value with line through origin. Bar graphs are presented as mean + S.E.M. *P<0.05, **P<0.01, ***P<0.001, ****P<0.0001.

Since changes in aEPSC frequency can reflect either alterations in the number of synapses or neurotransmitter release probability, we differentiated between these two possibilities by alternating recordings from neighboring CRF+ and CRF- neurons and independently measuring the paired-pulse ratio (PPR) of BLA-CeL synapses, a measure that is

inversely proportional to release probability (Supplementary Fig. 8). Although previous studies have noted changes in presynaptic release from the lateral amygdala (LA) to other neuronal populations in the CeL following fear conditioning (Li et al., 2013; Penzo et al., 2015), we did not find substantial differences in PPR of BLA-CeL synapses between CRF+ and CRF- neurons following fear conditioning or fear extinction (Supplementary Fig. 8), implying that the bidirectional changes in CRF+/CRF- aEPSC frequency ratios in this paradigm are more likely due to activity-driven adjustments in number of synaptic release sites onto these neurons. However, similarly to our observed changes in aEPSC amplitude ratios across fear states, examination of α-amino-3-hydroxy-5-methyl-4-isoxazoleproprionate receptor (AMPAR)/N-methyl-D-aspartate receptor (NMDAR) ratios further corroborated that post-synaptic modifications also contribute to shifts in relative input bias within the BLA-CeL CRF+/CRF- circuit (Supplementary Fig. 8). Overall, these studies provide converging evidence that the BLA-CeL circuit bidirectionally and dynamically changes its relative connectivity with CRF+ and CRF- neurons based on the animals' experience, with the naïve and fear-extinguished states associated with greater relative input strength onto CRF+ neurons, compared to the fear-conditioned state.

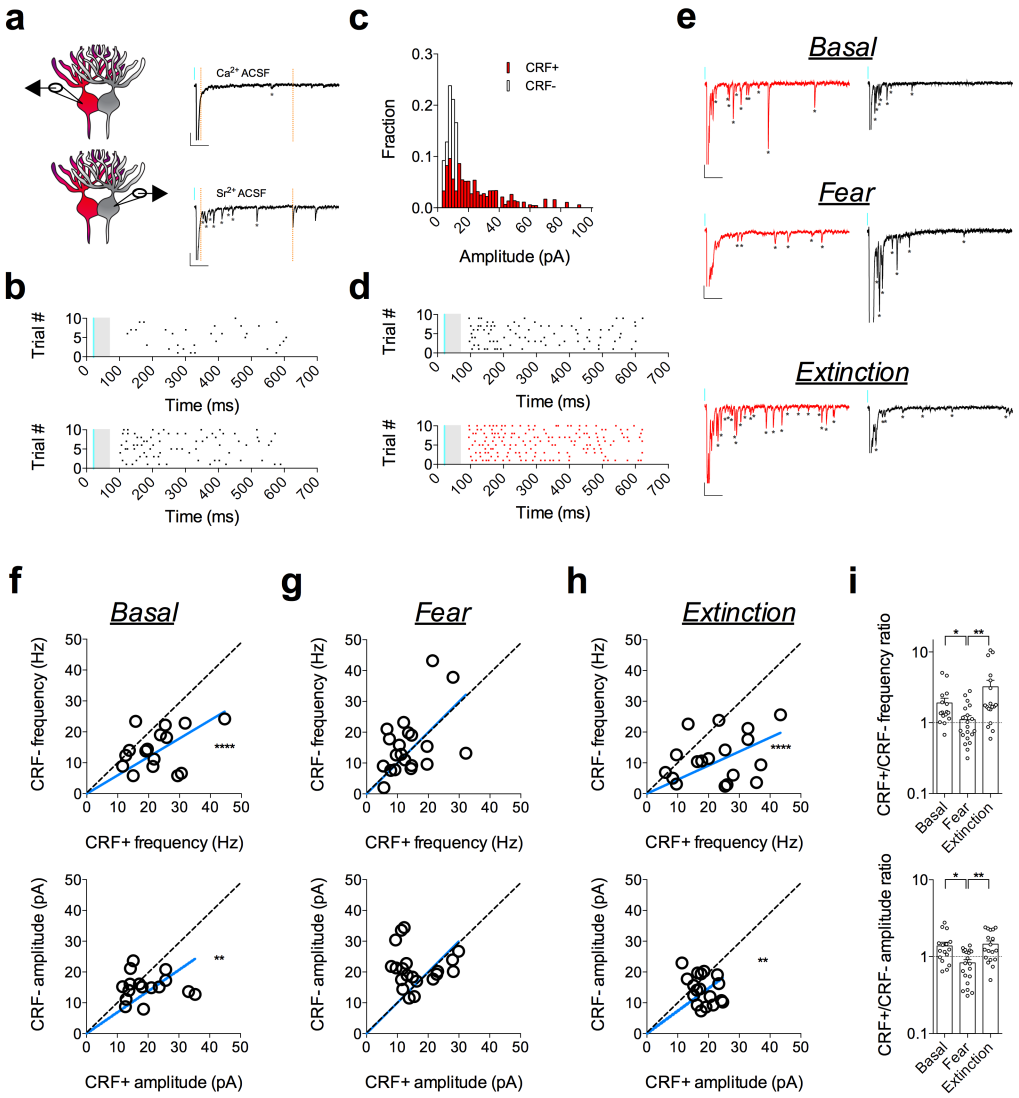

Fig. 4. Experience-dependent circuit remodeling of BLA-CeL input bias is driven by presynaptic and postsynaptic alterations. a, Alternating patch-clamp technique with representative traces from a CeL-cell recorded in the presence of extracellular calcium or strontium (scale bars 100ms, 20pA). **b,** Raster plot of asynchronous events in the presence of extracellular calcium or strontium for the cell depicted in panel a. **c,** Example of amplitude distribution from a recording of neighboring CRF+ and CRF- neurons. **d,** Raster plot of asynchronous events from example in panel c. **e,** Representative traces of strontium induced asynchronous release from neighboring CRF+ and CRF- neurons across conditions (*indicates presence of asynchronous event, scale bars 100ms, 20pA). **f,** XY graphs depicting skew-plot of aEPSC frequency and amplitude for neighboring CRF+ and CRF- neurons in naïve mice (basal condition) (n=16 cells per group, 4 mice, extra sum-of-squares F test, $F(1,15)=33.96$, $P=0.00003329$ for aEPSC frequency, and $F(1,15)=14.48$, $P=0.0017$ for aEPSC amplitude). **g,** XY graphs depicting skew-plot of aEPSC frequency and amplitude for neighboring CRF+ and CRF- neurons in fear conditioned mice (n=20 cells per group, 4 mice). **h,** XY graphs depicting skew-

plot of aEPSC frequency and amplitude for neighboring CRF+ and CRF- neurons in extinction mice (basal condition) (n=18 cells per group, 4 mice, extra sum-of-squares F test, $F(1,17)=54.07$, $P=0.00000113$ for aEPSC frequency, and $F(1,17)=11.02$, $P=0.0041$ for aEPSC amplitude) **i,** CRF+/CRF- frequency and amplitude ratios from neighboring CRF+ and CRF- neurons during aEPSC recordings (log scale; n=16 basal, n=20 fear, n=18 extinction cells for each group; Kruskal-Wallis tests, $P=0.0035$ for frequency and $P=0.0030$ for amplitude; post-hoc Dunn's multiple comparisons, basal vs. fear frequency $P=0.0405$, fear vs. extinction frequency $P=0.0025$, basal vs. fear amplitude $P=0.0112$, fear vs. extinction amplitude $P=0.0049$). XY skew-plots are presented as absolute value with line through origin. Bars graphs are presented as mean + S.E.M. *P<0.05, **P<0.01, ****P<0.0001.

Given that fear conditioning enhances excitatory plasticity onto CeL SOM+ neurons, we next sought to test whether the bidirectional shifts in relative input strength in the BLA-CeL circuit are reflected between populations of CRF+ and SOM+ neurons. To explicitly test this, we crossed CRF-IRES-Cre mice with SOM-IRES-Flp mice to gain genetic access to these distinct neuronal populations within the same animals, and co-injected Cre-dependent mCherry (AAV-hSyn-DIO-mCherry) and Flp-dependent YFP (AAV-EF1a-fDIO-YFP) into the CeA to label CRF+ and SOM+ neurons, respectively (Supplementary Fig. 1). The overall quantity of neurons co-expressing mCherry and YFP was low, with an average of 0.125, 1, and 2 neurons co-labeled in the rostral, middle, and caudal CeL respectively (Supplementary Fig. 1). We then used the same labeling approach along with injection of ChR2-eYFP into the BLA, and performed dual whole-cell patch-clamp recordings from identified CRF+ and SOM+ neurons while stimulating the BLA-CeL circuit. Using this technique, we discovered the same bidirectional changes in input bias as we did for CRF+ and CRF- neurons, again suggesting that many of the CRF- neurons used in our previous analysis are likely SOM+ cells (Supplementary Fig. 9). However, despite the total number of cells co-expressing these peptides being low, the possibility remains that inadvertent inclusion of CRF+/SOM+ neurons could affect the interpretability of electrophysiological results. We therefore determined changes in input bias in the BLA-CeL

circuit between CRF+/SOM+ and CRF-/SOM- synapses. Interestingly, we found that CRF+/SOM+ and CRF-/SOM- neuron pairs showed input bias and ratiometric changes following fear conditioning and extinction training that is most consistent with that of CRF+ and CRF- pairs (Supplementary Fig. 10). Thus, our data suggests that neurons expressing both CRF and SOM are more similar to neurons that only express CRF, at least in terms of their circuit-specific experience-dependent plasticity.

BLA-CeL circuit remodeling onto CRF+ and CRF- neurons is activity-dependent.

We next examined whether activity of the BLA is necessary for fear-conditioning-induced synaptic remodeling of BLA-CeL synapses onto CRF+/CRF- neurons. To test this, we used a chemogenetic method involving the use of designer receptors exclusively activated by designer drugs (DREADDs) (Armbruster et al., 2007). *CRF-IRES-Cre::Ai14* mice were bilaterally co-injected into the BLA with AAV-CamKIIα-ChR2-eYFP and the inhibitory Gαi-coupled DREADD (AAV-CamKIIα-hM4Di-mCherry), and subsequently administered VEH or the designer drug clozapine-*N*-oxide (CNO) prior to conditioning (Fig. 5a-c). Importantly, bath application of CNO in these mice depressed oEPSC amplitude from the BLA projection onto CeL neurons, suggesting this approach can inhibit neurotransmitter release and decrease the signaling fidelity of the BLA-CeL circuit (Fig. 5b). Consistent with our previous experiments, dual patch-clamp recordings yielded the same basal input bias from the BLA-CeL circuit onto CRF+ neurons and a high CRF+/CRF- amplitude ratio, which disappeared following fear-conditioning in VEH-treated mice (Fig. 5d-f). However, these changes in input strength following fear-conditioning were absent in CNO-treated animals (Fig. 5d-f), indicating that activity within principal BLA neurons during fear conditioning is necessary for driving the

relative shifts in BLA-CeL input strength away from CRF+ neurons. Similarly, we administered VEH or CNO prior to extinction training in a separate cohort of mice (Fig. 5g). We found that inhibiting the BLA prior to both days of extinction training blocked the shift in input bias back towards CRF+ neurons (Fig. 5h-j). Overall, these findings demonstrate that BLA activity is necessary for the bidirectional shifts in input bias onto CRF+ and CRF- neurons that occurs with the acquisition and extinction of conditioned fear. Importantly, mice given CNO that expressed mCherry instead of the Gαi-coupled DREADD in the BLA did not demonstrate differences in input bias from VEH treated mice, indicating CNO alone does not affect BLA-CeL circuit remodeling (Supplementary Fig. 11).

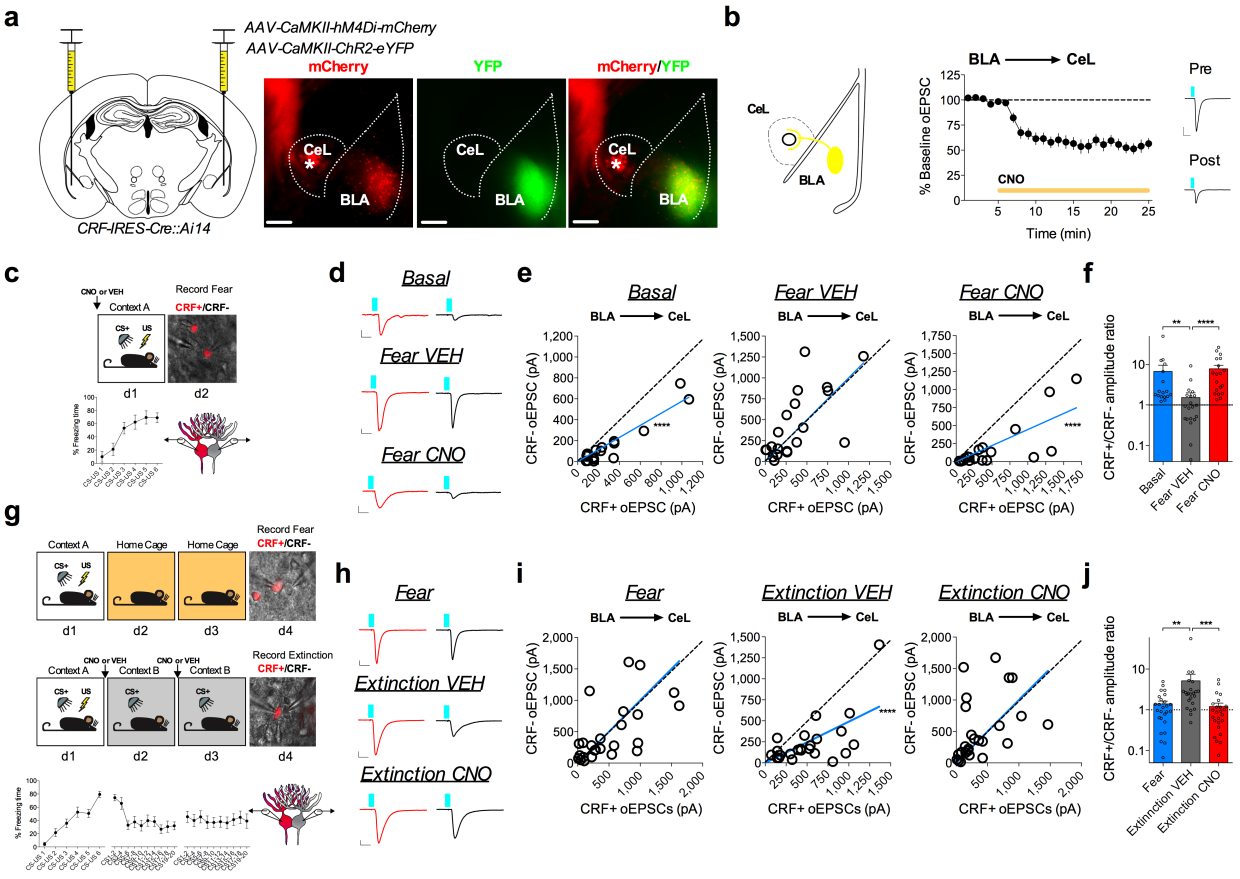

Figure 5. Activity of the BLA is necessary for remodeling input bias onto CRF+ and CRF- neurons. a, Left: mixed viral injection strategy for electrophysiological assessment of inhibiting the BLA-CeL circuit. Right: image of ChR2-eYFP and hM4D(Gi)-mCherry expression in the BLA from a coronal slice used for recordings (*indicates CRF+ neurons in the CeL expressing TdTomato; scale bars 200µm). **b,** Summary data from bath application of CNO while recording oEPSC amplitude in the CeL (see methods; n=13 cells, 5 mice). Top-left: depiction of co-infected ChR2-eYFP and hM4D(Gi)-mCherry projection of the BLA-CeL. Right: traces of oEPSCs before and after bath application of CNO (scale bar 10ms, and 200pA). **c,** Experimental paradigm of electrophysiological assessment of inhibiting the BLA prior to fear conditioning. Right: DIC and fluorescent overlay image of dual-patch clamp recording from CRF+ and CRF- pair. Bottom: learning curve. **d,** Traces of maximal oEPSC amplitude from CRF+ (red) and CRF- (black) neuronal pairs across treatment groups for stimulation of the BLA-CeL circuit (scale bars 10ms, and 50pA). **e,** XY graphs depicting skew-plot of maximal oEPSC amplitude from each CRF+ and CRF- neuronal pair for behavioral conditions (n=17 basal pairs, 5 mice, n=20 fear VEH pairs, 5 mice, and n=19 fear CNO pairs, 5 mice, extra sum-of-squares F test, $F(1,16)=105.5$, $P=0.00000002$ for basal, $F(1,18)=65.60$, $P=0.00000021$ for fear CNO). **f,** CRF+/CRF- maximal oEPSC amplitude ratio (log scale; n=17 basal pairs, n=20 fear VEH pairs, and n=19 fear CNO pairs, Kruskal-Wallis test, $P=0.00002$; post-hoc Dunn's multiple comparisons, basal vs. fear VEH $P=0.0048$, fear VEH vs. fear CNO $P<0.0001$). **g,** Experimental paradigm of electrophysiological assessment of inhibiting the BLA prior to fear extinction. **h,** Traces of maximal oEPSC amplitude from CRF+ (red) and CRF- (black) neuronal pairs across

treatment groups for stimulation of the BLA-CeL circuit (scale bars 10ms, and 100pA). Bottom: learning curves. **i,** XY graphs depicting skew-plot of maximal oEPSC amplitude from each CRF+ and CRF- neuronal pair for behavioral conditions (n=26 fear pairs, 4 mice, n=23 extinction VEH pairs, 5 mice, and n=25 extinction CNO pairs, 5 mice, extra sum-of-squares F test, $F(1,22)=46.26$, $P=0.00000078$). **j,** CRF+/CRF- maximal oEPSC amplitude ratio (log scale; n=26 fear pairs, n=23 extinction VEH pairs, and n=25 extinction CNO pairs, Kruskal-Wallis test, $P=0.0002$; post-hoc Dunn's multiple comparisons, fear vs. extinction VEH $P=0.0035$, extinction VEH vs. extinction CNO $P=0.0002$). XY skew-plots are presented as absolute value with line through origin and bar graphs are presented as mean + S.E.M. *P<0.05, **P<0.01, ***P<0.001, ****P<0.0001.

The BLA-CeL circuit is necessary for fear memory acquisition and the retrieval of extinction memory.

Because the BLA-CeL circuit remodels input to CeL neurons across fear states in an activity-dependent manner, we next tested the potential relevance of this circuit remodeling to the acquisition and extinction of conditioned fear. Whole BLA inhibition has been shown to differentially affect fear behavior compared to directed manipulations of distinct BLA projection neurons (Anglada-Figueroa and Quirk, 2005; Namburi et al., 2015; Tipps et al., 2018). Therefore, to selectively inhibit the BLA-CeL circuit, we used an intersectional genetic strategy in which we bilaterally injected the CeA with a retrograde virus that drives the expression of the cre-recombinase enzyme (AAVrg-Cre) (Tervo et al., 2016), and in the same mice bilaterally injected the BLA with a virus that drives the expression of the inhibitory Gαi-coupled DREADD in a cre-dependent manner (AAV-hSyn-DIO-hM4Di-mCherry) (Fig. 6a). Mice injected with CNO prior to conditioning had significantly diminished freezing relative to VEH-treated mice in response to CS presentation the following day (Fig. 6b,c), indicating that the activity of BLA-CeL projection neurons critically contributes to the acquisition of fear memories as assessed by memory recall the following day, without affecting freezing during conditioning. In separate mice injected with CNO prior to extinction training sessions, we did not find differences in

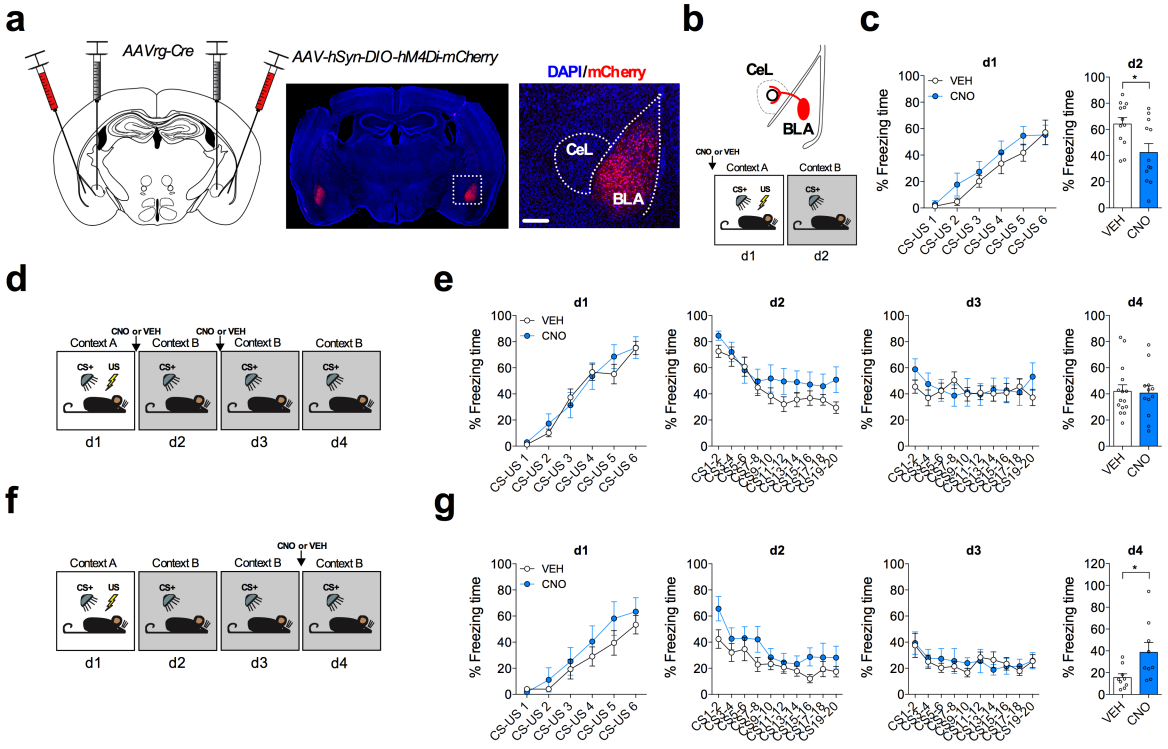

Fig. 6. The BLA-CeL circuit is critical for both the acquisition of fear memory and the retrieval of extinction memory. a, Left: intersectional viral strategy for behavioral assessment of inhibiting the BLA-CeL circuit. Right: images depicting bilateral expression of cre-dependent hM4D(Gi)-mCherry in the BLA with close up of inset (scale bar 200µm). **b,** Experimental paradigm for behavioral assessment of inhibiting the BLA-CeL circuit during fear conditioning. Top: schematic of hM4D(Gi)-mCherry expression specifically in BLA neurons projecting to the CeL. **c,** Learning curve for VEH or CNO treated mice during fear acquisition on day 1 (d1), and fear memory recall on day 2 (d2), after VEH or CNO injection prior to fear conditioning (d1) (n=12 mice per group, two-tailed unpaired t-test, P=0.0172). **d,** Experimental paradigm for behavioral assessment of inhibiting the BLA-CeL circuit during extinction training. **e,** Learning curves for VEH and CNO treated mice. Left to right, conditioning day 1 (d1), extinction session 1 on day 2 (d2), extinction session 2 on day 3 (d3), and extinction memory recall test on day 4 (d4) (n=15 mice for VEH, and n=12 mice for CNO).**f,** Experimental paradigm for behavioral assessment of inhibiting the BLA-CeL circuit during an extinction memory recall test. **g,** Learning curves for VEH and CNO treated mice. Left to right, conditioning day 1 (d1), extinction session 1 on day 2 (d2), extinction session 2 on day 3 (d3), and extinction memory recall test on day 4 (d4) (n=9 mice for VEH, and n=9 mice for CNO, two-tailed unpaired t-test, P=0.0293).Learning curves are presented as mean ± S.E.M. and bar graphs are presented as mean + S.E.M. *P<0.05.

within-session conditioned freezing responses or freezing responses during an extinction memory recall test the following day (Fig. 6d,e), suggesting that the activity of the BLA-CeL

circuit is not necessary for within-session extinction or the acquisition of extinction memory. However, since the BLA-CeL circuit remodels in favor of greater relative input strength onto CRF+ neurons after extinction training, it is possible that CRF+ neurons may negatively regulate fear responses, and that the BLA-CeL circuit may instead be important for regulating the expression of extinction memories after training and synaptic remodeling has occurred. Consistent with this possibility, we found that decreasing the excitability of the BLA-CeL circuit with CNO during an extinction memory recall test, at a time point in which the circuit input bias has shifted back towards favoring CRF+ neurons, caused a significantly greater level of freezing compared to VEH-treated controls, suggesting the BLA-CeL circuit is also important for the retrieval of extinction memory (Fig. 6 f,g).

CRF+ neuron activity is sufficient to impair fear memory acquisition and facilitate within session extinction, and is necessary for extinction memory retrieval.

CeA CRF+ neurons have been shown to form mutually inhibitory synapses with SOM+ neurons, a circuit motif that may allow for rapid selection of divergent threat-adaptive motor responses via a mechanism of competitive lateral inhibition (Fadok et al., 2017). Given our data demonstrating that CRF+ neurons receive greater relative BLA excitatory input under basal and fear-extinguished conditions than CRF-/SOM+ neurons, and SOM+ neurons drive freezing responses (Fadok et al., 2017; Li et al., 2013; Penzo et al., 2015), it is possible that CRF+ neuronal activity may serve to reduce freezing behavior. To test this idea, and probe the functional role of CeA-CRF+ neurons in regulating fear behavior, CRF-IRES-Cre mice were bilaterally injected into the CeA with a cre-dependent excitatory Gαq-coupled DREADD tagged with a mCherry fluorescent protein (AAV-hSyn-DIO-hM3Dq-mCherry, Fig. 7a). Using this

method, we selectively increased the excitability of CRF+ neurons via the application of CNO. Importantly, we found that bath application of CNO, while recording from mCherry+ neurons in the CeL, produced a significant depolarization of the resting membrane potential (Fig. 7b), and that systemic injection of CNO increased the expression of the immediate early gene Fos in mCherry+ neurons, a commonly used marker for cellular activity (Supplementary Fig. 13).

Next, we increased the excitability of CRF+ neurons by injecting CNO or VEH prior to fear conditioning, at a time point when the relative input bias of the CeL network favors CRF+ neurons, but when a shift in relative input away from CRF+ neurons would be expected to be initiated (Fig. 7c,d). Animals injected with CNO had lower freezing to the CS than VEH-treated animals during fear memory recall the following day, without differences in within-session freezing during conditioning, suggesting impaired fear memory acquisition. Moreover, increasing the excitability of CRF+ neurons during extinction training, at a time point when relative input bias has already shifted away from CRF+ neurons towards equal input onto CRF+ and CRF- neurons, caused a significant reduction in within-session freezing behavior (Fig. 7f,g). However, enhancement of CRF+ neuron activity did not affect the initial retrieval of fear memory (freezing during the first 2 CS presentations on d2), suggesting that activity of CRF+ neurons promotes within-session extinction rather than simply gating the expression of freezing responses. Additionally, enhancing the excitability of CRF+ neurons did not affect the speed of the same mice when they were presented with the CS, or cause signatures of CRF-mediated plasticity within the CeL, indicating that activity of CRF+ neurons does not induce escape or flight-like responses in this paradigm, and that our rapid behavioral effects may not be due to local CRF release within the CeL (Supplementary Fig. 12). Overall, these data reveal that CeA-CRF+ neuron activity is sufficient to diminish passive fear expression and enhance within-

session extinction, an effect consistent with the relatively greater excitatory input from the BLA onto these cells in low fear states.

We further addressed the necessity of CRF+ neurons for the extinction of conditioned freezing by bilaterally expressing a cre-dependent inhibitory Gαi-coupled DREADD (AAV-hSyn-DIO-hM4Di-mCherry) in the CeA of our CRF-IRES-Cre mice (Fig. 7h). As expected, we found that bath application of CNO, while recording from mCherry+ neurons in the CeL, produced a significant hyperpolarization of the resting membrane potential, resulting in the complete blockade of action potential firing in CRF+ neurons (Fig. 7i). We then injected CNO or VEH prior to extinction training sessions and found that decreasing the excitability of CRF+ neurons, at a time-point where the relative excitatory input bias onto CRF+ and CRF- neurons is equal, did not prevent within-session extinction or extinction memory recall (Fig. 7j,k). However, our whole-cell recordings indicate that relative excitatory input bias shifts back onto CRF+ neurons following two days of extinction training (i.e. day 4, Fig. 7c), suggesting that CRF+ neurons may be important for the subsequent retrieval, rather than acquisition, of extinction memory *per se*. To test this hypothesis, we injected a separate cohort of mice with CNO or VEH prior to an extinction memory recall session (Fig. 7l). Consistent with this hypothesis, decreasing CRF+ neuronal activity at a time point at which CRF+ neurons receive greater excitatory input caused a significantly greater level of freezing relative to VEH treatment (Fig. 5l,m), revealing the necessity of CeL CRF+ neurons for full extinction memory retrieval. Importantly, CNO administration in wild-type or mCherry-only expressing mice at each of the time points examined for DREADD manipulations did not affect freezing levels, indicating our results were not due to off-target actions of CNO (Supplementary Fig. 13) (Gomez et al., 2017).

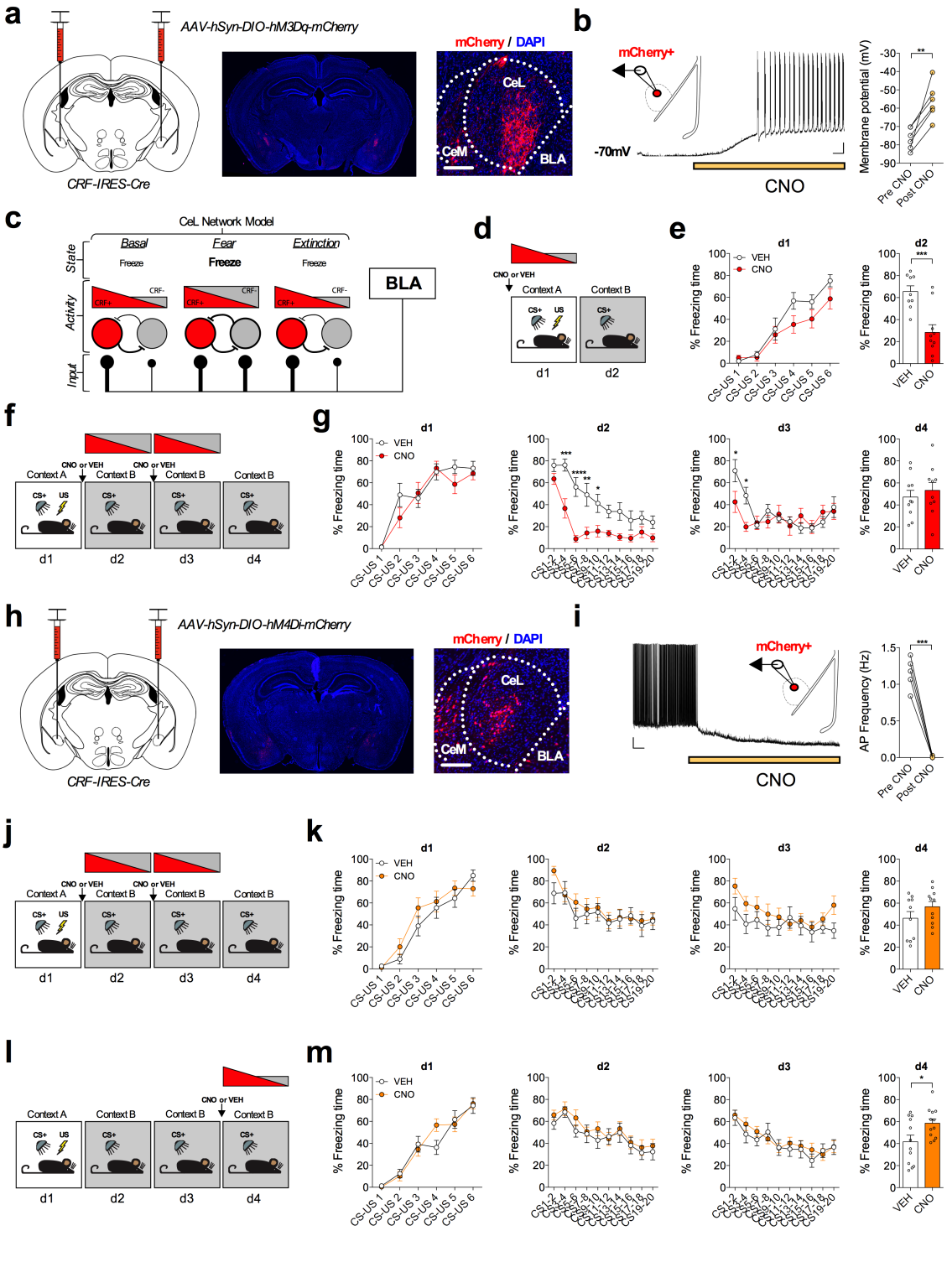

Fig. 7. CRF+ neuron activity impairs fear memory acquisition, facilitates within session extinction, and is necessary for extinction retrieval. a, Left: injection strategy for cre-dependent hM3D(Gq)-mCherry expression in CRF+ neurons of the CeA. Right: images depicting bilateral targeting of hM3D(Gq)-mCherry to CRF neurons in the CeA with

magnification demonstrating mCherry fluorescence (scale bar 200μm). **b,** Patch-clamp recording from mCherry+ neurons in the CeL with representative trace of CNO bath application causing depolarization to action potential threshold in mCherry+ neuron (scale bar 0.5min, and 10mV). Right: Summary of change in resting membrane potential following bath application of CNO (n=6 cells, 3 mice, two-tailed paired t-test, P=0.0046). **c,** Tiered hypothetical model for the CeL network reflecting input bias from the BLA-CeL circuit and expected cellular activity level when the BLA is recruited. **d,** Experimental paradigm for enhancing excitability of CeA-CRF+ neurons during fear conditioning with input bias depicted at time of injection. **e,** Learning curves for VEH and CNO treated mice. Left to right, conditioning day 1 (d1), fear memory recall test on day 2 (d2) (n=9 VEH mice, and n=10 CNO mice, two-tailed unpaired t-test, P=0.0006). Learning curves are presented as mean ± S.E.M., and bar graphs are presented as mean + S.E.M. ***P<0.001. **f,** Experimental paradigm for enhancing excitability of CeA-CRF+ neurons during extinction training with current activity bias depicted at time of injection. **g,** Learning curves for VEH and CNO treated mice. Left to right, conditioning day 1 (d1), extinction session 1 on day 2 (d2), extinction session 2 on day 3 (d3), and extinction memory recall test on day 4 (d4) (n=10 mice per group, two-way repeated measures ANOVA, F(1,18)=20.19, P=0.0003 for effect of treatment; post-hoc Holm-Sidak's multiple comparisons, d1 CS3-4 P=0.0001, CS5-6 P=0.000000317409, CS7-8 P=0.0011, CS910 P=0.0335, d2 CS1-2 P=0.0272, CS3-4 P=0.0272). **h,** Left: injection strategy for cre-dependent hM4D(Gi)-mCherry expression in CRF+ neurons of the CeA. Right: images depicting bilateral targeting of hM4D(Gi)-mCherry to CRF neurons in the CeA with magnification demonstrating mCherry fluorescence (scale bar 200μm). **i,** Patch-clamp recording from mCherry+ neurons in the CeL with representative trace of CNO bath application causing hyperpolarization and reduction in action potential frequency (scale bar 0.5min, and 10mV). Right: Summary of change in action potential frequency following bath application of CNO (n=5 cells, 3 mice, two-tailed paired t-test, P=0.0003). **j,** Experimental paradigm for decreasing excitability of CeA-CRF+ neurons during extinction training with input bias depicted at time of injection. **k,** Learning curves for VEH and CNO treated mice. Left to right, conditioning day 1 (d1), extinction session 1 on day 2 (d2), extinction session 2 on day 3 (d3), and extinction memory recall test on day 4 (d4) (n=10 VEH mice, and n=11 CNO mice). **l,** Experimental paradigm for decreasing excitability of CeA-CRF+ neurons during an extinction memory recall test with input bias depicted at time of injection. **m,** Learning curves for VEH and CNO treated mice. Left to right, conditioning day 1 (d1), extinction session 1 on day 2 (d2), extinction session 2 on day 3 (d3), and extinction memory recall test on day 4 (d4) (n=12 mice per group, two-tailed unpaired t-test, P=0.0291). Learning curves are presented as mean ± S.E.M., and bar graphs are presented as mean + S.E.M. *P<0.05, **P<0.01, ***P<0.001, ****P<0.0001.

Anatomical substrates subserving divergent roles of CeA CRF+ and SOM+ neurons.

Cumulatively, our findings and those of previous studies suggest CRF+ and SOM+ neurons are important for passive fear inhibition and expression, respectively (Dedic et al., 2018; Gafford et al., 2014; Li et al., 2013). Given the functional differences in these cell-types, we next

explored differences in the output circuitry of these neurons, which could inform upon their divergent behavioral roles. Whole-brain optogenetic output mapping revealed a large number of convergent brain structures between these classes of CeA neurons, as well as a number of divergent brain structures in which CRF+ and SOM+ neurons differentially project (Supplementary Fig. 14-16). Considering the periaqueductal gray (PAG) and the CeA are brain regions that are indispensable for the expression of defensive fear behaviors (Evans et al., 2018; Tovote et al., 2016), we examined the degrees of connectivity within sub-regions of these nuclei from CRF+ and SOM+ neurons. Notably, whole-cell recordings in the CeL and PAG demonstrated optically evoked inhibitory postsynaptic currents (oIPSCs) that were blocked by application of the $GABA_A$ receptor antagonist picrotoxin, consistent with both local and long-range projections of SOM+ and CRF+ neurons signaling through GABAergic neurotransmission (Supplementary Fig. 16). Furthermore, SOM+ efferent projections terminate in the ventral/ventrolateral PAG (v/vlPAG) with a smaller degree of terminals also present in the dorsal/dorsolateral PAG (d/dlPAG), whereas CRF+ efferent projections primarily terminate in the v/vlPAG (Supplementary Fig. 14,16). The distribution of terminals in this region corresponded to the percentage of responsive neurons, where 35.3% of v/vlPAG neurons and 9.1% of d/dlPAG neurons were reliably responsive to ChR2 terminal stimulation from SOM+ neurons. However, we found that only 11.1% of v/vlPAG neurons and 0% of d/dlPAG neurons were reliably responsive to ChR2 terminal stimulation from CRF+ neurons, suggesting that CeA-CRF+ neurons have less connectivity with the v/vlPAG than SOM+ neurons, and that CRF+ neurons lack functional synaptic projections to the d/dlPAG. These results indicate that each neuronal population may differentially affect motor output from the PAG in cooperation with

signals from other upstream brain structures. A similar connectivity pattern was seen for CRF+ neuronal output to brain regions with high or low terminal expression (Supplementary Fig. 17).

Discussion

The acquisition of conditioned fear responses is essential to survival, allowing organisms to properly assess and avoid harm when re-exposed to threat-predictive stimuli in the environment. Conversely, learning to suppress and diminish conditioned fear responses when a CS no longer signals immediate danger is also essential. Indeed, impairments in extinction learning are a phenotypic hallmark of posttraumatic stress disorder (Pitman et al., 2012). Although significant advances have been made in understanding cellular substrates for fear learning within the amygdala, how top-down or bottom-up excitatory signals are modified by previous experience to influence CeA neuronal output to initiate or suppress fear responses is incompletely understood. Here we show that acquisition of conditioned fear memories is associated with an activity-dependent shift in BLA glutamatergic input bias away from CRF+ CeL neurons while extinction training is associated with a normalization of input bias back toward favoring CRF+ neurons. Interestingly, changes in overall spontaneous glutamatergic neurotransmission in the CeL demonstrated these same shifts in relative input bias regardless of the afferent source, although dynamic and opposing shifts in the INS-CeL and PBN-CeL circuits remodel in favor of input onto CRF+ neurons and may appear to counterbalance mechanisms of postsynaptic or presynaptic alterations from the BLA-CeL circuit. Thus, future studies are needed in examining the behavioral consequences and relevance of impaired network remodeling from afferent sources other than the BLA.

We also found that reducing neuronal activity within the BLA during conditioning prevents the relative shift in input bias away from CRF+ cells, while specifically decreasing signaling of the BLA-CeL circuit reduces fear memory acquisition as assessed by next-day recall, without affecting freezing behavior during conditioning. Although our plasticity experiments were restricted to global manipulations of all BLA projection neurons, these data provide indirect but converging evidence that activity-dependent remodeling of the BLA-CeL circuit away from CRF+ neurons may be a physiological correlate for fear memory acquisition. Additionally, previous work has demonstrated that inhibition of the BLA-CeM circuit reduces within-session freezing during conditioning but not fear memory recall the following day (Namburi et al., 2015), suggesting that BLA neurons that project distinctly to the CeM and CeL may play separate but complimentary roles in driving defensive freezing responses during initial threat exposure versus the future behavioral selection of these responses following associative learning, respectively. In contrast, inhibition of the BLA-CeL circuit during extinction training in our studies did not impair extinction learning or the acquisition of extinction memory as assessed by within-session freezing during extinction training or during extinction memory recall the following day, although our reductions in BLA activity during extinction training did prevent extinction-induced synaptic remodeling. Together, these results suggest that compensatory circuits are still able to support fear extinction in the face of compromised BLA-CeL remodeling. However, BLA-CeL circuit remodeling is likely still an important correlate for suppressing fear memories following extinction learning because, once relative input bias has shifted back toward CRF+ neurons (i.e. on day 4), inhibition of the BLA-CeL circuit, or inhibition of CRF+ neurons downstream of the BLA, impairs extinction memory retrieval, suggesting compensatory circuits cannot override a lack of function in this circuit after proper remodeling has already taken place.

Our data also support a novel role for CeL CRF+ neuron activity in the context of fear acquisition and extinction. Specifically, while activation of CRF+ neurons is sufficient to impair fear memory acquisition (as assessed during next-day memory recall), and facilitate within-session extinction, CRF+ neuron activity is only necessary for the retrieval, rather than the acquisition, of extinction memory. These data are consistent with the relative input bias of the BLA-CeL circuit favoring CRF+ neurons after extinction training and our data indicating BLA-CeL circuit inhibition impairs extinction retrieval but not within session extinction of conditioned freezing. These findings provide insight into how experience-dependent plasticity at BLA-CeL synapses may instruct behavioral selection across fear states via dynamic changes in excitatory drive to distinct CeL neuronal subpopulations.

A key finding of the present work is that CeL CRF+ neurons receive greater excitatory synaptic input under basal and fear-extinguished conditions relative to their CRF-lacking counterparts, while CRF- neurons receive enhanced excitatory drive after fear conditioning. It is likely at least a subpopulation of CRF- neurons in this study are SOM+ neurons, which have been shown to be essential in producing conditioned and unconditioned freezing behavior (Fadok et al., 2017; Li et al., 2013; Penzo et al., 2015). Consistent with this possibility, we found bidirectional enhancement and reduction of excitatory neurotransmission onto SOM+ neurons following fear conditioning and extinction training that closely mirrored that of CRF- neurons, and shifts in input bias that favored excitatory drive onto CRF+ neurons over SOM+ neurons in basal and fear-extinguished states. That ectopic activation of CeA CRF+ neurons reduces conditioned freezing further supports the notion CRF+ and SOM+ neurons generate antagonistic behavioral responses to threat-predictive cues (Fadok et al., 2017; Yu et al., 2016). Consistent with this, we found evidence that SOM+ neurons demonstrate a greater degree of synaptic

connectivity to the PAG than that of CRF+ neurons, with functional inputs to both the v/vlPAG and d/dlPAG, whereas CRF+ neurons only form functional input to the v/vlPAG. Given that both CRF+ and SOM+ neurons are GABAergic, differences in connectivity and signaling fidelity to converging brain structures or distinct projections to diverging brain structures may represent a neural substrate for the antagonistic effects of CRF+ and SOM+ neurons on freezing behavior, and require further investigation.

Temporally precise control of CRF+ neuronal activity using *in vivo* optogenetics has shown that CRF+ neurons drive active motor responses, involving escape and conditioned flight behavior to CSs, which is primarily driven by strong inhibitory control over SOM+ neurons (Fadok et al., 2017). Therefore, it appears CRF+ neurons may use fast GABAergic neurotransmission and lateral inhibition of SOM+ neurons to trigger active phenotypes, whereas CRF peptide release from these cells has been implicated in generating passive freezing responses via the enhancement of synaptic neurotransmission onto CRF1 receptor expressing neurons in the CeA (of which a large proportion are SOM+; Supplementary Fig. 18)[13]. In line with this idea, neuropeptides are often only released from dense core vesicles following bouts of prolonged neural activity or high firing rates, and signal through G-protein coupled receptors, which generally have a slower influence on membrane excitability than fast neurotransmission (van den Pol, 2012). As a parallel to this idea, SOM signaling in the amygdala has been shown to decrease anxiety and fear expression (Kahl and Fendt, 2014; Yeung et al., 2011; Yeung and Treit, 2012), suggesting SOM+ neurons may utilize fast neurotransmission to drive freezing responses, but SOM release may serve as a homeostatic feedback mechanism for preventing fear generalization and maladaptive fear expression over time. Future studies should aim at

investigating the interplay and differences between the use of fast neurotransmission and neuropeptide signaling within genetically defined cell populations in the CeL.

Of note, the relative input strength between CRF+ and CRF-/SOM+ neurons is approximately equal following fear conditioning. Consequently, our findings emphasize that the balance of relative BLA input to distinct CeL cell-types may be more informative for assessing experience-dependent learning within this system than changes in the absolute input-magnitude onto a single cell-type. It has been previously suggested that the BLA is responsible for switching between states of high and low fear expression and that separate BLA "fear-on" and "fear-off" neurons contribute to fear expression and extinction, respectively (Herry et al., 2008; McCullough et al., 2016). These findings raise the possibility that changes in relative excitatory drive to CRF+ and CRF- neurons after fear conditioning and extinction training could be driven by inputs from distinct BLA cell populations. For example, "fear-on" neurons within the BLA may preferentially signal to CRF-/SOM+ neurons and undergo activity-dependent bidirectional remodeling after acquisition and extinction of conditioned freezing, whereas "fear-off" neurons may preferentially recruit CRF+ neurons during extinction learning. Future studies will be required to experimentally test this intriguing hypothesis.

In light of the diverse behavioral responses CRF+ neurons can influence, we propose a model in which these neurons regulate an animal's motor output by promoting active motivational responses. In naive mice, activity of these neurons would stimulate motor output to influence the expression of active responses associated with appetitive drive (Kim et al., 2017), such as foraging or surveying the environment for resources (Supplementary Fig. 18). Alternatively, under conditions of imminent threat activity of these neurons can promote active motor behavior relevant to the animal's internal state and context, such as escape or flight-like

responses (Evans et al., 2018; Fadok et al., 2017), whereas under conditions of safety or subsiding fear, the activity of CRF+ neurons will prompt active exploration (Kim et al., 2017). Thus, as the contingency between the CS and US degrades during extinction training, greater relative input is restored back onto CRF+ neurons to diminish passive freezing responses and promote active exploration of the environment (Supplementary Fig. 18).

During exposure to a threat, an animal's survival depends on rapidly assessing environmental cues and mounting appropriate freezing, escape, or avoidance behavior. Conversely, under non-threatening conditions, survival depends on the ability to explore and pursue meaningful stimuli in the environment. In any given environmental context, multiple brain circuits coordinate through parallel processes to determine the ultimate behavioral strategies an animal selects. Our findings support an emerging view that experience-dependent plasticity mechanisms that shift the balance of excitatory drive to distinct classes of sub-cortical output neurons may represent a conserved mechanism for optimizing behavioral action selection in response to previous experiences (MacAskill et al., 2014).

Methods

Animals

All experiments were approved by the Vanderbilt University Institutional Animal Care and Use Committees and were conducted in accordance with the National Institute of Health Guide for the Care and Use of Laboratory Animals. Male 7-15 week old wild type, CRF-IRES-Cre (Jackson Laboratory strain B6(Cg)-Crhtm1(cre)Zjh/J; stock #: 012704; donating investigator Z. Josh Huang, Cold Spring Harbor Laboratory), CRF-IRES-Cre::Ai14 (CRF-IRES-Cre crossed to Jackson Laboratory strain B6.Cg-Gt(ROSA)26Sortm14(CAG-tdTomato)Hze/J; stock #:

007914; donating investigator Hongkui Zeng, Allen Institute for Brain Science), SOM-IRES-Cre (Jackson Laboratory strain B6J.Cg-Ssttm2.1(cre)Zjh/MwarJ; stock #: 028864; donating investigator Z. Josh Huang, Cold Spring Harbor Laboratory & Melissa R Warden, Cornell University), SOM-IRES-Cre::Ai14, CRF-IRES-Cre::SOM-IRES-Flp (CRF-IRES-Cre crossed to Jackson Laboratory strain Ssttm3.1(flpo)Zjh/J; stock #028579; donating investigator Z. Josh Huang, Cold Spring Harbor Laboratory) mice on a C57/BL6J background, or a mixed C57/BL6J/?+pN1F9 background for CRF-IRES-Cre::SOM-IRES-Flp mice were used for all experiments where indicated in the text. Mice were housed no more than 5 animals per cage in a temperature and humidity-controlled housing facility under a 12h light/dark cycle with ad libitum access to food and water. For electrophysiology recordings from naïve, fear, or extinction groups, mice were single housed following behavioral manipulation to avoid naïve mice being exposed to stressed littermates. All experiments were performed during the light cycle.

Viruses

For ex vivo circuit mapping of inputs and outputs to the CeL, we used AAV5-CaMKIIα-ChR2(H134R)-eYFP (0.15-0.25µL) and AAV5-EF1α-DIO-ChR2(H134R)-eYFP (0.3µL), respectively (UPenn Vector Core, Philadelphia, PA, or Addgene, Watertown, MA). For chemogenetic manipulations in the CeA we used AAV5-hSyn-DIO-hM3D(Gq)-mCherry and AAV5-hSyn-DIO-hM4D(Gi)-mCherry (1µL). For bilateral co-injection of AAV5-CaMKIIα-hM4D(Gi)-mCherry and AAV5-CaMKIIα-ChR2(H134R)-eYFP or AAV5-hSyn-mCherry into the BLA (0.15µL), we combined viruses in a 1:1 ratio. For circuit specific DREADD approaches we bilaterally injected the retrograde specific AAV2rg-pmSyn1-eBFP-Cre variant (0.1µL) into the CeA and bilaterally injected the cre-dependent AAV5-hSyn-DIO-hM4D(Gi)-mCherry or

AAV5-hSyn-DIO-mCherry (0.2µL) into the BLA. For fluorescent labeling of CRF+ and SOM+ neurons in CRF-IRES-Cre::SOM-IRES-Flp mice with bilateral targeting to the CeA (0.3µL), we combined AAV5-hSyn-DIO-mCherry and AAV5-EF1a-fDIO-eYFP in a 1:1 ratio. AAV2rg-pmSyn1-eBFP-Cre was a generous gift from Hongkui Zeng (Addgene viral prep # 51507-AAVrg)(Madisen et al., 2015)). AAV5-hSyn-DIO-hM3D(Gq)-mCherry, AAV5-hSyn-DIO-hM4D(Gi)-mCherry, AAV5-CaMKIIα-hM4D(Gi)-mCherry, and AAV5-hSyn-DIO-mCherry were all generous gifts from Bryan Roth (Addgene viral preps # 44361-AAV5, # 44362-AAV5, and # 50477-AAV5)(Krashes et al., 2011). AAV5-CaMKIIα-ChR2(H134R)-eYFP, AAV5-EF1α-DIO-ChR2(H134R)-eYFP, AAV5-EF1a-fDIO-eYFP and AAV5-hSyn-mCherry were all generous gifts from Karl Deisseroth (UPenn Vector Core, Philadelphia, PA, and Addgene viral preps # 26969-AAV5, # 20298-AAV5, # 55641-AAV5, # 114472).

Surgery

Mice were anesthetized with 5% isoflurane and then transferred to a stereotaxic frame (Kopf Instruments, Tujunga, CA) and kept under constant 2.5% isoflurane anesthesia. The skull surface was exposed via a midline sagittal incision and treated with the local anesthetic benzocaine (Medline Industries, Brentwood, TN). For each surgery, a 10uL microinjection syringe (Hamilton Co., Reno, NV) with a Micro4 pump controller (World Precision Instruments, Sarasota, FL) was guided by a motorized digital software (NeuroStar; Stoelting Co., Wood Dale, IL) to each injection coordinate. Virus was administered bilaterally into the CeA (coordinates in mm: AP: -0.70-1.15, ML: ±2.93, DV: 4.31-4.60 from Bregma), the BLA (coordinates in mm: AP: -1.25-1.50, ML: ±3.35-3.60, DV: 5.00 from Bregma), the INS (coordinates in mm: AP: -0.10, ML: ±4.10, DV: 4.30 from Bregma), and the PBN (coordinates in mm: AP: -4.75, ML:

±1.40, DV: 3.67 from bregma). Following completion of surgery, 10mg/kg ketoprofen (AlliVet, St. Hialeah, FL) was administered as an analgesic.

Immunohistochemistry and imaging

Mice were anesthetized using isoflurane (Abbott Labs, Chicago, IL) and transcardially perfused with cold phosphate buffered saline (PBS, 10mL) followed by cold 4% paraformaldehyde in 0.1M phosphate buffer (PFA, 15-20mL). Brains were dissected and stored overnight at 4o C in 4% PFA and then transferred to a 30% sucrose solution for 4 days, were cut at 40μm using a Leica CM3050 S cryostat (Leica Microsytems, Weitzlar, Germany), and subsequently placed in an ethylene-glycol-based antifreeze solution at -20o C for long-term storage. Brain slices were washed in Tris-Buffered Saline (TBS) for 3X 10min, placed in TBS with 4% Horse serum and 0.2% Triton X-100 (TBS+) for 30min, followed by overnight incubation with primary antibodies: mouse anti-PKCδ (1:500; BD Biosciences, San Jose, CA, 611463), rabbit anti-c-Fos (1:500; Millipore, Burlington, MA, ABE457), or chicken anti-GFP (1:500; Abcam, Cambridge, UK, ab13970). Slices were washed 3X 10min in TBS+ and incubated for 2.5hrs with secondary antibody: Alexa Fluor 488 donkey anti-rabbit or donkey anti-mouse (1:1000; Invitrogen, Carlsbad, CA, A21206), or Cy2 AffiniPure donkey anti-chicken (1:1000; Jackson ImmunoResearch Laboratories Inc., 703-225-155), washed for 3X 10min in TBS and then mounted and cover-slipped. For slices stained with 4′,6-diamidin-2-phenylindol (DAPI, 1:12,000; Thermo Fisher Scientific, Waltham, MA, 62248) we incubated for 5 min, followed by an extra 3X 10min washes in TBS. Imaging was conducted using an upright Axio Imager M2 epifluorescent microscope or a Zeiss inverted LSM 710 Meta confocal microscope (Zeiss, Oberkochen, Germany). Whole brain section images were acquired by tiling using a 5X

objective, and higher magnification images were acquired by tiling the amygdala using a 20X objective. Brightness and contrast of images were adjusted using Image J or Adobe CS4 software for clarity and presentation in figures.

Cell counting and co-localization

Fluorescently labeled neurons in the CeC, CeL, and CeM were counted using ImageJ software (Public Domain license, Wayne Rasband) between stereotaxic brain coordinates -1.06mm and -1.70mm from Bregma. Cell counts were analyzed along the rostrocaudal axis of the CeA by identifying a representative coronal slice from each animal for rostral (-1.06-1.22mm from bregma), middle (-1.34-1.46mm), and caudal (-1.58-1.70mm) subdivisions using whole-brain stereotaxic coordinates atlas as a reference (Franklin & Paxinos, 2007). Exposure was kept the same between groups when imaging C-fos positive neurons in the CeL, and adjustments for brightness or contrast were done equally in parallel between groups.

RNAscope® fluorescent in situ hybridization

RNAscope® cDNA probes and detection kits were purchased from ACD and used according to the company's online protocol for fresh frozen tissue. The probe sets directed against CRF, SOM, and PKCδ were designed from sequence information from the mouse RefSeq mRNA IDs NM_205769.2, NM_009215.1, and NM_011103.3, respectively (more information available on ACD's website). Mice were anesthetized using isoflurane and the brains were quickly removed and frozen in Tissue Tek® O.C.T. compound (Sakura Finetek, Torrance, CA) using Super Friendly Freeze-It Spray (Fisher Scientific, Hampton, NH). Brains were stored at -20°C until cut on a cryostat to produce 16 um coronal sections. Sections were

adhered to warm slides and immediately refrozen before being stored at -80°C until ready to undergo the RNAscope® procedure. Following the ACD protocol for fresh frozen tissue, slides were fixed for 15 mins in ice cold 4% paraformaldehyde and then dehydrated in a sequence of ethanol serial dilutions (50%, 70% and 100%, twice each). Slides were briefly air-dried and then a hydrophobic barrier was drawn around the tissue sections using a Pap Pen (Vector Labs). Slides were then incubated with ACD's protease IV solution for 30 mins at room temperature in a humidified chamber. Following protease treatment, sections were incubated with RNAscope® cDNA probes (2 hours), and then with a series of signal amplification reagents provided by the Multiplex Fluorescence Kit from ACD; in brief, Amp 1-FL (30 mins), Amp 2-FL (15 mins), Amp 3-FL (30 mins) and Amp 4-FL ALT A (15 mins). Two minutes of washing in RNAscope® wash buffer (1x from 50x stock, ACD) were performed between each step, and all incubation steps with the cDNA probes and amplification reagents were preformed using a HybEZ oven (ACD) at 40°C. cDNA probe mixtures were prepared at a dilution of 50:1:1 for SOM, CRF and PKCδ, respectively. Sections were also stained for DAPI using the reagent provided by the Fluorescent Multiplex Kit. Immediately following DAPI staining, sections were mounted and cover slipped using Aqua-Polymount (PolySciences) and left to dry overnight. Slides from the anterior, medial and posterior CeA were collected in pairs, using one section for incubation with the cDNA probes, and another for incubation with a 3 probe set for bacterial mRNA (DapB; ACD) to serve as a negative control.

Sections were imaged using a Zeiss inverted LSM 710 Meta confocal microscope at 20X and 63X magnification. Images from sections treated with the negative control probe for each pair of slides were used to determine brightness and contrast parameters that minimized observation of bacterial transcripts and auto-fluorescence, and these adjustments were then

applied to the images in parallel from experimental sections treated with the cDNA probes. Adjusted experimental images were then analyzed in a designated region of interest around the CeL. Cells in these regions of interest were identified using both the DAPI stained nuclei and the borders present between cells (identified with the help of gray scale differential interference contrast (DIC) overlays), and the total number of cells in each region were counted. Cells were then counted for presence of CRF, SOM, and PKCδ signal in order to determine totals for each cell population expressing these signals either alone or in various combinations. Transcripts were readily identified as round, fraction delimited spots over and surrounding DAPI-labeled nuclei.

Fear conditioning and extinction training

Mice underwent fear conditioning and extinction training as previously described(Hartley et al., 2016). Briefly, mice were placed in Context A for fear conditioning, which consisted of a chamber with dimensions: 30.5 × 24.1 × 21.0cm and an automated freezing analysis software (Med Associates, Burlington, VT, USA), which was cleaned prior to and in between mice using MB-10 disinfectant (Quip Laboratories, Wilmington, DE). For conditioning (day 1), mice were presented with six conditioned stimulus– unconditioned stimulus (CS–US) pairings (tone–foot shock) separated by a 30s inter-trial interval (ITI). Each tone (80 dB, 3000 Hz) lasted 30s. Mice were presented with the electric foot shock at 0.7mA during the last 2s of each 30s tone. For fear extinction training, day 2 and day 3, mice were placed in Context B, which consisted of the same chamber with a white floor, a curved white wall contextual insert, and a distinct vanilla extract olfactory cue (McCormick, Sparks, MD). A short 30s baseline was used to test initial freezing as a measure of fear generalization to the novel context. Mice were then presented with 20 CS presentations (30s) with a 30s ITI. For extinction recall (day 4), mice were placed back into

Context B the following day and presented with 6 CS presentations with a 30s ITI. For some experiments, a full drug-free extinction session on day 2 or day 4 was conducted to compare early and late phase fear or extinction recall, and the first 5-6 CS presentations were used as a measure of recall in the absence of drug administration. Conditioned flight behavior was scored by measuring the speed of mice during extinction training using ANY-maze automated software (Stoelting, Wood Dale, IL).

Ex vivo electrophysiology

Coronal brain sections were collected at 250μm using standard procedures. Mice were anesthetized using isoflurane, and transcardially perfused in an ice-cold/oxygenated (95% v/v O2, 5% v/v CO2) cutting solution consisting of (in mM): 93 N-Methyl-D-glucamine (NMDG), 2.5 KCl, 20 HEPES, 10 MgSO4 . 7H2O, 1.2 NaH2PO4, 30 NaHCO3, 0.5 CaCl2 . 2H2O, 25 glucose, 3 Na+-pyruvate, 5 Na+-ascorbate, and 5 N-acetylcysteine. The brain was subsequently dissected, hemisected, and sectioned using a vibrating LeicaVT1000S microtome (Leica Microsytems, Bannockburn, IL). The brain slices were then transferred to an oxygenated 34°C chamber filled with the same cutting solution for a 10 min recovery period. Slices were then transferred to a holding chamber containing a buffered solution consisting of (in mM): 92 NaCl, 2.5 KCl, 20 HEPES, 2 MgSO4 7H2O, 1.2 NaH2PO4, 30 NaHCO3, 2 CaCl2 2H2O, 25 glucose, 3 Na-pyruvate, 5 Na-ascorbate, 5 N-acetylcysteine and were allowed to recover for ≥30 min. For recording, slices were placed into a perfusion chamber where they were constantly exposed to oxygenated artificial cerebrospinal fluid (ACSF; 31-33°C) consisting of (in mM): 113 NaCl, 2.5 KCl, 1.2 MgSO4 . 7H2O, 2.5 CaCl2 . 2H2O, 1 NaH2PO4, 26 NaHCO3, 20 glucose, 3 Na+-pyruvate, 1 Na+-ascorbate, at a flow rate of 2-3ml/min.

Cells were visually identified from Ai14 reporter lines or virally injected animals under illumination from a series 120Q X-cite lamp at 40X magnification using an immersion objective in coordination with differential interference contrast microscopy (DIC). CeL neurons were voltage clamped in whole cell configuration at -70mV using borosilicate glass pipettes (3-6MΩ) filled with intracellular solution containing (in mM): 125 K+-gluconate, 4 NaCl, 10 HEPES, 4 MgATP, 0.3 Na-GTP, and 10 Na-phosphocreatine (pH 7.30-7.35). To assess basal membrane properties and sEPSCs onto distinct CeL cell types, alternating whole-cell patch clamp recordings were made from neighboring (≤30μm) TdTomato expressing somata (CRF+) or TdTomato lacking somata (CRF-) within the same depth and plane of the slice, or independently from SOM+ neurons in other animals as depicted in figures. Following break-in to each cell, ≥3 min of time elapsed before initiation of experiments to allow for internal solution exchange and stabilization of membrane properties. Spontaneous excitatory post-synaptic currents (sEPSCs) were recorded over 3 min in the presence of the $GABA_A$ receptor antagonist picrotoxin (25μM) so as to isolate excitatory neurotransmission. After sEPSC recordings, cells were switched to current clamp configuration, resting membrane potential was recorded, and then current injection was manually applied to maintain the cell near a stable resting potential of -70mV. Depolarizing current injections (20, 600ms) were administered in incremental steps (Δ40pA) beginning with an initial hyperpolarizing current injection of -100pA. The afterhyperpolarization (AHP) amplitude was measured by applying 5 sweeps of a 600pA current injection (400ms). The time constant was determined using 5 sweeps of a -100pA current injection (10ms). Input resistance was measured using 10 sweeps of a -20pA current injection (500ms). When possible, all membrane properties were measured from each recorded neuron following sEPSC recordings. For recordings of PPR and AMPAR/NMDAR ratios we used an internal solution containing (in

mM): 120 Cs-gluconate, 2.8 NaCl, 20 HEPES, 2.5 MgATP, 0.25 Na-GTP, and 5 TEA-Cl (pH 7.30-7.35). All data was acquired using a Multiclamp 700B amplifier, Digidata 1440A A/D converter, Clampex version 10.6 software (Axon Instruments, Union City, CA), was sampled at 20kHz and low pass filtered at 1 kHz, and analyzed in Multiclamp version 10.6 software (Axon Instruments).

Ex vivo optogenetics

For input mapping experiments, mice were bilaterally injected with AAV5-CaMKIIα-ChR2(H134R)-eYFP into the BLA, INS, or PBN using cohorts of CRF-IRES-Cre::Ai14 mice. When possible, cohorts of littermate mice were equally distributed between experimental groups to limit inter-cohort variability. Mice recovered for 4 weeks to allow for maximal virus expression and then were randomly assigned to naïve (basal), fear, or extinction groups. For the majority of experiments, recordings from each group were interleaved daily when applicable. For comparisons between inputs onto CRF+ neurons, we performed input/output curves by incrementally stepping light exposure time while keeping light intensity constant (3.0 mW/mm^2). Dual whole-cell patch clamp recordings were conducted from neighboring CRF+ and CRF- neurons (somata ~ ≤30μm), CRF+ and SOM+ neurons (somata ~ ≤60μm), or CRF+/SOM+ and CRF-/SOM- neurons (somata ~ ≤30μm). Series resistance compensation (≤75%) was used to approximately match access resistance values between each cell (within 0-3MΩ). We recorded oEPSCs elicited from the BLA, INS, and PBN inputs by illuminating the central amygdala with ~470nm wavelength light using a LEDD1B T-Cube LED driver (ThorLabs, Newton, NJ). To compare input bias onto CRF+ and CRF- neurons, input/output curves were generated by incrementally stepping the light intensity at fixed values set along the LED driver and averaging

the oEPSC amplitude at each step across 5 sweeps while keeping light exposure constant (5ms). Fixed light-density values correspond to the following intensity steps listed in figures (in mW/mm^2): 1) 0.2, 2) 0.4, 3) 0.6, 4) 1.4, 5) 2.6, and 6) 3.0. Due to the close proximity of the BLA to the CeA, we controlled for transient infection of ChR2 in CeL neurons from occasional viral spread past the intermediate capsule by performing a 200ms light pulse prior to experimentation. Neuronal pairs that demonstrated a prolonged ChR2-mediated inward current were discarded. For some paired INS projection experiments, we manually turned down the exposure time of light until stimulation would not reliably evoke sodium channel currents via voltage-clamp escape. For TTX experiments, light intensity and exposure was kept constant at maximum values used for data collection (3.0 mW/mm^2, and 5ms exposure time), and TTX (500nM) was bath applied after a 5 min baseline recording. For measurements of aEPSCs we replaced extracellular calcium with 4mM strontium and kept maximum stimulation (3.0 mW/mm^2, and 5ms exposure time) constant across conditions. Measurements of aEPSCs were captured in a 500ms window 50ms following onset of the light stimulus. To further assess changes in presynaptic release probability, we manually adjusted stimulation intensity to provide adequate voltage clamping and minimize space clamp error of oEPSCs from BLA-CeL synapses and measured PPR (oEPSC2/oEPSC1) at various inter-stimulus intervals (ISIs; 25ms, 50ms, 100ms, and 200ms). From the same neurons, AMPAR/NMDAR ratios were calculated by keeping light intensity and exposure time constant between neighboring neurons and measuring the AMPAR-mediated current when voltage-clamping at -70mV for 10 sweeps followed by the same stimulation while voltage clamping at +40mV for the dual component AMPAR and NMDAR-mediated current. The magnitude of the NMDAR-mediated current was calculated at 20ms following the onset of

stimulation, when the average AMPAR responses at -70mV had decayed from 95% to 5% of its peak value back to baseline holding current.

For output mapping, CRF-IRES-Cre, CRF-IRES-Cre::Ai14, or SOM-IRES-Cre mice were bilaterally injected with AAV5-EF1α-DIO-ChR2(H134R)-eYFP into the CeA. Mice were allowed to recover for 6-8 weeks for maximal virus expression and entire brains were sectioned and examined for eYFP terminal expression. In separate mice, whole-cell recordings were isolated from brain regions reliably demonstrating a moderate to high degree of YFP expression downstream of the CeA (the CeL, CeM, BNST, PBN, and PAG) and were patched where YFP expression was visibly highest in the slice. Whole-cell recordings were conducted using a high-chloride based internal solution, containing (in mM): 106 K+-gluconate, 40 KCl, 10 HEPES, 4 MgATP, 0.3 Na-GTP, and 20 Na-phosphocreatine (pH 7.20-7.25). Neurons were voltage clamped at -70mV in the presence of AMPA and NMDA receptor blockers CNQX (20μM) and APV (50μM), respectively, so as to isolate GABA dependent currents. Cells that lacked time-locked oIPSCs were scored as non-responsive, and cells that demonstrated time-locked oIPSCS were scored as responsive. To test for $GABA_A$-mediated responses, picrotoxin was bath applied to the perfusate (50μM).

Ex vivo DREADD validation

To test for the efficacy of DREADDs in regulating the excitability of infected neurons, we performed whole-cell patch clamp recordings from mCherry+ cells in the CeL of DREADD injected animals. Neurons were kept in current clamp configuration and CNO (10μM, Cayman Chemical, Ann Arbor, MI) was bath applied to the slice while the resting membrane potential was monitored for 10min. CNO was applied to the slice after a 3min baseline recording of the

resting membrane potential. The average change in resting membrane potential for hM3D(Gq)-infected neurons was calculated to the Vm value at which neurons reached threshold for action potential firing. For hM4D(Gi)-infected neurons, current was injected to keep cells near action potential threshold at a low spontaneous firing frequency (~1Hz) and decreases in action potential frequency were monitored following bath application of CNO.

For experiments examining the presence of CRF-mediated plasticity or release, we recorded sEPSCs from CeL neurons in the presence of picrotoxin (25μM) for a baseline of 3 min followed by bath application of CRF (300nM) or VEH while sEPSCs were monitored for 15 min. In separate experiments, we recorded CRF- neurons in the CeL (mCherry-) of CRF-IRES-Cre mice expressing hM3D(Gq)-infected neurons, and repeated the same analysis while bath applying CNO (10μM) or VEH and monitoring sEPSCs for 20 min. Cells in which the access resistance fluctuated more than 20% of the baseline during recording were excluded from analysis.

For hM4D(Gi)-mediated inhibition of the BLA to CeL pathway, indiscriminate voltage clamp recordings were made from CeL neurons in the presence of picrotoxin (25μM), and oEPSCs were evoked at 0.1 Hz for a baseline of 5min followed by a 20min bath application of CNO (10μM). Access resistance was monitored throughout experiments by injection of a 5mV hyperpolarizing current, and cells in which the access resistance fluctuated more than 20% of the baseline were discarded from analysis. Data from global hM4D(Gi) and ChR2 expression in the BLA, and mice with Cre-dependent hM4D(Gi) and ChR2 pathway specific expression were pooled for analysis.

Behavioral experiments using DREADDs

Mice were allowed to recover for 5 weeks to allow maximal DREADD expression in the CeL or BLA. For DREADD-mediated block of BLA-CeL plasticity, mice were allowed to recover for 4 weeks before undergoing behavioral manipulation and whole-cell recordings. For all DREADD experiments, CNO (10mg/kg) was administered 30min prior to behavioral testing, as outlined in figures.

Randomization and inclusion/exclusion criteria

Mice were selected at random and without bias from group housed cages and assigned to each treatment group for electrophysiology experiments. For behavioral experiments, mice were pseudorandomly assigned to VEH or CNO groups in alternating pairs to best control for age and experiments were run by alternating between treatment groups (running pairs of mice at the same time in identical fear conditioning chambers to control for time of day). Mice in behavioral tests were excluded from analysis only when they exhibited signs of serious illness or discomfort (i.e. extreme lethargy accompanied with akinesia) or if they demonstrated missed bilateral injections of target structures. For electrophysiology experiments, outliers were removed as determined by Grubbs or ROUT test. Experimenters were not blinded to condition, but behavioral analysis was conducted without bias by automated freezing software.

Statistical Analysis

Statistical analyses were conducted using GraphPad Prism 6.0 software. All statistical tests used are reported where they appear in the figure legends. We assumed normality and equal variance for each data set, but normality was not formally tested. Nonparametric tests were only

used for comparing the ratio of averages of maximal current amplitudes from dual recordings, as this has been described as a more robust method of comparing ratiometric data (MacAskill et al., 2014). A power analysis was not conducted a priori to determine sample sizes, but our sample sizes for behavior and electrophysiology manipulations are consistent with similar experiments from previously published work (Li et al., 2013; MacAskill et al., 2014; Penzo et al., 2015; Sanford et al., 2017).

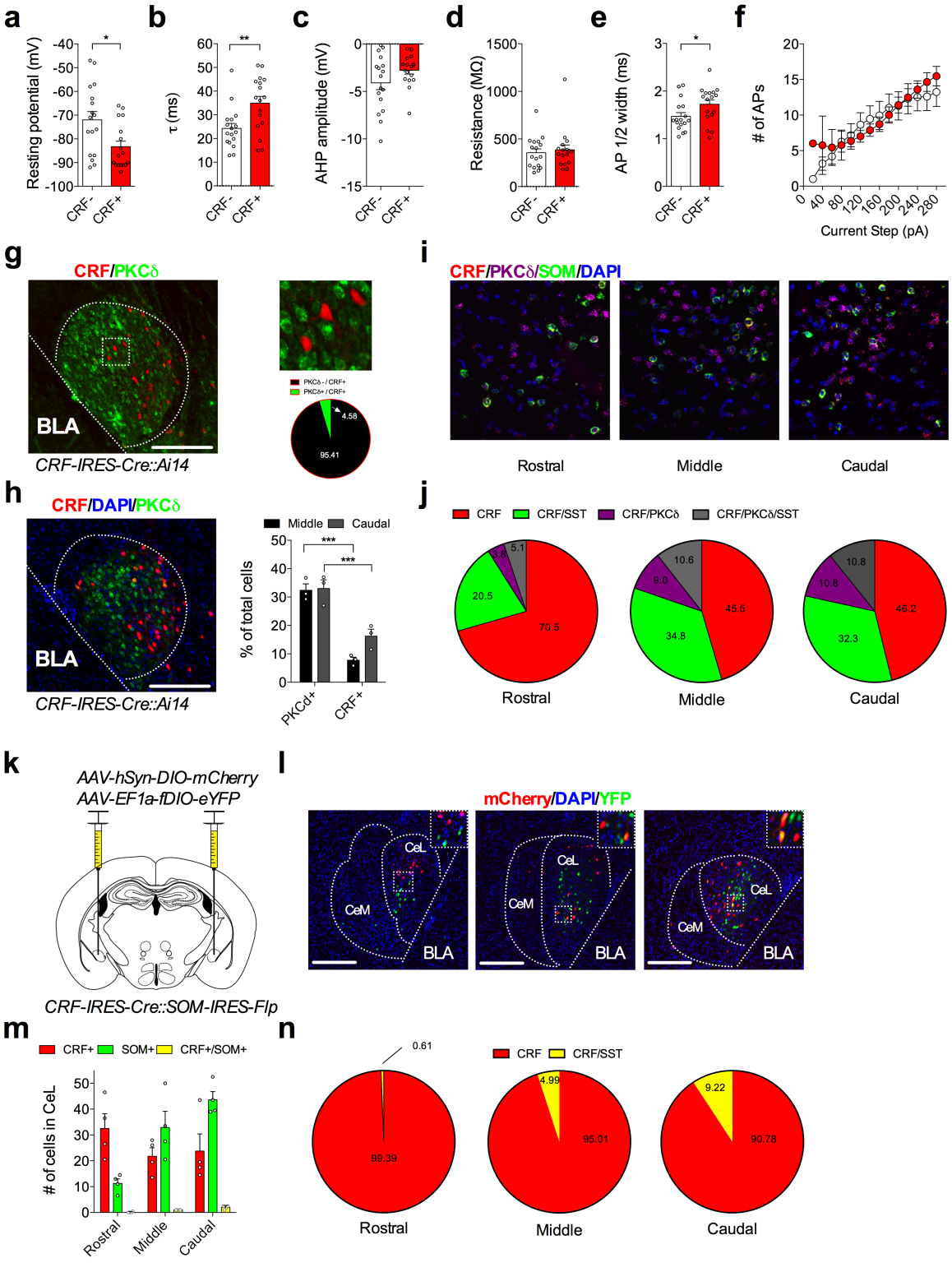
a
Resting potential (mV)
CRF-
CRF+
b
τ (ms)
c
AHP amplitude (mV)
d
Resistance (MΩ)
e
AP 1/2 width (ms)
f
# of APs
Current Step (pA)
g
CRF/PKCδ
BLA
CRF-IRES-Cre::Ai14
PKCδ-/CRF+
PKCδ+/CRF+
4.58
95.41
i
CRF/PKCδ/SOM/DAPI
Rostral
Middle
Caudal
h
CRF/DAPI/PKCδ
BLA
CRF-IRES-Cre::Ai14
Middle
Caudal
% of total cells
PKCd+
CRF+
j
CRF
CRF/SST
CRF/PKCδ
CRF/PKCδ/SST
20.5
70.5
3.8
5.1
9.0
10.6
34.8
45.5
10.8
10.8
32.3
46.2
Rostral
Middle
Caudal
k
AAV-hSyn-DIO-mCherry
AAV-EF1a-fDIO-eYFP
CRF-IRES-Cre::SOM-IRES-Flp
l
mCherry/DAPI/YFP
CeL
CeM
BLA
m
CRF+
SOM+
CRF+/SOM+
# of cells in CeL
Rostral
Middle
Caudal
n
CRF
CRF/SST
0.61
99.39
4.99
95.01
9.22
90.78
Rostral
Middle
Caudal

Supplementary Fig. 1. Characterization of CRF+ neurons in the CeL. a, Resting membrane potential of neighboring CRF+ and CRF- neurons (n=17 cells per group, 4 mice, two-tailed unpaired t-test P=0.0115). **b,** Time constant of neighboring CRF+ and CRF- neurons (n=17 cells per group, two-tailed unpaired t-test P=0.0049). **c,** Afterhyperpolarization amplitude of neighboring CRF+ and CRF- neurons (n=17 cells per group). **d,** Input resistance of neighboring CRF+ and CRF- neurons (n=17 cells per group). **e,** Action potential half-width of neighboring CRF+ and CRF- neurons (n=17 cells per group, two-tailed unpaired t-test P=0.0439). **f,** Number of action potentials per current injection of neighboring CRF+ and CRF- neurons (n=17 cells per group). **g,** Left: image showing immunohistochemical analysis of PKCδ overlap with CRF+ neurons (scale bar 250μm). Top-right: close up inlet of image on left. Bottom-right: percentage overlap of CRF+ and PKCδ+ neurons (n=4 mice). **h,** Image demonstrating immunohistochemical analysis of PKCδ and CRF+ neurons in the CeA with DAPI stain for quantification of total neurons in CeL. Right: percent of PKCδ+ and CRF+ neurons in the CeL along the rostrocaudal axis (note that PKCδ staining of cell somata was absent in anterior CeL; n=3 mice, two-way ANOVA, $F(1,8)=80.08$, $P=0.0000193255$ for rostrocaudal axis; post-hoc Holm-Sidak's multiple comparisons, P=0.0001 for PKCδ and P=0.0009 for CRF+). **i,** Images of fluorescent *in situ* hybridization for CRF, SOM, and PKCδ mRNA in the CeL. Images are pseudocolored for consistency with CRF+ neurons depicted as red throughout figures. **j,** Percentage overlap of SOM and PKCδ with CRF in the CeL along the rostrocaudal axis (n=3 mice). **k,** Injection strategy for targeting fluorophore expression to CRF and SOM neurons in the CeA. **l,** Representative images of the rostral, middle, and caudal CeA. YFP signal indicates SOM+ neurons, and mCherry signal indicates CRF+ neurons (inlet indicates either the presence or absence of co-localization between YFP and mCherry; scale bars 200μm). **m,** Average quantity of CRF+, SOM+, and co-labeled CRF+/SOM+ neurons in the CeL along the rostrocaudal axis (n=4 mice). **n,** Average percentage of co-labeled CRF+/SOM+ neurons in the CeL along the rostrocaudal axis (n=4 mice). Action potentials per current injection are presented as mean ± S.E.M., and bar graphs are presented as mean + S.E.M. *P<0.05, **P<0.01, ***P<0.001.

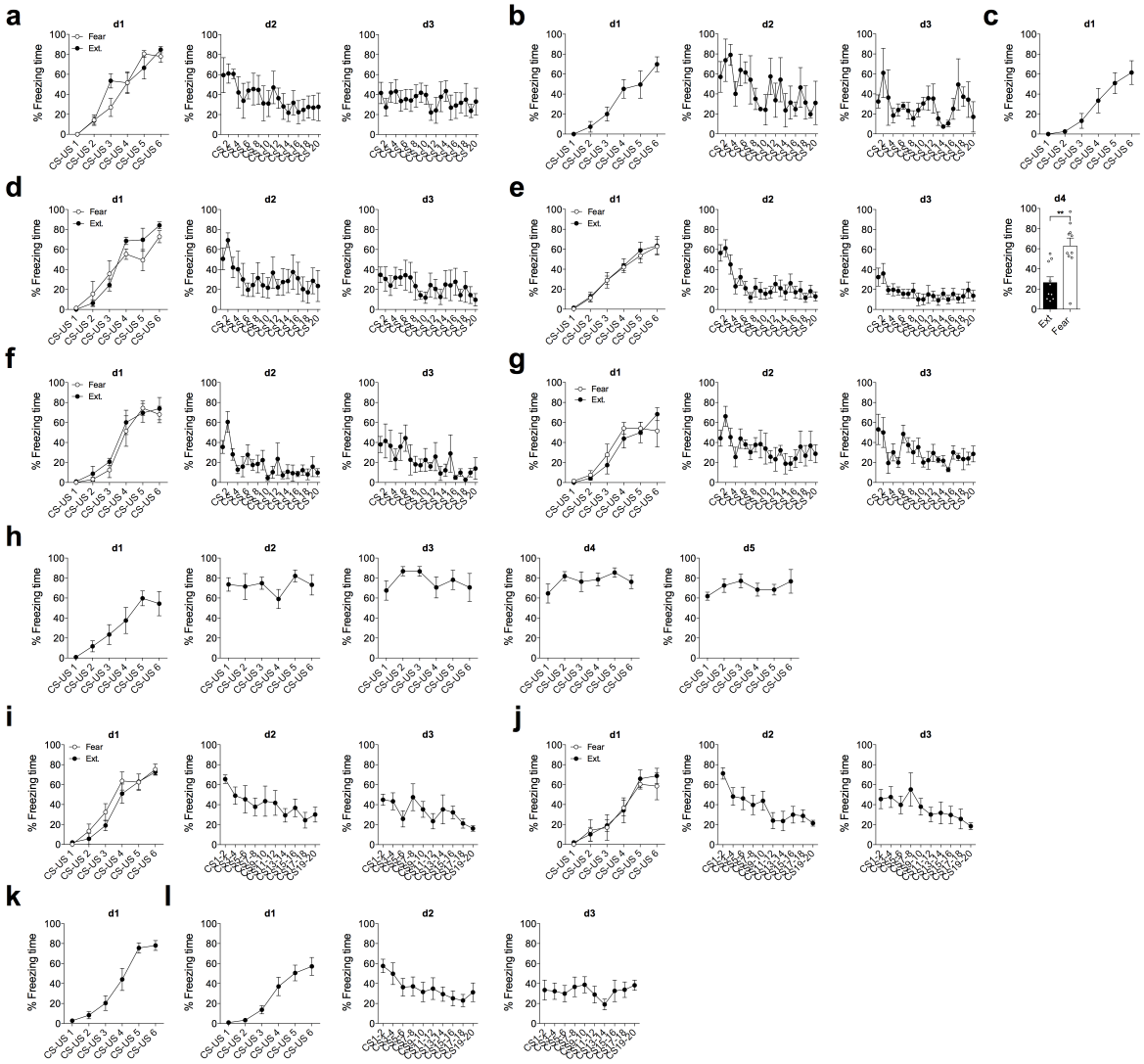

Supplementary Fig. 2. Learning curves for electrophysiological and control experiments. a, Fear conditioning and extinction learning curves from experiment in Fig. 1. **b,** Fear conditioning and extinction learning curves from experiment in Supplementary Fig. 3. **c,** Fear conditioning learning curve from experiments in Fig. 2. **d,** Fear conditioning and extinction learning curves from experiment in Fig. 3. **e,** Comparison of fear recall on day 4 (d4) from mice left in their home cage (Fear) compared to mice that have undergone extinction training (Ext) (n=10 mice per group, two-tailed unpaired t-test, P=0.0016). **f,** Fear conditioning and extinction learning curves from experiment in Fig. 4. **g,** Fear conditioning and extinction learning curves from experiment in Supplementary Fig. 8. **h,** Learning curves of 5 days of fear conditioned overtraining from experiments in Supplementary Fig. 7. **i,** Fear conditioning and extinction learning curves from experiment in Supplementary Fig. 9. **j,** Fear conditioning and extinction learning curves from experiment in Supplementary Fig. 10. **k,** Fear conditioning learning curve from experiment in Supplementary Fig. 13c-f. **l,** Fear conditioning and extinction learning curves from experiment in Supplementary Fig. 13g-j. Learning curves are presented as mean ± S.E.M., and bar graphs are presented as mean + S.E.M. **P<0.01.

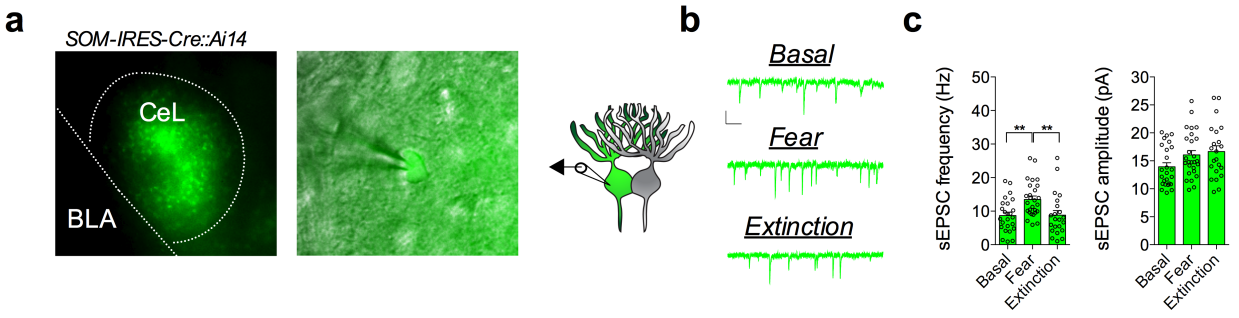

Supplementary Fig. 3. Fear conditioning and extinction training bidirectionally remodel excitatory input onto SOM+ neurons. a, Left: image of fluorescent SOM+ neurons in the CeL from a coronal slice used in recordings (pseudocolored in green). Middle: DIC and fluorescent overlay of patch-clamp recording from a SOM+ neuron. Right: recording schematic of SOM+ neuron in the CeL. **b,** Traces of sEPSC recordings from SOM+ neurons across behavioral conditions (scale bar 100ms, and 10pA). **c,** Average sEPSC frequency and amplitude of SOM+ neurons from naïve (basal), fear conditioned, and fear extinction mice (n=25 basal, 3 mice, n=27 fear, 4 mice, n=22 extinction cells, 3 mice, one-way ANOVA, F(2,71)=0.1380, P=0.0030; post-hoc Holm-Sidak's multiple comparisons, basal vs. fear P=0.0051, fear vs. extinction P=0.0051). Bar graphs are presented as mean + S.E.M. **P<0.01.

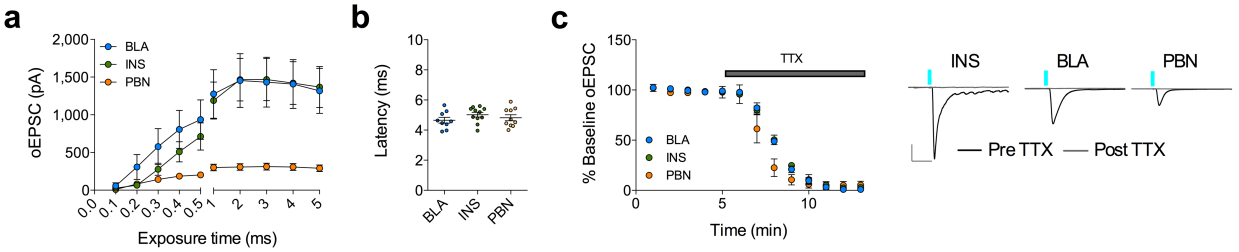

Supplementary Fig. 4. CRF+ neurons in the CeL receive greater top-down excitatory input strength relative to bottom-up input. a, Input-output oEPSC exposure curve for BLA (n=9 cells, 3mice), INS (n=11 cells, 5 mice), and PBN (n=10 cells, 6 mice) inputs onto CRF+ neurons in the CeL. **b,** Latency of oEPSCs from the BLA (n=9 cells, 3mice), INS (n=11 cells, 5 mice), and PBN (n=10 cells, 6 mice) inputs to the CeL at maximal stimulation parameters. **c,** Left: Summary data from bath application of TTX while recording oEPSC amplitude of BLA (n=3 cells, 1 mouse) INS (n=2 cells, 1 mouse), or PBN (n=4 cells, 2 mice) input onto CRF+ neurons in the CeL. Right: traces of INS, BLA, and PBN oEPSCs before and after TTX application (scale bar 20ms, 500pA).

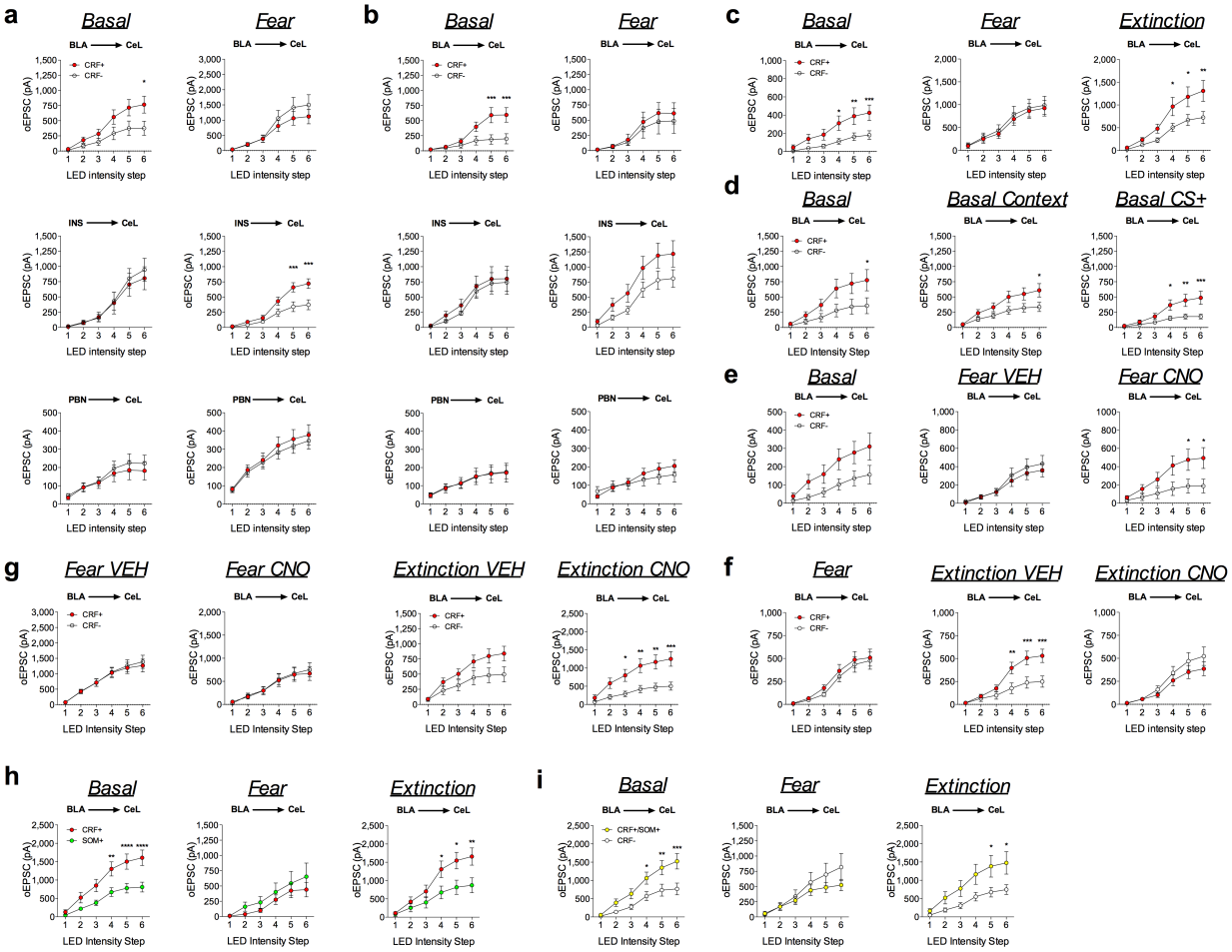

Supplementary Fig. 5. Input-output curves from dual patch-clamp recordings in the CeL. **a,** I/O curves of data from Fig. 2 (two-way ANOVAs, F(1,168)=14.98, P=0.0002 for BLA-CeL basal group effect, and F(1,228)=25.04, P=0.00000112 for INS-CeL fear group effect; post-hoc Holm-Sidak's multiple comparisons, BLA-CeL basal step 6 P=0.0208, INS-CeL fear step 5 P=0.0004, step 6 P=0.0001). **b,** I/O curves for data from Supplementary Fig. 7 (two-way ANOVAs, F(1,72)=11.13, P=0.001345902 for BLA-CeL basal group effect, and F(1,144)=13.15, P=0.0004 for INS-CeL fear group effect; post-hoc Holm-Sidak's multiple comparisons, BLA-CeL basal step 5 P=0.0008, step 6 P=0.0009). **c,** I/O curve of data from Fig. 3 (two-way ANOVAs, F(1,216)=25.43, P=0.00000097 for basal group effect, and F(1,204)=19.33, P=0.00001769 for extinction group effect; post-hoc Holm-Sidak's multiple comparisons, basal step 4 P=0.0360, step 5 P=0.0154, step 6 P=0.0085, extinction step 4 P=0.0492, step 5 P=0.0275, step 6 P=0.0091). **d,** I/O curve of data from Supplementary Fig. 6 (two-way ANOVAs, F(1,168)=15.64, P=0.0001 for basal group effect, F(1,192)=16.10, P=00008605 for basal context group effect, and F(1,168)=22.91, P=0.00000370 for basal CS+ group effect; post-hoc Holm-Sidak's multiple comparisons, basal step 6 P=0.0446, basal context step 6 P=0.0373, basal CS+ step 4 P=0.0310, step 5 P=0.0058, step 6 P=0.0011). **e,** I/O curve of data from Fig. 5c-f (two-way ANOVAs, F(1,192)=17.69, P=0.00003986 for basal group effect, and F(1,216)=18.38, P=0.00002727 for fear CNO group effect; post-hoc Holm-Sidak's multiple comparisons, fear step 5 P=0.0368, step 6 P=0.0270). **f,** I/O curve of data from Fig. 5g-j (two-way ANOVAs,

F(1,264)=25.08, P=0.00000101 for extinction VEH group effect; post-hoc Holm-Sidak's multiple comparisons, extinction VEH step 4 P=0.0081, step 5 P=0.0010, step 6 P=0.0006). **g,** I/O curve of data from Supplementary Fig. 11c-j (two-way ANOVAs, F(1,192)=14.70, P=0002 for extinction VEH group effect, and F(1,180)=44.76, P<0.0001 for extinction CNO group effect; post-hoc Holms-Sidak's multiple comparisons, extinction CNO step 3 P=0.0220, step 4 P=0.0030, step 5 P=0.0015, step 6 P=0.0006). **h,** I/O curve of data from Supplementary Fig. 9 (two-way ANOVAs, F(1,156)=38.74, P<0.0001 for basal group effect, and F(1,132)=19.76, P=0.00001843 for extinction group effect; post-hoc Holm-Sidak's multiple comparisons, basal step 4 P=0.0066, step 5 P=0.0017, step 6 P=0.0005, extinction step 4 P=0.0406, step 5 P=0.0156, step 6 P=0.0093). **i,** I/O curve of data from Supplementary Fig. 10 (two-way ANOVAs, F(1,120)=29.29, P=0.00000032 for basal group effect, and F(1,156)=22.20, P=0.00000540 for extinction group effect; post-hoc Holm-Sidak's multiple comparisons, basal step 4 P=0.0411, step 5 P=0.0074, step 6 P=0.0006, extinction step 5 P=0.0319, step 6 P=0.0303). XY graphs for each intensity step are presented as mean of the absolute value for oEPSC amplitude ± S.E.M. *P<0.05, **P<0.01, ***P<0.001, ****P<0.0001.

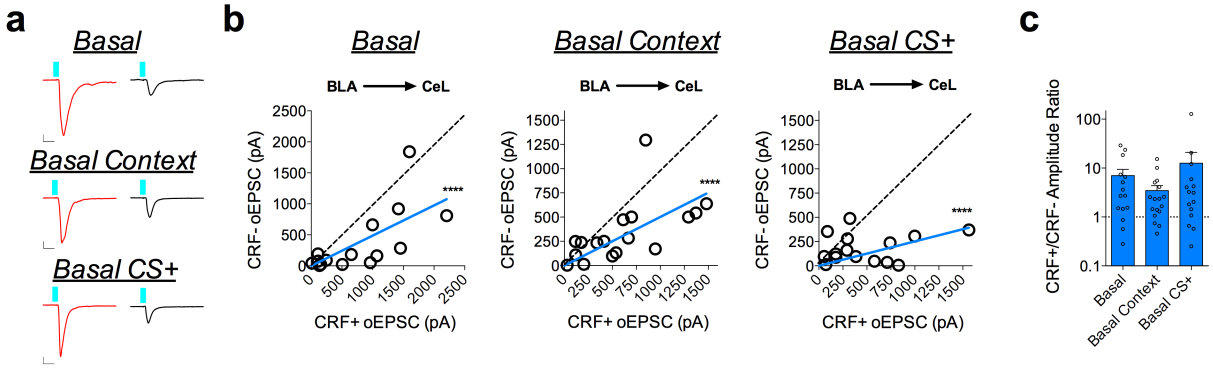

Supplementary Fig. 6. Conditioning context or CS exposure does not affect BLA-CeL circuit input bias onto CRF+ and CRF- neurons. a, Traces of maximal oEPSC amplitude from CRF+ (red) and CRF- (black) neuronal pairs across behavioral conditions for stimulation of the BLA-CeL circuit (scale bars 10ms, 100pA). **b,** XY graphs depicting skew-plot of maximal oEPSC amplitude from each CRF+ and CRF- neuronal pair for behavioral conditions (n=15 basal pairs, 4 mice, n=17 basal context pairs, 4 mice, and n=15 basal CS+ pairs, 5 mice, extra sum-of-squares F test, F(1,14)=30.55, P=0.00007452 for basal, F(1,16)=35.56, P=0.00001986 for basal context, and F(1,14)=113.2, P=0.00000004 for basal CS+). **c,** CRF+ and CRF- maximal oEPSC amplitude ratio (log scale; n=14 basal pairs, n=17 basal context, and n=14 basal CS+ pairs, Kruskal-Wallis test, non-signinficant). XY skew-plots are presented as absolute value with line through origin. Bar graphs are presented as mean + S.E.M. ****P<0.0001.

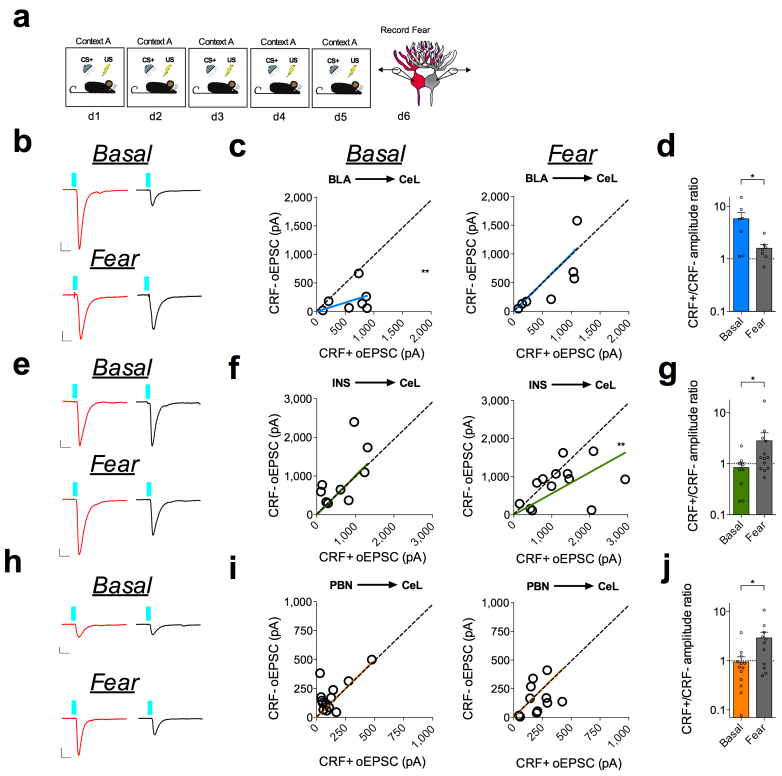

Supplementary Fig. 7. Conditioned fear overtraining remodels circuit specific input bias onto CRF+ and CRF- neurons in the CeL. a, Experimental paradigm for dual patch-clamp recordings from neighboring CRF+ and CRF- neurons in over-trained mice. Right: DIC and fluorescent overlay image of dual-patch clamp recording from CRF+ and CRF- pair. **b,** Traces of maximal oEPSC amplitude from CRF+ (red) and CRF- (black) neuronal pairs across behavioral conditions for stimulation of the BLA-CeL circuit (scale bar 10ms, 200pA for basal, and 10ms, 50pA for fear). **c,** XY graphs depicting skew-plot of maximal oEPSC amplitude from each CRF+ and CRF- neuronal pair for behavioral conditions (n=7 basal pairs, 2 mice, n=7 fear pairs, 2 mice, extra sum-of-squares F test, $F(1,6)=31.76$, $P=0.0013$). **d,** CRF+/CRF- maximal oEPSC amplitude ratio (log scale; n=7 basal pairs, n=7 fear pairs, Mann-Whitney test, $P=0.0364$). **e,** Traces of maximal oEPSC amplitude from CRF+ (red) and CRF- (black) neuronal pairs across behavioral conditions for stimulation of the INS-CeL circuit (scale bar 10ms, 50pA for basal, and 10ms, 200pA for fear). **f,** XY graphs depicting skew-plot of maximal oEPSC amplitude from each CRF+ and CRF- neuronal pair for behavioral conditions (n=9 basal pairs, 2 mice, n=13 fear pairs, 2 mice, extra sum-of-squares F test, $F(1,12)=17.88$, $P=0.0012$). **g,** CRF+/CRF- maximal oEPSC amplitude ratio (log scale; n=9 basal pairs, n=13 fear pairs, Mann-Whitney test, $P=0.0151$). **h,** Traces of maximal oEPSC amplitude from CRF+ (red) and CRF- (black) neuronal pairs across behavioral conditions for stimulation of the PBN-CeL circuit (scale bars 10ms, 50pA). **i,** XY graphs depicting skew-plot of maximal oEPSC amplitude from each CRF+ and CRF- neuronal pair for behavioral conditions (n=13 basal pairs, 2 mice, n=11 fear pairs, 2 mice, extra sum-of-squares F test, not significant). **j,** CRF+/CRF- maximal oEPSC amplitude ratio (log scale; n=13 basal pairs, n=11 fear pairs, Mann-Whitney test, $P=0.0204$). XY skew-plots are presented as absolute value with line through origin. Bars graphs are presented as mean + S.E.M. *P<0.05, **P<0.01.

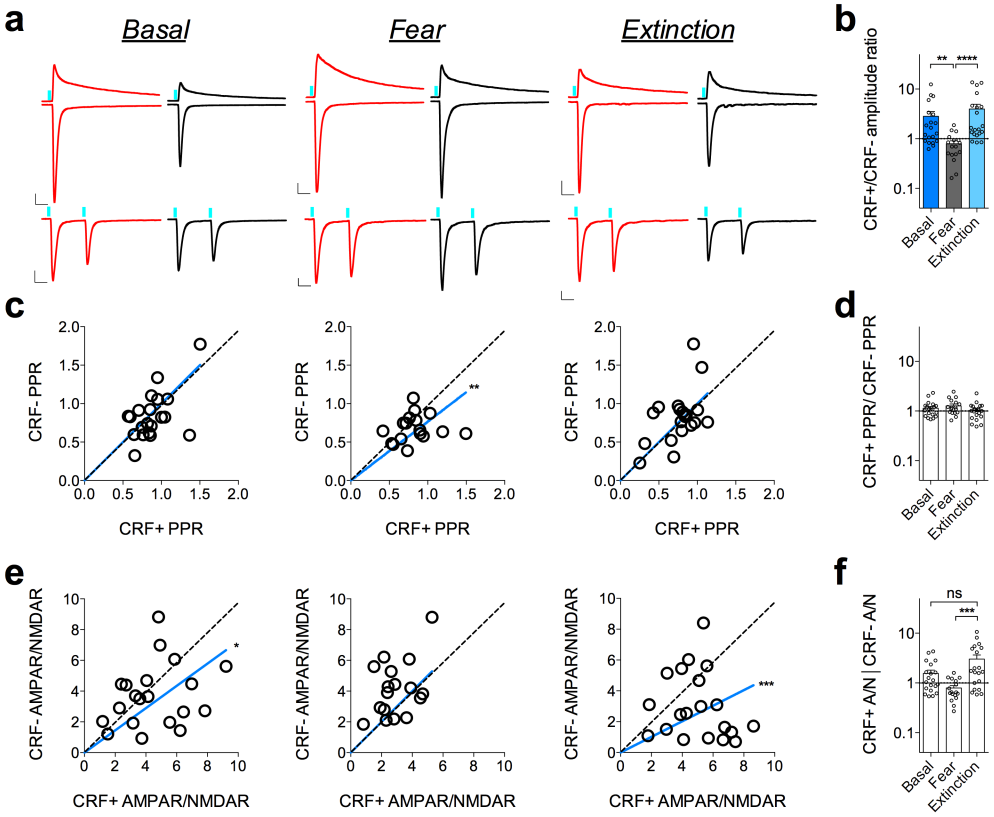

Supplementary Fig. 8. Experience-dependent remodeling of BLA-CeL input bias is not due to changes in presynaptic release probability. **a,** Traces of AMPAR/NMDAR ratios and PPR from neighboring CRF+ and CRF- neurons following stimulation of the BLA-CeL circuit (scale bars 20ms, 200pA). **b,** CRF+ and CRF- maximal oEPSC amplitude ratio (log scale; n=20 basal pairs, n=17 fear pairs, and n=20 extinction pairs, Kruskal-Wallis test, P=0.00008; post-hoc Dunn's multiple comparisons, basal vs. fear P=0.0025, fear vs. extinction P<0.0001). **c,** XY graphs depicting skew-plot of PPR from neighboring CRF+ and CRF- neurons across behavioral conditions (n=20 basal pairs, 5 mice, n=17 fear pairs, 5 mice, and n=20 extinction pairs, 5 mice, extra sum-of-squares F test, F(1,16)=11.29, P=0.0040 for fear). **d,** Ratio of PPR between neighboring CRF+ and CRF- neurons (log scale; n=20 basal pairs, n=17 fear pairs, and n=20 extinction pairs). **e,** XY graphs depicting skew-plot of AMPAR/NMDAR from neighboring CRF+ and CRF- neurons across behavioral conditions (n=20 basal pairs, 5 mice, n=17 fear pairs, 5 mice, and n=20 extinction pairs, 5 mice, extra sum-of-squares F test, F(1,19)=7.374, P=0.0137 for basal, and F(1,19)=20.89, P=0.0002 for extinction). **f,** Ratio of AMPAR/NMDAR between neighboring CRF+ and CRF- neurons (log scale; n=20 basal pairs, n=17 fear pairs, and n=20 extinction pairs, Kruskal-Wallis test, P=0.0013; post-hoc Dunn's multiple comparisons, fear vs. extinction P=0.0008). XY skew-plots are presented as absolute value with line through origin. Bar graphs are presented as mean + S.E.M. *P<0.05, **P<0.01, ***P<0.001, ****P<0.0001.

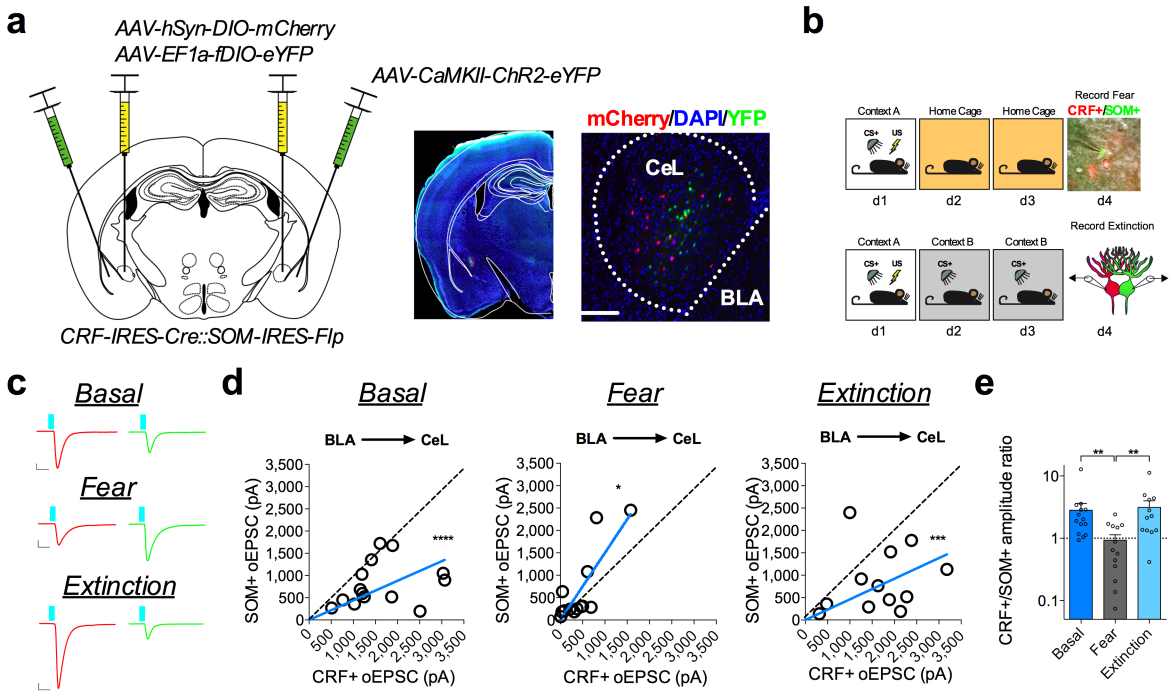

Supplementary Fig. 9. Fear conditioning and extinction training bidirectionally remodel the BLA-CeL circuit input bias onto CRF+ and SOM+ neurons. a, Left: optogenetic circuit mapping approach with viral injection. Right: image of YFP and mCherry expression in SOM+ and CRF+ neurons (image is from an animal with no injection of ChR2 expression in the BLA for clarity of fluorophore expression in adjacent CeA; scale bar 175µm). **b,** Experimental paradigm for dual patch-clamp recordings from CRF+ and SOM+ neurons in fear conditioned and fear extinguished mice. Bottom-right: DIC and fluorescent overlay image of dual-patch clamp recording from CRF+ and SOM+ pair. **c,** Traces of maximal oEPSC amplitude from CRF+ (red) and SOM+ (green) neuronal pairs across behavioral conditions for stimulation of the BLA-CeL circuit (scale bars 10ms, 200pA). **d,** XY graphs depicting skew-plot of maximal oEPSC amplitude from each CRF+ and SOM+ neuronal pair for behavioral conditions (n=14 basal pairs, 5 mice, n=13 fear pairs, 6 mice, and n=12 extinction pairs, 5 mice, extra sum-of-squares F test, $F(1,13)=47.34$, $P=0.00001118$ for basal, $F(1,12)=5.444$, $P=0.03784$ for fear, and $F(1,11)=21.16$, $P=0.00076493$ for extinction). **e,** CRF+/CRF- maximal oEPSC amplitude ratio (log scale; n=14 basal pairs, n=13 fear pairs, and n=12 extinction pairs, Kruskal-Wallis test, $P=0.0042$; post-hoc Dunn's multiple comparisons, basal vs. fear $P=0.0091$, fear vs. extinction $P=0.0076$). XY skew-plots are presented as absolute value with line through origin. Bar graphs are presented as mean + S.E.M. *P<0.05, **P<0.01, ***P<0.001, ****P<0.0001.

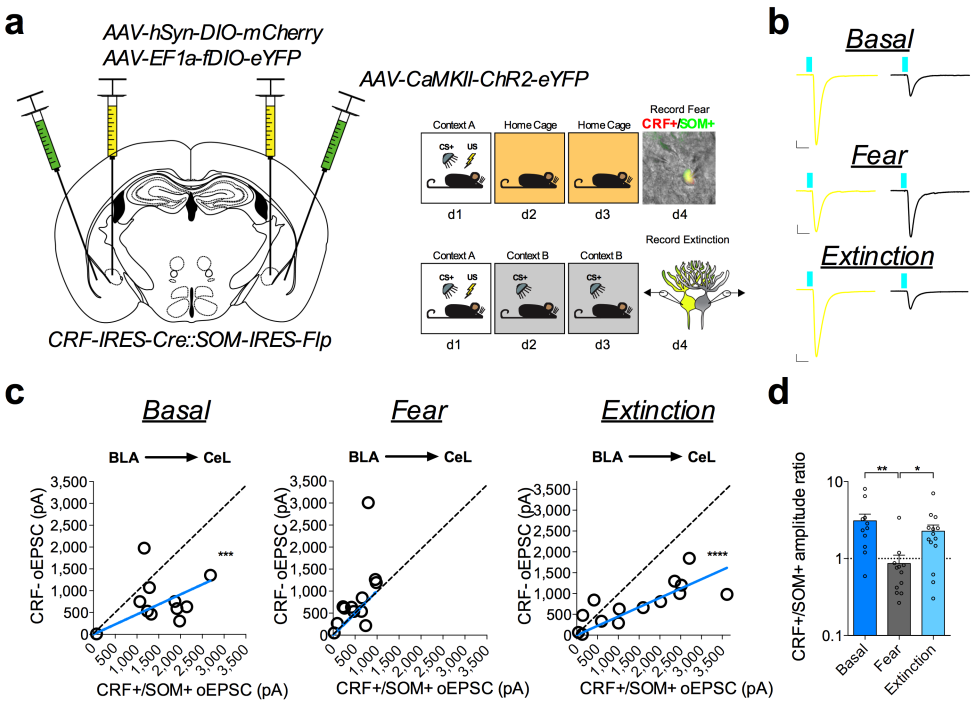

Supplementary Fig. 10. CRF+/SOM+ neurons demonstrate plasticity associated with CRF+ neurons. a, Left: optogenetic circuit mapping approach with viral injection. Right: experimental paradigm for dual patch-clamp recordings from CRF+/SOM+ (mCherry+/YFP+) neurons and adjacent CRF- neurons in fear conditioned and fear extinguished mice. Bottom-right: DIC and fluorescent overlay image of dual-patch clamp recording from CRF+/SOM+ and CRF- pair. **b,** Traces of maximal oEPSC amplitude from CRF+/SOM+ (yellow) and CRF- (black) neuronal pairs across behavioral conditions for stimulation of the BLA-CeL circuit (scale bars 10ms, 200pA basal, 10ms, 100pA fear, 10ms, 400pA extinction). **c,** XY graphs depicting skew-plot of maximal oEPSC amplitude from each CRF+/SOM+ and CRF- neuronal pair for behavioral conditions (n=11 basal pairs, 4 mice, n=12 fear pairs, 4 mice, and n=14 extinction pairs, 5 mice, extra sum-of-squares F test, $F(1,10)=29.83$, $P=0.00027627$ for basal, and $F(1,13)=121.0$, $P=0.00000006$ for extinction). **d,** CRF+/SOM+ and CRF- maximal oEPSC amplitude ratio (log scale; n=11 basal pairs, n=12 fear pairs, and n=14 extinction pairs, Kruskal-Wallis test, $P=0.0026$; post-hoc Dunn's multiple comparisons, basal vs. fear $P=0.0022$, fear vs. extinction $P=0.0185$). XY skew-plots are presented as absolute value with line through origin. Bar graphs are presented as mean + S.E.M. *P<0.05, **P<0.01, ***P<0.001, ****P<0.0001.

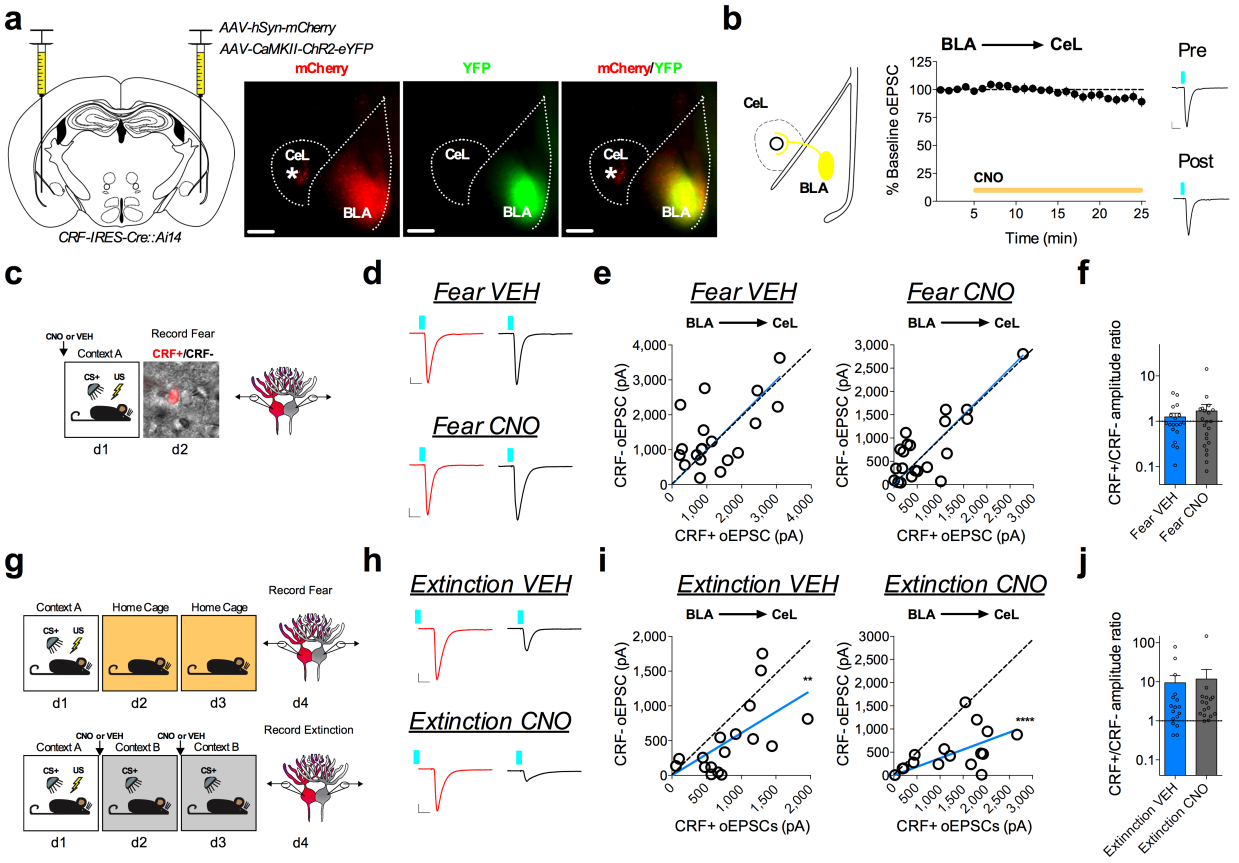

Supplementary Fig. 11. CNO administration does not affect plasticity in the BLA-CeL circuit. a, Left: mixed viral injection strategy for electrophysiological assessment of the BLA-CeL circuit in mCherry control animals. Right: image of ChR2-eYFP and mCherry expression in the BLA from a coronal slice used for recordings (*indicates CRF+ neurons in the CeL expressing TdTomato; scale bars 200µm). **b,** Left: schematic of ChR2-eYFP and mCherry co-expression in the BLA-CeL circuit. Right: summary data from bath application of CNO while recording oEPSC amplitude in the CeL (n=12 cells, 5 mice). Right: traces of oEPSCs before and after bath application of CNO (scale bar 10ms, and 200pA). **c,** Experimental paradigm of electrophysiological assessment of BLA-CeL circuit in mCherry control animals after fear learning. Bottom-right: DIC and fluorescent overlay image of dual-patch clamp recording from CRF+ and CRF- pair. **d,** Traces of maximal oEPSC amplitude from CRF+ (red) and CRF- (black) neuronal pairs across fear treatment groups for stimulation of the BLA-CeL circuit (scale bars 10ms, and 200pA). **e,** XY graphs depicting skew-plot of maximal oEPSC amplitude from each CRF+ and CRF- neuronal pair for behavioral conditions (n=19 fear VEH pairs, 5 mice, n=21 fear CNO pairs, 5 mice). **f,** CRF+/CRF- maximal oEPSC amplitude ratio (log scale; n=19 fear VEH pairs, n=21 fear CNO pairs). **g,** Experimental paradigm of electrophysiological assessment of BLA-CeL circuit in mCherry control animals after extinction training. **h,** Traces of maximal oEPSC amplitude from CRF+ (red) and CRF- (black) neuronal pairs across extinction treatment groups for stimulation of the BLA-CeL circuit (scale bars 10ms, and 200pA). **i,** XY graphs depicting skew-plot of maximal oEPSC amplitude from each CRF+ and CRF- neuronal pair for behavioral conditions (n=17 extinction VEH pairs, 4 mice, and n=16 extinction CNO

pairs, 4 mice, extra sum-of-squares F test for extinction VEH, $F(1,16)=15.43$, $P=0.0012$, extra sum-of-squares F test for extinction CNO, $F(1,15)=92.60$, $P=0.00000008$). **j,** CRF+/CRF- maximal oEPSC amplitude ratio (log scale; n=17 extinction VEH pairs, n=16 extinction CNO pairs). XY skew-plots are presented as absolute value with line through origin. Bar graphs are presented as mean + S.E.M. **P<0.01, ****P<0.0001.

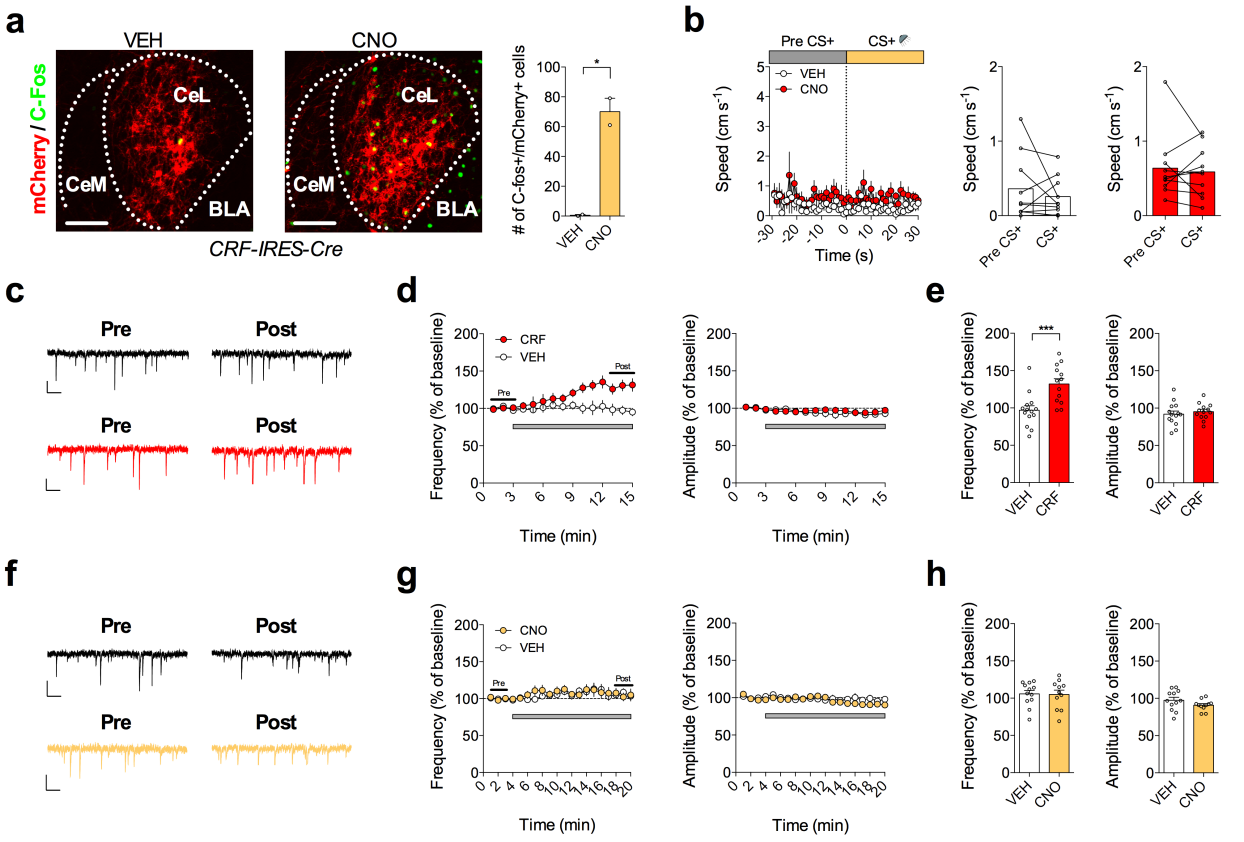

Supplementary Fig. 12. Gαq-coupled-DREADD excites CRF+ neurons in the CeL and does not cause local CRF release. a, Left: images representing immunohistochemical analysis of immediate early gene c-Fos in *CRF-IRES-Cre* mice expressing cre-dependent hM3D(Gq)-mCherry in the CeL, followed by systemic administration of VEH or CNO (scale bar 200µm). Right: quantification of c-Fos+ neurons overlapping with hM3D(Gq)-mCherry+ neurons in the CeL (n=2 VEH, n=2 CNO mice, two-tailed unpaired t-test, P=0.0164). **b,** Average time-locked speed trace during early fear memory recall phase for mice injected with VEH or CNO (first 5 CS+ presentations on extinction session 1 day 2 (d2)) from the same mice in experiment presented in Fig. 5d,e. **c,** Representative traces of sEPSCs from CeL neurons before (pre) and after (post) VEH or CRF application (scale bars 100ms, 10pA). **d,** Effects of VEH or CRF bath application on sEPSC frequency and amplitude over time (gray bar indicates application of CRF or VEH). **e,** Summary of sEPSC frequency and amplitude after application of VEH or CRF (n=14 VEH neurons, 5 mice, n=13 CNO neurons, 5 mice, two-tailed unpaired t-test, P=0.0008). **f,** Representative traces of sEPSCs from CeL neurons before (pre) and after (post) VEH or CNO application in mice expressing hM3D(Gq)-mCherry in CRF+ neurons of the CeL (scale bars 100ms, 10pA). **g,** Effects of VEH or CNO bath application on sEPSC frequency and amplitude over time in mice expressing hM3D(Gq)-mCherry in CRF+ neurons of the CeL (gray bar indicates application of CNO or VEH). **h,** Summary of sEPSC frequency and amplitude after application of VEH or CNO in mice expressing hM3D(Gq)-mCherry in CRF+ neurons of the CeL (n=12 VEH neurons, 5 mice, n=11 CNO neurons, 5 mice). Effects of CRF on sEPSC frequency or amplitude over time are presented as mean ± S.E.M., and bar graphs are presented as mean + S.E.M. *P<0.05, ***P<0.001.

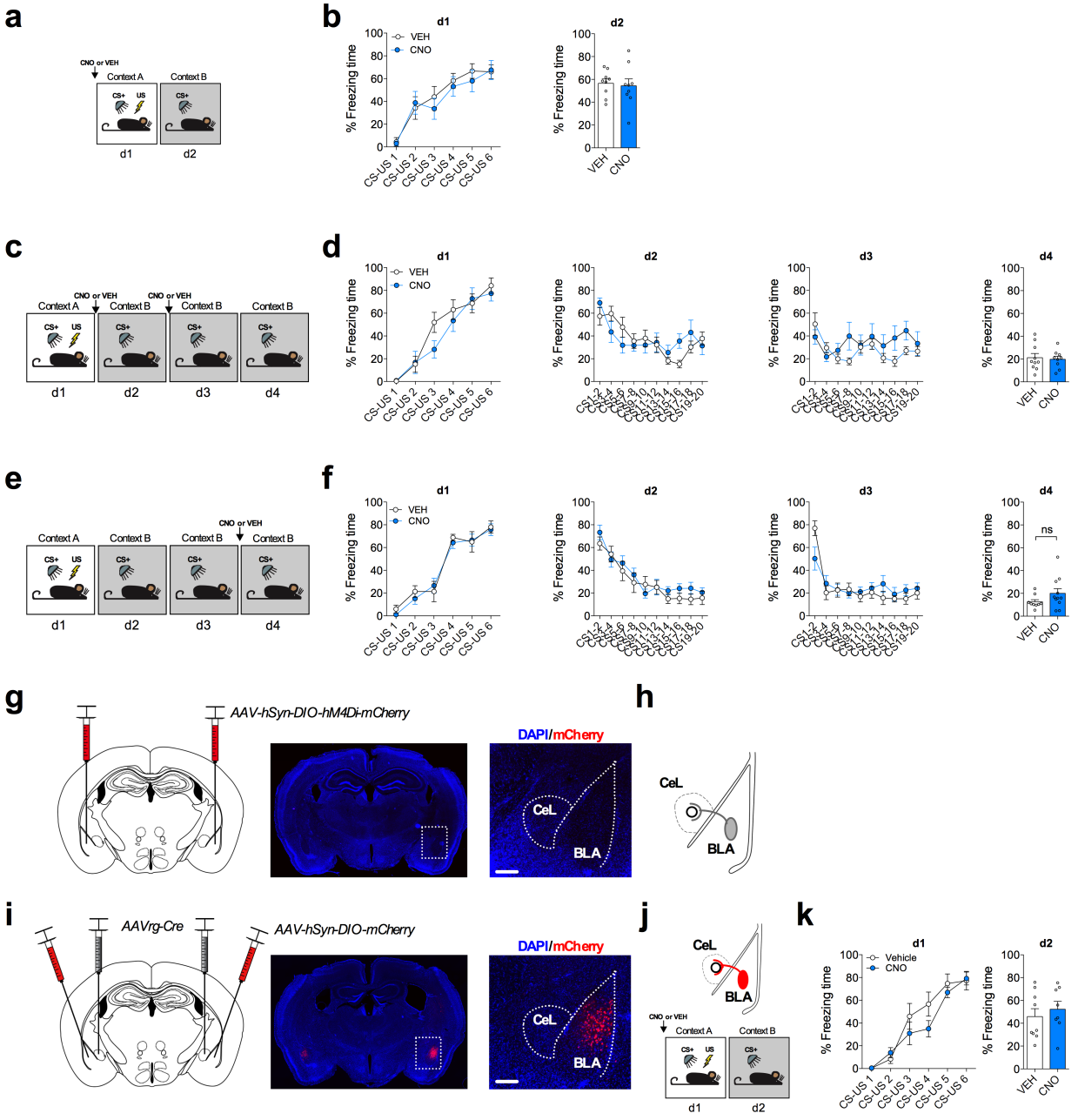

Supplementary Fig. 13. CNO administration does not affect freezing behavior. a, Experimental paradigm for administration of VEH or CNO during fear conditioning. **b,** Learning curves for VEH and CNO treated mice. Left to right, fear conditioning day 1 (d1), and fear memory recall test day 2 (d2) (n=9 mice per group). **c,** Experimental paradigm for administration of VEH or CNO during extinction learning. **d,** Learning curves for VEH and CNO treated mice. Left to right, conditioning day 1 (d1), extinction session 1 on day 2 (d2), extinction session 2 on day 3 (d3), and extinction memory recall test on day 4 (d4) (n=10 VEH mice, and n=9 CNO mice). **e,** Experimental paradigm for administration of VEH or CNO during an extinction memory recall test. **f,** Learning curves for VEH and CNO treated mice. Left to right,

conditioning day 1 (d1), extinction session 1 on day 2 (d2), extinction session 2 on day 3 (d3), and extinction memory recall test on day 4 (d4) (n=9 VEH mice, and n=11 CNO mice). **g,** Left: lack of intersectional injection strategy for delivery of cre-dependent hM4D(Gi)-mCherry to the BLA. Right: images depicting absence of hM4D(Gi)-mCherry expression in the BLA when AAVrg-Cre is not injected into the CeA (scale bar 200μm). **h,** Schematic of lack of hM4D(Gi)-mCherry expression specifically in BLA neurons projecting to the CeL when AAVrg-Cre is not injected into the CeA. **i,** Left: intersectional viral strategy for behavioral assessment of control fluorophore expression in the BLA-CeL circuit. Right: images depicting bilateral expression of cre-dependent mCherry in the BLA with close up of inset (scale bar 200μm). **j,** Experimental paradigm for administration of VEH or CNO during fear conditioning. Top: schematic of mCherry expression specifically in BLA neurons projecting to the CeL. **k,** Learning curves for VEH and CNO treated mice. Left to right, fear conditioning day 1 (d1), and fear memory recall test day 2 (d2) (n=9 VEH mice, and n=8 CNO mice). Learning curves are presented as mean ± S.E.M., and bar graphs are presented as mean + S.E.M.

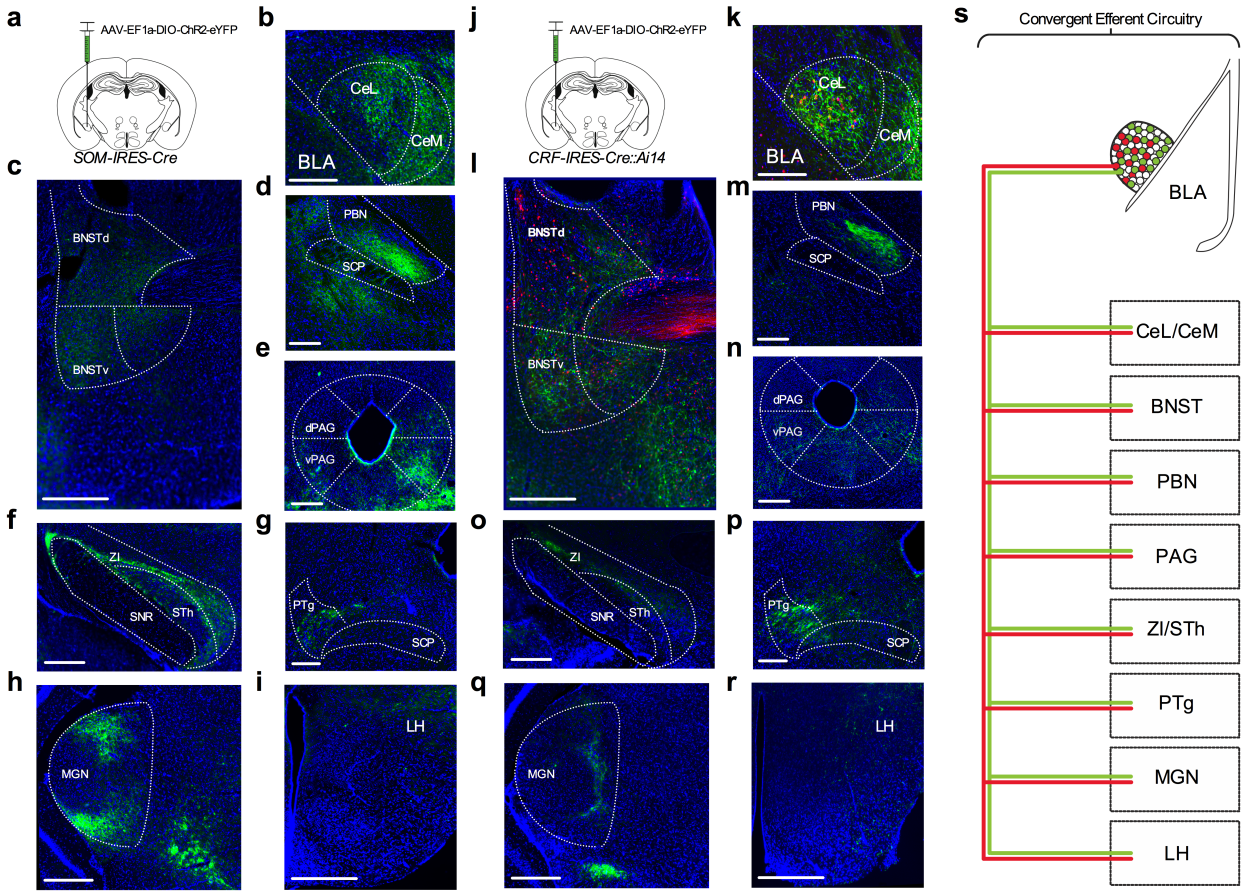

Supplementary Fig. 14. Convergent efferent projections of SOM and CRF neurons from the CeA. a, Optogenetic output circuit-mapping approach for Cre-dependent expression of ChR2-eYFP in SOM+ neurons of the CeA (n=5 mice). **b,** Local ChR2-eYFP cell body and synaptic terminal expression from SOM+ neurons in the CeL (scale bar 300µm). **c,** ChR2-eYFP synaptic terminal expression from SOM+ neurons in the dorsal and ventral BNST (scale bar 500µm). **d,** ChR2-eYFP synaptic terminal expression from SOM+ neurons in the PBN (note distribution of YFP in ventrolateral border of PBN; scale bar 200µm). **e,** ChR2-eYFP synaptic terminal expression from SOM+ neurons in the PAG (note distribution of YFP in the ventral and dorsal PAG; scale bar 400µm). **f,** ChR2-eYFP synaptic terminal expression from SOM+ neurons in the zona incerta/subthalamic nucleus (ZI/STh; scale bar 250µm). **g,** ChR2-eYFP synaptic terminal expression from SOM+ neurons in the pedunculotegmental nucleus (PTg; scale bar 250µm). **h,** ChR2-eYFP synaptic terminal expression from SOM+ neurons in the medial geniculate nucleus (note distribution of YFP in the dorsal and ventral MGN; scale bar 375µm). **i,** ChR2-eYFP synaptic terminal expression from SOM+ neurons in the lateral hypothalamus (LH; scale bar 500µm). **j,** Optogenetic output circuit-mapping approach for Cre-dependent expression of ChR2-eYFP in CRF+ neurons of the CeA (n=8 mice). **k,** Local ChR2-eYFP cell body and synaptic terminal expression from CRF+ neurons in the CeL (scale bar 300µm). **l,** ChR2-eYFP synaptic terminal expression from CRF+ neurons in the dorsal and ventral BNST (scale bar 400µm). **m,** ChR2-eYFP synaptic terminal expression from CRF+ neurons in the PBN (note distribution of YFP in dorsolateral border of PBN; scale bar 500µm). **n,** ChR2-eYFP synaptic

terminal expression from CRF+ neurons in the PAG (note transient distribution of YFP in the ventral PAG relative to the dorsal PAG; scale bar 400μm). **o,** ChR2-eYFP synaptic terminal expression from CRF+ neurons in the ZI/STh (scale bar 250μm). **p,** ChR2-eYFP synaptic terminal expression from CRF+ neurons in the PTg (scale bar 250μm). **q,** ChR2-eYFP synaptic terminal expression from CRF+ neurons in the MGN (note distribution of YFP in the medial MGN; scale bar 375μm). **r,** ChR2-eYFP synaptic terminal expression from CRF+ neurons in the LH (scale bar 500μm). **s,** Summary of convergent output structures of SOM+ and CRF+ neurons of the CeA.

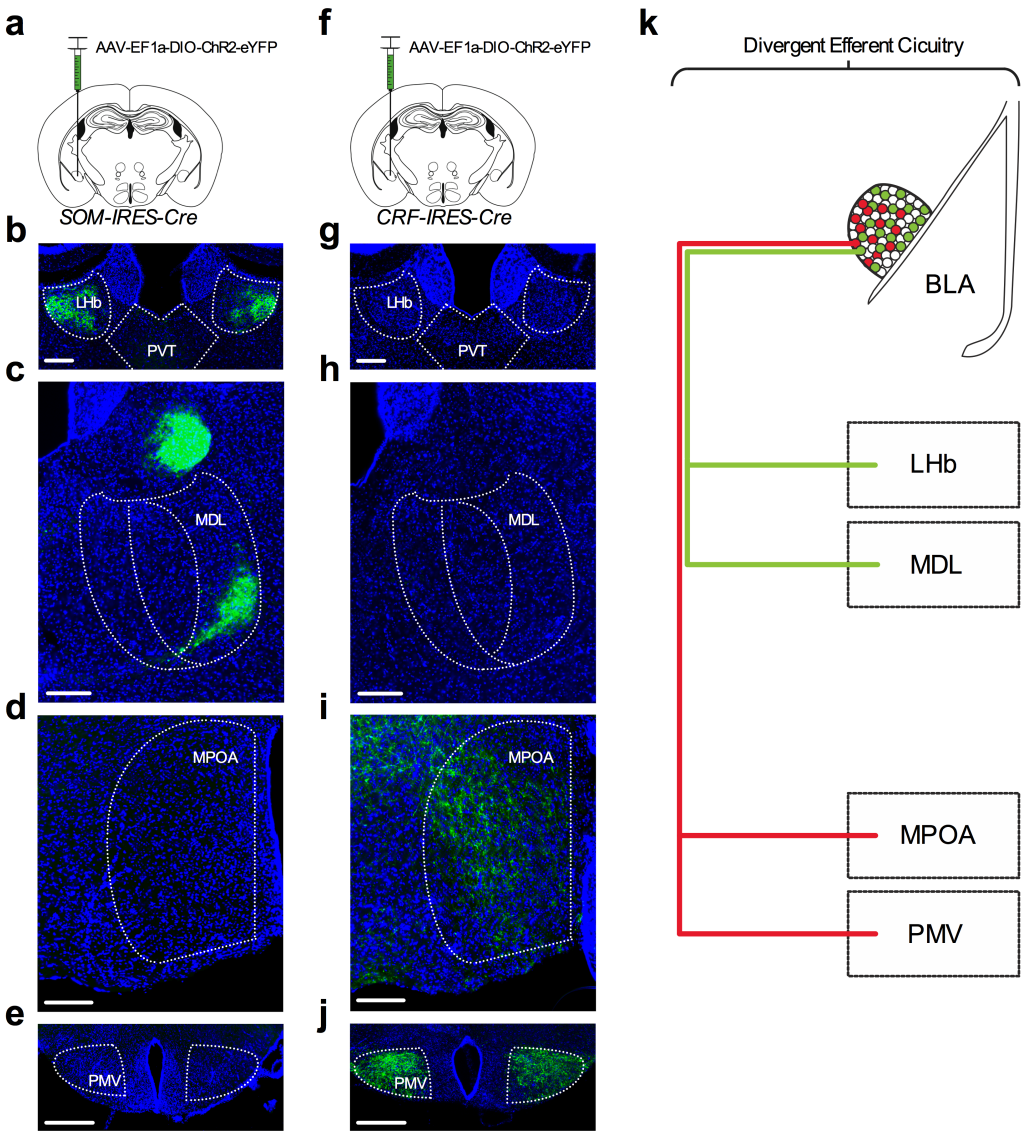

Supplementary Fig. 15. Divergent efferent projections of SOM and CRF neurons from the CeA. a, Optogenetic output circuit-mapping approach for Cre-dependent expression of ChR2-eYFP in SOM+ neurons of the CeA (n=3 mice). **b,** ChR2-eYFP synaptic terminal expression from SOM+ neurons in the lateral habenula (LHb; scale bar 250µm). **c,** ChR2-eYFP synaptic terminal expression from SOM+ neurons in the lateral portion of the medial dorsal thalamus (MDL; scale bar 125µm). **d,** Lack of ChR2-eYFP synaptic terminal expression from SOM+ neurons in the medial preoptic area (MPOA; scale bar 250µm). **e,** Lack of ChR2-eYFP synaptic terminal expression from SOM+ neurons in the ventral premammillary nucleus (PMV; scale bar 400µm). **f,** Optogenetic output circuit-mapping approach for Cre-dependent expression of ChR2-eYFP in CRF+ neurons of the CeA (n=3 mice). **g,** Lack of ChR2-eYFP synaptic terminal expression from CRF+ neurons in the LHb. **h,** Lack of ChR2-eYFP synaptic terminal expression from CRF+ neurons in the MDL. **i,** ChR2-eYFP synaptic terminal expression from CRF+ neurons in the MPOA (scale bar 250µm). **j,** ChR2-eYFP synaptic terminal expression from CRF+ neurons in the PMV (scale bar 400µm).

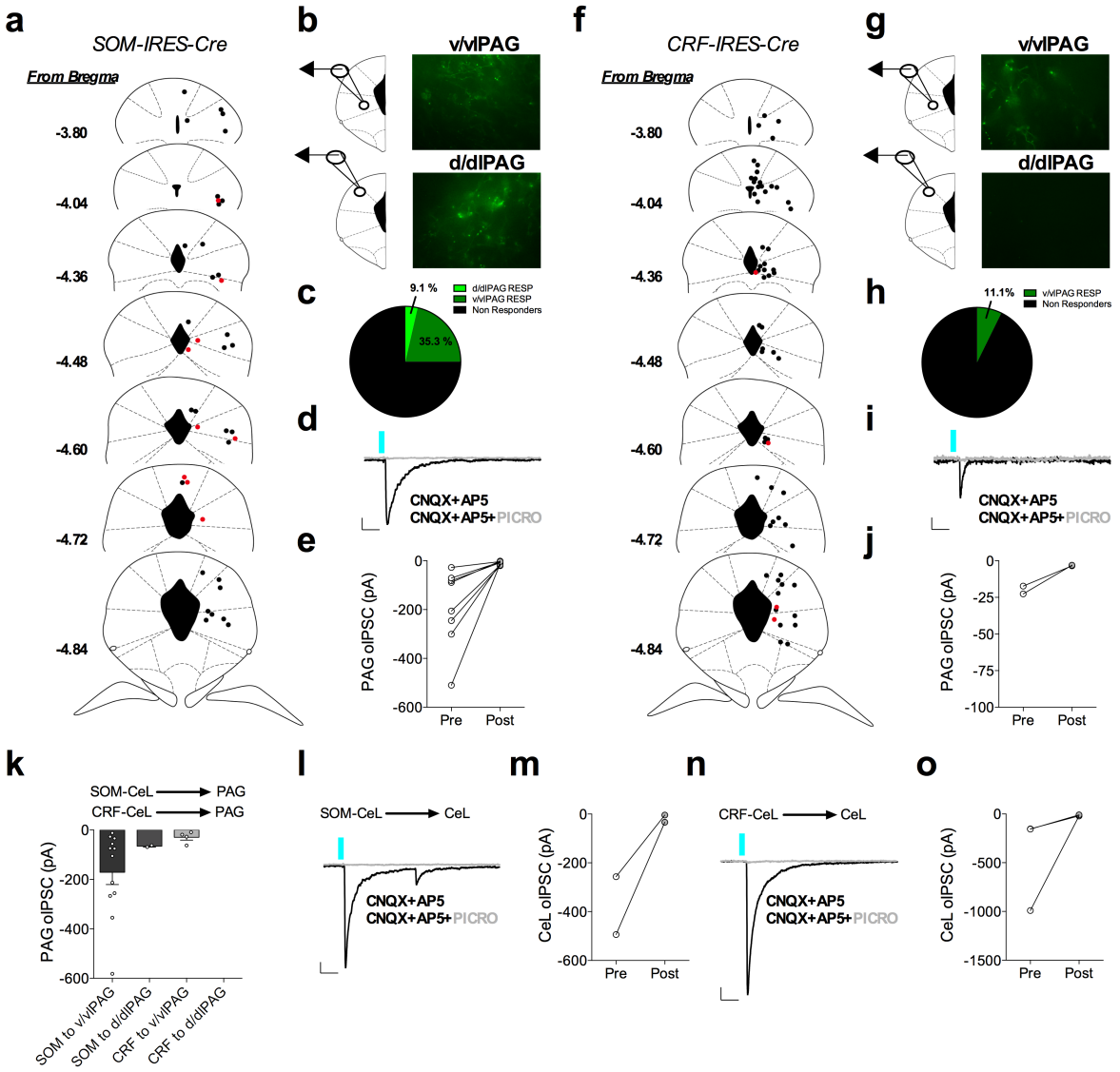

Supplementary Fig. 16. CRF and SOM neurons in the CeA signal through long-range and local GABAergic synapses to the PAG and CeL. a, Recording sites for long-range projections of SOM+ CeA neurons to the PAG. Red dots indicate responsive neurons demonstrating oIPSCs following ChR2 stimulation of axon terminals, and black dots indicate non-responsive neurons. **b,** Fluorescent images taken from slice recordings demonstrating the presence of ChR2-eYFP terminals in the ventral/ventrolateral PAG and the dorsal/dorsolateral PAG. **c,** Connectivity index indicating percentage of responsive and non-responsive PAG neurons from SOM+ input (n=56 neurons, 4 mice; RESP=responsive neurons). **d,** Example trace of time-locked oIPSC recorded from a responsive neuron in the PAG, which was blocked following application of picrotoxin (scale bars 20ms, 20pA). **e,** Summary of oIPSCs blocked by picrotoxin in the PAG (n=8 neurons, 4 mice). **f,** Recording sites for long-range projections of CRF+ CeA neurons to the PAG. Red dots indicate responsive neurons demonstrating oIPSCs following ChR2 stimulation of axon terminals, and black dots indicate non-responsive neurons. **g,** Fluorescent images taken from slice recordings demonstrating the presence of ChR2-eYFP terminals in the ventral/ventrolateral PAG and lack of terminals in the dorsal/dorsolateral PAG. **h,** Connectivity

index indicating percentage of responsive and non-responsive PAG neurons from CRF+ input (n=62 neurons, 4 mice; RESP=responsive neurons). **i,** Example trace of time-locked oIPSC recorded from a responsive neuron in the PAG, which was blocked following application of picrotoxin (scale bars 20ms, 20pA). **j,** Summary of oIPSCs blocked by picrotoxin in the PAG (n=2 neurons, 2 mice). **k,** Average amplitude of oIPSCs from SOM+ and CRF+ neuronal projections to the PAG (n=14 neurons, 4 mice for SOM+ input, n=2 neurons, 4 mice for CRF+ input). **l,** Example trace of time-locked oIPSC recorded from a SOM- responsive neuron in the CeL, which was blocked following application of picrotoxin (scale bars 20ms, 50pA). **m,** Summary of oIPSCs blocked by picrotoxin in the CeL (n=2 neurons, 2 mice). **n,** Example trace of time-locked oIPSC recorded from a CRF- responsive neuron in the CeL, which was blocked following application of picrotoxin (scale bars 20ms, 100pA). **o,** Summary of oIPSCs blocked by picrotoxin in the CeL (n=3 neurons, 3 mice). Bar graphs are presented as mean + S.E.M.

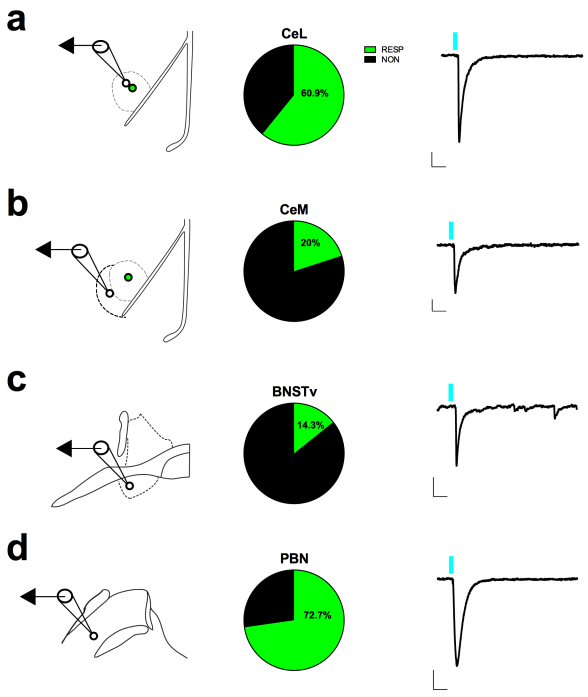

Supplementary Fig. 17. Connectivity index of CeA CRF+ neurons to areas with high or low ChR2-YFP terminal density. a-d, Percentage of responsive neurons from patch-clamp recordings of areas expressing visible YFP signal in slice (n=46 CeL, n=5 CeM, n=7 vBNST, and n=11 PBN cells, 17 mice; RESP=responsive, NON=non-responsive). Right column: representative traces of oIPSCs from responsive neurons in the CeL, CeM, vBNST, and PBN (scale bars 50ms, 100pA).

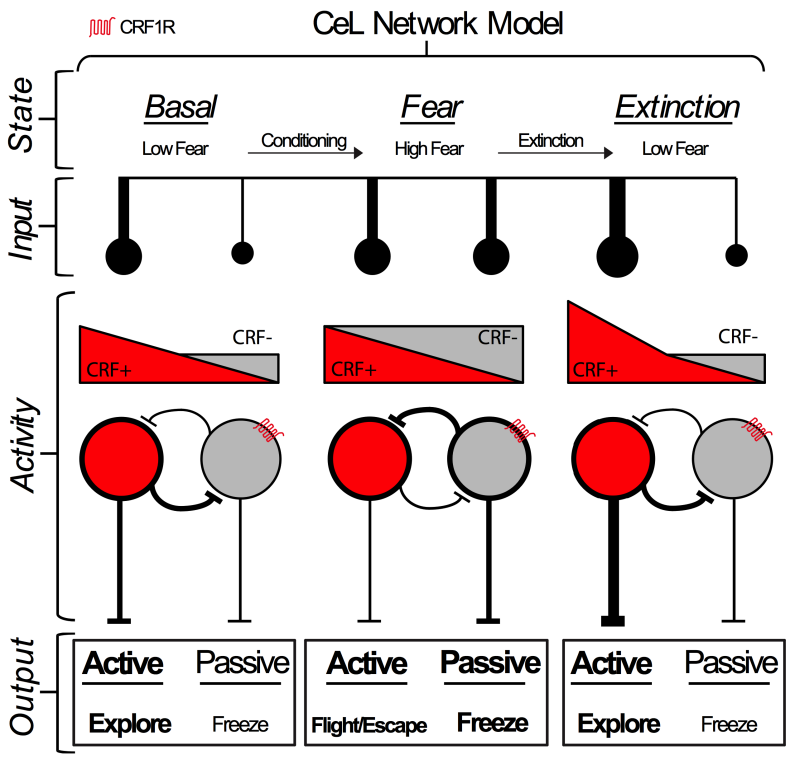

Supplementary Fig. 18. Summary of dynamic experience-dependent remodeling of CeL neuronal activity on the expression of fear behavior. This tiered CeL network model reflects overall input bias onto CRF+ and CRF- neurons across contextual states, the hypothesized activity of CeL neurons during excitatory drive from input sources, and the expected behavioral outputs. Since there is greater input onto CRF+ neurons in basal conditions, it is possible that salient sensory cues from the environment serve to drive active motivational states, such as exploration and foraging, behaviors that would require suppressing motor inhibition and are consistent with CeA-CRF+ neurons contributing to the expression of appetitive behavior under non-threatening contexts. Previous findings suggest that during early or weak threat assessment, when association between stimuli and danger is still ambiguous, CRF+ neurons are recruited to selectively enhance associative learning through CRF release and subsequent CRFR1-mediated synaptic plasticity onto CeL neurons, which we further show results in equal relative sensory input from the BLA onto CRF+ and CRF-/SOM+ neurons. Following re-exposure to a threat-predictive CS, an animal can mount conditioned active or passive fear responses via mutually inhibitory connections between CRF+ and CRF-/SOM+ neurons, a result that reflects the predicted imminence or proximity of a threat and can be learned during extended training paradigms. However, we propose that as the contingency between the CS and US degrades during extinction learning, such that the CS no longer accurately predicts threat exposure, there is a restoration of greater relative sensory input back onto CRF+ neurons, resulting in the suppression of passive freezing and the promotion of active exploration of the environment. This model is consistent with the overall role of CeA neurons impinging on hindbrain effector nuclei that tightly regulate motivational motor programs critical to survival.

CHAPTER III

CONCLUSIONS AND FUTURE DIRECTIONS

To Freeze or Not to Freeze: A Model for Experience-Dependent Behavioral Selection Across Fear States

The CeL is a unique structure in that it can regulate both positive and negative valence behaviors to promote survival. Genetically distinct or partially overlapping populations of CeL neurons can individually drive positive emotional states, negative emotional states, or both. Consequently, the CeL may serve as nexus for integrating internal and external sensory information to expedite proper behavioral control. The data presented in Chapter II provide a novel framework for how excitatory afferents to the CeL may serve this purpose. Since the BLA is responsible for multisensory processing and determining the valence of sensory information (Beyeler et al., 2018; Beyeler et al., 2016; Correia and Goosens, 2016; Kim et al., 2016; Tye, 2018; Zhang and Li, 2018), it is not surprising that we find this circuit to be the main determinant of gluatamatergic remodeling onto CRF+ and CRF- neurons. Although the INS-CeL and PBN-CeL circuits serve important functions in regulating fear in their own right, the BLA-CeL circuit appears the most relevant in shifting the scales of excitatory input in favor of one CeL population over another, as input bias in this circuit mostly closely reflects the net changes in excitatory transmission in the CeL across fear states. It is hypothesized that CS information from the BLA can be relayed to the CeL following fear learning to drive the selection of distinct classes of neurons and modulate fear levels. We have expanded upon this concept and amassed our data into a working model for how behavioral control over fear occurs in the CeL following

extinction training as well (Supplementary Fig. 18). Intriguingly, we find that CRF+ neurons can diminish passive fear responses, such as freezing, and that they receive greater relative excitatory input under conditions of low-fear. This would suggest that excitatory inputs have a greater influence on CRF+ neuronal activity when passive fear expression is expected to be low, such as in non-conditioned (i.e. non-stressed) animals or animals that have undergone extinction training (both scenarios when it is inappropriate or maladaptive to mount defensive fear responses). However, we have not specifically tested how excitatory afferents to the CeL regulate the firing rates of individual CeL neurons *ex vivo* in the absence of GABA receptor blockers. It will be important for future studies to expand upon our model by examining the firing rates of CRF+ neurons *in vivo* during our behavioral assays, and how these neurons can be driven to fire action potentials from various inputs.

In the absence of associative fear learning (i.e. naive/basal condition), it is feasible that positive valence information from the BLA may be relayed to the CeL to guide behavior. In support of this idea, CRF+ neurons have been shown to regulate appetitive behavior in non-threatening contexts, which is thought to depend on input from pro-appetitive and positive-valence neurons upstream in the BLA (Kim et al., 2016). These BLA neurons are characterized by their expression of protein phosphatase 1 regulatory inhibitory subunit B (Ppp1r1b), which produce the same appetitive behaviors that are associated with CRF+ neuronal activation, and whose activation also reduces negative valence behaviors such as conditioned freezing (Kim et al., 2016). Notably, these positive-valence neurons project heavily to the CeL and infralimbic mPFC, and are genetically distinct from negative-valence neurons in the BLA that express R-spondin-2 (Rspo2). Rspo2+ neurons are necessary for conditioned freezing, project to the prelimbic mPFC, and form mutually inhibitory interactions with Ppp1r1b+ neurons. Thus, it is

likely "fear on" and "fear off" neurons are Rspo2+ and Ppp1r1b+, respectively. One intriguing explanation of our results is that BLA-CeL remodeling involves adjustments in the weight of excitatory synapses from these separate populations of BLA cells onto CRF+ and CRF- neurons. Future studies should examine the overlap of Ppp1r1b+ neurons with previously identified extinction neurons in the BLA (i.e Thy1+ neurons) and how these positive-valence neurons functionally regulate the excitability of CeA cell-types, as opposed to Rspo2+ neurons.

Of note, appetitive responses are typically promotor and instrumental behaviors, which require suppression of circuits that cause immobility. As such, a bias in the activation of CRF+ neurons by BLA afferents would likely serve to prevent freezing behavior via local competitive and inhibitory interactions with other CeL neurons, likely CRF-/SOM+ neurons, and drive promotor motivational responses (Supplementary Fig. 18) (Fadok et al., 2017). For example, the fact that CRF+ neurons regulate positively reinforcing behaviors in non-threatening contexts suggests the possibility that excitatory afferents recruit CRF+ neuron activity to stimulate exploration of the environment. This increase in exploration may also occur during the late stage of extinction training when the CS-US contingency has significantly degraded. Yet, other findings suggest that CRF+ neurons promote active fear responses in highly threatening contexts, in which a stimulus predicts imminent danger (i.e. during the early phases of fear recall or extinction training) (Fadok et al., 2017). Although these findings in the literature are seemingly conflicting, one consistent aspect across all of these results is that each behavioral paradigm produces an active motor phenotype. In non-threatening (low fear) contexts CRF+ neurons can drive active motivational responses that are appetitive: self-stimulation, exploration, and water consumption (Kim et al., 2017), and in threatening contexts (high fear) also can drive active motivational responses that are aversive: flight, escape, and avoidance (Fadok et al., 2017).

Given that CeL neurons impinge on hindbrain nuclei that tightly regulate survival-oriented motor programs, we propose that CRF+ neurons simply regulate active motor phenotypes. Importantly, the CeL does not work in isolation, and corresponding brain networks relevant to an animal's context and internal state will work in parallel to determine the behavioral strategy that is selected. Thus, the functional output that CeL-CRF+ neurons influence is always the same, but the behaviors may seem qualitatively different depending on the context and cooperation from other brain circuits. Future studies using different learning paradigms could further test our model. For instance, unlike inescapable USs, which promote the acquisition of passive conditioned fear responses, shuttle-box paradigms provide animals with an option for escaping a US by moving to a new location, allowing animals to acquire active conditioned fear responses to threat-predictive cues. Therefore, if CRF+ neurons simply regulate active motor responses, we might expect greater relative excitatory transmission onto CRF+ neurons than CRF-/SOM+ neurons following shuttle-box/avoidance learning. Alternatively, we might also expect greater relative excitatory transmission onto CRF+ neurons following positive reinforcement learning in non-threatening contexts, where the CS predicts the presence of a potential reward the animal can actively seek out.

Although local GABAergic inhibitory interactions between CRF+ and SOM+ neurons are thought to mediate the decision to freeze or not to freeze, another possible mechanism could be differences in long-range efferent projection patterns. We find CRF+ and SOM+ neurons have differential projection patterns to the LHb, MDL, MPOA, and PMV. SOM+ neurons project heavily to the LHb and MDL, whereas CRF+ neurons project to the MPOA and PMV. Our output-mapping results indicate these are the main brain regions in which these CeL populations do not seem to have significant overlapping projections. Interestingly, the LHb has

long been implicated in flexible decision-making and rapidly integrating internal and external sensory information during behavioral selection in complex environments (Baker and Mizumori, 2017; Mizumori and Baker, 2017). Furthermore, the LHb drives adaptive behavioral responses based on the expected outcomes of sensory information (Baker and Mizumori, 2017; Mizumori and Baker, 2017). SOM+ neurons may therefore impart the decision to freeze during fear recall by biasing activity of the LHb towards the expected outcome of the CS. Additionally, the MDL is heavily implicated in associative memory and action-outcome relationships (Mitchell and Chakraborty, 2013), suggesting SOM+ neurons may relay fear memory information to the MDL to promote freezing responses. Conversely, the MPOA and PMV are essential for prosocial and aggressive behaviors related to mating, social bonding, and copulation. Individual neurons in these regions can drive appetitive and rewarding social behaviors or aggressive responding towards conspecifics, respectively (Lin et al., 2011; McHenry et al., 2017; Soden et al., 2016). Thus, it is conceivable that CRF+ neurons may signal to the MPOA or PMV to regulate approach, exploration, or fight-or-flight responses causing a shift in behavioral strategy to presentation of the CS during extinction learning. These CRF-specific projection patterns may also explain some of the appetitive behaviors that occur when CRF+ neurons are ectopically stimulated. Given that the functions of various efferent projection patterns from the CeL are not well understood, dissecting the role of these circuitries from individual CeL populations is of great importance for future studies examining shifts in behavioral strategies across fear states, and will be an important update to our model.

Despite the different projection patterns between CRF+ and SOM+ neurons, we also find that these neurons converge on the PAG. Since the PAG is critical for defensive behaviors and the CeA-PAG circuit is believed to drive freezing responses, we further explored the degree of

connectivity to the PAG from each of these neuronal populations. Consistent with the critical role of the v/vlPAG in generating conditioned freezing, we found a greater degree of connectivity from SOM+ neurons, with only minimal connectivity from CRF+ neurons. Overall, the fact that CRF+ and SOM+ neurons also share many converging efferent projections suggests that their differences in regulating freezing responses could also be mediated by differences in their connectivity with GABAergic or glutamatergic cell classes in downstream microcircuits. The CeA-PAG circuit has been shown to disinhibit v/vlPAG projection neurons, which would be expected to generate freezing responses (Tovote et al, 2016), but it remains to be determined if this is true for all classes of CeA neurons or differs between various populations. We also find that SOM+ neurons synapse onto d/dlPAG neurons, but CRF+ neurons do not, providing another potential explanation for differences in the regulation of defensive behavioral strategies. Parsing out the microcircuits of long-range efferents from these neurons within the same brain structures could provide more information as to how these neurons regulate behavioral responses across fear learning and extinction. Furthermore, an intriguing line of investigation for future research would be to examine potential changes in the GABAergic output of CRF+ and SOM+ neurons following fear acquisition and extinction, as plasticity and remodeling of the inhibitory synapses downstream of these neurons may further determine behavioral responses across fear states.

Fast Neurotransmission Versus Neuromodulation in High or Low Fear States

A surprising phenomenon of CeL function is that individual cell-types appear to regulate opposing behaviors to that which would be expected from release of their neuropeptides. For instance, excitation of SOM+ neurons produces rapid and unconditioned freezing responses, whereas SOM peptide signaling within the amygdala has been shown to reduce anxiety and fear

expression (Kahl and Fendt, 2014; Yeung et al., 2011; Yeung and Treit, 2012). Similarly, stimulation of CRF+ neurons produces active phenotypes and impairs freezing, while CRF peptide signaling in the amygdala typically enhances conditioned freezing behavior and fear acquisition (Sanford et al., 2017; Wiersma et al., 1998). These data suggest that the real-time expression of rapid behavioral responses during activity of CRF+ or SOM+ neurons is more likely driven by fast neurotransmission, while the neuropeptides they release may subserve latent or delayed effects on plasticity, learning, and memory.

Neuropeptides are often released following bouts of high-frequency stimulation and signal primarily through GPCRs, which have a slower effect on cellular excitability and synaptic transmission than canonical neurotransmitters. One possibility is that CRF and SOM peptides serve as a feedback mechanism that is meant to stabilize or regulate CeL function after sustained or robust activity. In this case, extensive activation of SOM+ neurons under highly stressful scenarios will adaptively drive freezing responses, but may also release SOM peptide to dampen passive fear responses so that fear behavior can normalize following stress. This could serve as one means of homeostasis following chronic or highly traumatic stress exposure, and could be an endogenous mechanism for preventing the development of trauma-induced illness, reducing stress-induced anxiety, or counteracting maladaptive fear learning. Alternatively, activation of CRF+ neurons could prevent passive freezing responses when they are unwarranted, but prolonged activation may produce CRF peptide release and facilitate behavioral sensitization to stressful stimuli. In support of this hypothesis, CRF peptide signaling in the CeA has been shown to boost acquisition of conditioned freezing responses during fear learning by enhancing excitatory transmission onto CRF1R+ neurons (Sanford et al., 2017). CRF1R+ neurons have robust colocalization with SOM+ neurons and demonstrate excitatory synaptic potentiation

following application of CRF, a result that is congruent with our findings of enhanced sEPSCs onto CeL neurons following bath application of CRF onto acute brain slices. Remarkably, this phenomenon of CRF-induced plasticity and enhancement of fear acquisition only seems to occur under low-threat conditions where the CS-US association is more ambiguous (low-intensity foot-shocks). Accordingly, our data suggests activation of CRF+ neurons would be more robust in conditions where the predictability of the CS outcome is low. In low-threat circumstances, freezing levels are not high, and thus it would be expected that CRF+ neurons in the CeL would be more active. CRF peptide release in this case may then serve to accelerate fear learning and memory formation by enhancing long-term plasticity in the CeL. Overall, the CeL as a system could balance appropriate behavioral responding through mechanisms of negative feedback by altering cellular activity of the CeM or remodeling excitatory drive to neurons that promote distinguishable defensive behaviors in the CeL. With the development of new genetic tools for measuring neuropeptide release *in vivo*, these hypotheses can be tested more directly.

Timing is Everything: Necessity and Redundancy in Corticolimbic Fear Circuits

A common goal of neuroscience research is to understand which components of the CNS determine a specific emergent property of behavior or physiology. This process spans all levels of analysis, from molecules, to individual cells, to cell ensembles, to nuclei, to circuits, and even to whole networks in the brain. On a cellular and system level, our goal was to examine the sufficiency or necessity of the BLA-CeL circuit and its experience-dependent plasticity in regulating learning across fear states, and how the downstream bias in excitatory input strength onto CRF+ neurons could be explained by the function of these neurons. To this end, we used ectopic excitation or inhibition with DREADDs to manipulate the BLA-CeL circuit and CRF+

neurons in the CeL. Importantly, we found that activity of principal BLA neurons is necessary for remodeling of the BLA-CeL input bias following both fear conditioning and extinction training. Because BLA activity is required for this bidirectional shift in input bias, we further attempted to test whether this plasticity is necessary for the bidirectional expression in freezing behavior that occurs with fear conditioning and extinction training, albeit indirectly. Surprisingly, the results of these experiments were dependent on the time-point in which the circuit was inhibited. Inhibition of the circuit during extinction memory recall increases freezing, which is why the circuit and its plasticity following extinction training are required for the full retrieval of extinction memory. Yet, our inhibition of the BLA-CeL circuit during extinction training sessions does not impact within-session freezing levels or extinction memory recall the following day. This finding suggests that reductions in within-session freezing during extinction training or extinction memory recall are not solely reliant on BLA inputs to CeL neurons.

Since BLA-CeL circuit is not required for within-session extinction, it is likely compensatory circuits in the brain can still drive extinction learning in the face of compromised circuit remodeling. Candidate circuits for this compensatory action could be the efferent projections of the infralimbic mPFC. As previously mentioned, the infralimbic mPFC is a key brain region in driving extinction learning, and this form of top-down control over subcortical regions could still guide behavior during extinction sessions. Nevertheless, once remodeling has already occurred, BLA inputs to CeL neurons are then critical for reducing conditioned freezing, suggesting other brain regions cannot provide compensation at this point. A possible explanation for the timing dependency of these results could be that the infralimbic mPFC-BLA projections recruit *vm*ICMs to reduce CeM activity during extinction training, while the plasticity at BLA-CeL neurons is ongoing and being consolidated. Supporting this idea, infralimbic mPFC neurons

send dense and direct excitatory projections to *vm*ICMs and activation of the infralimbic mPFC causes high-frequency firing of *vm*ICMs (Amir et al., 2011; Cassell and Wright, 1986; McDonald et al., 1996). Subsequently, once plasticity has been fully established a memory trace is formed, and the recruitment of BLA "fear off"/extinction neurons during CS exposure in the extinction context can recruit activity of CRF+ neurons in the CeL to dampen any CS-elicited freezing. In support of this notion, our DREADD manipulations of CRF+ neuronal inhibition downstream of the BLA yield the exact same results when inhibition occurs at the same time-points as our circuit-specific manipulations. Much like the function of their BLA inputs, CeL-CRF+ neurons do not appear to be necessary for inhibiting conditioned freezing, only for extinction memory retrieval. Therefore, it is possible that CRF+ neurons are only a subpopulation of a much larger genetically or functionally defined group of CeL neurons that are necessary for suppressing within-session freezing responses during extinction training sessions, and CRF+ neuronal activation alone is not necessary for preventing within-session freezing. Given the rapid progress in defining new genetic markers and functionally defined neurons in the CeL, further characterization of genetic overlap of CRF+ neurons with other markers will be important for determining this possibility.

Despite the convergence of our behavioral and physiological results, there are notable differences in the sufficiency versus necessity of CRF+ neurons in regulating freezing during fear conditioning and extinction training. Although CRF+ neurons are not necessary for diminishing freezing during extinction training sessions, our excitatory DREADD experiments indicate that CRF+ neurons are sufficient to reduce freezing responses, which is consistent with the relatively greater strength of BLA afferent input onto these neurons over CRF-/SOM+ neurons in low fear states. Firstly, we show that excitation of CRF+ neurons during extinction is

sufficient to rapidly diminish freezing responses, which we interpret as a facilitation of within session extinction. Secondly, we find that excitation of CRF+ neurons during fear conditioning is sufficient to reduce freezing during fear memory recall the following day, which further indicates that activity of these neurons is sufficient to impair fear memory formation. Somewhat surprisingly, excitation of CRF+ neurons during fear conditioning does not reduce within-session freezing, but it does reduce within-session freezing during extinction training. However, this result could be explained by the differences in reciprocal inhibitory connections between CeL neuronal populations. Approximately 75% of SOM+ neurons receive inhibitory synapses during excitation of CRF+ neurons, and *vice versa* (Fadok et al., 2017). Conversely, only about 25% of PKCδ+ neurons receive inhibitory synapses upon excitation from CRF+ neurons or SOM+ neurons, and *vice versa*. Thus, inhibitory interactions between CRF+ and PKCδ+ neurons are low, while inhibitory interactions between CRF+ and SOM+ neurons are high. Given that PKCδ+ neurons are also necessary for the acquisition of conditioned freezing responses, it is likely that excitation of CRF+ neurons during fear conditioning cannot override the influence of PKCδ+ neuronal activity on driving freezing responses, or prevent salient incoming signals to the CeL that reflect the US. However, in this case CRF+ neurons may still be sufficient to impair BLA-CeL plasticity onto SOM+ neurons via local inhibition. It will be important for future studies to further elucidate the degree of GABAergic signaling between each of these populations across fear states to provide more detail to our model.

Survival depends on an animal's ability to forage and seek out resources, which are exploratory behaviors aimed at achieving positive outcomes. These beneficial resources come in many forms (i.e. food, water, shelter, mates, companionship), but the choice to seek out these resources can become withheld by the experience of fear. In a naturalistic setting, animals need

to balance the risk of predation or injury while simultaneously dealing with the necessity to seek out natural rewards. This balance can involve complex computations in the brain that facilitate proper behavioral selection, and if these computations do not occur correctly disease or death may result. Out of necessity, associative fear learning evolved as simple means of understanding the potential exposure to danger when it is most likely to present itself, whereas extinction learning provides a means for understanding danger is no longer forthcoming so that one can return to everyday life. The use of animal models to measure these learning mechanisms has profound benefits, but is unfortunately limited by the fact that we are unable to fully understand the internal state and subjective experience of an animal without relying on some form of behavioral or endocrinological readout.

In our studies, the main dependent variable for assessing the level of fear is the percent time an animal spends freezing during the CS, and thus we interpret decreases in freezing as a decrease in fear expression. However, it is important to note that the decision an animal makes not to freeze can be driven by motivations other than just a dissipating experience of fear. Thus, it is equally important to consider a decrease in freezing as a possible increase in arousal and anxiety, avoidance, or an attempt to escape, as well as a potential increase in a positive exploration or assessment of the environment. We cannot exclude these possible explanations without future studies aimed at providing a more in depth examination of fear responses that compare threat-proximity and threat-intensity with the choice for alternate behavioral strategies. Hence, the neural computations in the amygdala that determine the decision to freeze or not to freeze are likely more complex than the current model of "fear on" and "fear off" interactions. As such, future models of CeL network function should take into consideration counteracting

circuits that regulate different internal states, or signal positive and negative valence information about the environment.

Overall, our data raise important questions about circuit remodeling across fear states in the context of neuropsychiatric disorders like PTSD. Future studies should seek to determine if impaired BLA-CeL circuit remodeling reflects the development or presence of maladaptive learning. Since BLA-CeL circuit remodeling appears to be an important determinant for proper fear learning, perturbations in the mechanisms contributing to this remodeling may reflect over-learning, and elevated expression of fear. Conversely, impairments of BLA-CeL circuit remodeling during extinction training could be an explanation for the recurrent expression of fear memory and resilience to extinction training found in humans with PTSD. New studies using rodent models of fear generalization and impaired extinction may allow us to test this possibility, and provide an avenue for translational research initiatives aimed at alleviating the symptoms of debilitating trauma disorders.

Summary

In conclusion, we have provided novel evidence for a mechanism by which synaptic remodeling in excitatory glutamatergic circuits to the CeL drive the acquisition of passive fear memory and fear memory extinction via bidirectional biases in relative input strength to functionally segregated and genetically distinct neurons in the CeA. The bidirectional changes in this excitatory input bias following fear acquisition and fear extinction are primarily driven by plasticity at BLA-CeL synapses. Activity-dependent remodeling of these BLA-CeL synapses as well as the net excitatory input favors excitatory drive onto CRF+ neurons over CRF-/SOM+ neurons in low fear states, resulting in the suppression of conditioned freezing responses. As a

result, this dynamic form of synaptic remodeling is necessary for the full acquisition of fear memory, and the retrieval of extinction memory, providing a mechanism by which experience-dependent modification of amygdala circuitry drives behavioral selection and learning processes through the recruitment of subcortical output neurons that differentially impinge on motor responses.

REFERENCES

Abraham, W.C., Bliss, T.V., and Goddard, G.V. (1985). Heterosynaptic changes accompany long-term but not short-term potentiation of the perforant path in the anaesthetized rat. The Journal of physiology 363, 335-349.

Abraham, W.C., Jones, O.D., and Glanzman, D.L. (2019). Is plasticity of synapses the mechanism of long-term memory storage? NPJ science of learning 4, 9.

Amano, T., Duvarci, S., Popa, D., and Pare, D. (2011). The fear circuit revisited: contributions of the basal amygdala nuclei to conditioned fear. The Journal of neuroscience : the official journal of the Society for Neuroscience 31, 15481-15489.

Amano, T., Unal, C.T., and Pare, D. (2010). Synaptic correlates of fear extinction in the amygdala. Nature neuroscience 13, 489-494.

Amir, A., Amano, T., and Pare, D. (2011). Physiological identification and infralimbic responsiveness of rat intercalated amygdala neurons. Journal of neurophysiology 105, 3054-3066.

Amir, A., Lee, S.C., Headley, D.B., Herzallah, M.M., and Pare, D. (2015). Amygdala Signaling during Foraging in a Hazardous Environment. The Journal of neuroscience : the official journal of the Society for Neuroscience 35, 12994-13005.

An, B., Kim, J., Park, K., Lee, S., Song, S., and Choi, S. (2017). Amount of fear extinction changes its underlying mechanisms. eLife 6.

Anglada-Figueroa, D., and Quirk, G.J. (2005). Lesions of the basal amygdala block expression of conditioned fear but not extinction. The Journal of neuroscience : the official journal of the Society for Neuroscience 25, 9680-9685.

Armbruster, B.N., Li, X., Pausch, M.H., Herlitze, S., and Roth, B.L. (2007). Evolving the lock to fit the key to create a family of G protein-coupled receptors potently activated by an inert ligand. Proceedings of the National Academy of Sciences of the United States of America 104, 5163-5168.

Arruda-Carvalho, M., and Clem, R.L. (2014). Pathway-selective adjustment of prefrontal-amygdala transmission during fear encoding. The Journal of neuroscience : the official journal of the Society for Neuroscience 34, 15601-15609.

Asok, A., Draper, A., Hoffman, A.F., Schulkin, J., Lupica, C.R., and Rosen, J.B. (2018). Optogenetic silencing of a corticotropin-releasing factor pathway from the central amygdala to the bed nucleus of the stria terminalis disrupts sustained fear. Molecular psychiatry 23, 914-922.

Baeg, E.H., Kim, Y.B., Jang, J., Kim, H.T., Mook-Jung, I., and Jung, M.W. (2001). Fast spiking and regular spiking neural correlates of fear conditioning in the medial prefrontal cortex of the rat. Cereb Cortex 11, 441-451.

Baker, P.M., and Mizumori, S.J.Y. (2017). Control of behavioral flexibility by the lateral habenula. Pharmacology, biochemistry, and behavior 162, 62-68.

Bale, T.L., and Vale, W.W. (2004). CRF and CRF receptors: role in stress responsivity and other behaviors. Annual review of pharmacology and toxicology 44, 525-557.

Bauer, E.P., and LeDoux, J.E. (2004). Heterosynaptic long-term potentiation of inhibitory interneurons in the lateral amygdala. The Journal of neuroscience : the official journal of the Society for Neuroscience 24, 9507-9512.

Baum, M. (1988). Spontaneous recovery from the effects of flooding (exposure) in animals. Behaviour research and therapy 26, 185-186.

Berret, E., Kintscher, M., Palchaudhuri, S., Tang, W., Osypenko, D., Kochubey, O., and Schneggenburger, R. (2019). Insular cortex processes aversive somatosensory information and is crucial for threat learning. Science.

Beyeler, A., Chang, C.J., Silvestre, M., Leveque, C., Namburi, P., Wildes, C.P., and Tye, K.M. (2018). Organization of Valence-Encoding and Projection-Defined Neurons in the Basolateral Amygdala. Cell reports 22, 905-918.

Beyeler, A., Namburi, P., Glober, G.F., Simonnet, C., Calhoon, G.G., Conyers, G.F., Luck, R., Wildes, C.P., and Tye, K.M. (2016). Divergent Routing of Positive and Negative Information from the Amygdala during Memory Retrieval. Neuron 90, 348-361.

Biane, J.S., Takashima, Y., Scanziani, M., Conner, J.M., and Tuszynski, M.H. (2016). Thalamocortical Projections onto Behaviorally Relevant Neurons Exhibit Plasticity during Adult Motor Learning. Neuron 89, 1173-1179.

Blaise, J.H. (2013). Long-term potentiation of perforant pathway-dentate gyrus synapse in freely behaving mice. Journal of visualized experiments : JoVE.

Blanchard, D.C., and Blanchard, R.J. (1972). Innate and conditioned reactions to threat in rats with amygdaloid lesions. Journal of comparative and physiological psychology 81, 281-290.

Blanchard, R.J., and Blanchard, D.C. (1969a). Crouching as an index of fear. Journal of comparative and physiological psychology 67, 370-375.

Blanchard, R.J., and Blanchard, D.C. (1969b). Passive and active reactions to fear-eliciting stimuli. Journal of comparative and physiological psychology 68, 129-135.

Bliss, T.V., and Lomo, T. (1973). Long-lasting potentiation of synaptic transmission in the dentate area of the anaesthetized rabbit following stimulation of the perforant path. The Journal of physiology 232, 331-356.

Botta, P., Demmou, L., Kasugai, Y., Markovic, M., Xu, C., Fadok, J.P., Lu, T., Poe, M.M., Xu, L., Cook, J.M., *et al.* (2015). Regulating anxiety with extrasynaptic inhibition. Nature neuroscience 18, 1493-1500.

Bouton, M.E. (2004). Context and behavioral processes in extinction. Learn Mem 11, 485-494.

Bouton, M.E., and King, D.A. (1983). Contextual control of the extinction of conditioned fear: tests for the associative value of the context. Journal of experimental psychology Animal behavior processes 9, 248-265.

Bryda, E.C. (2013). The Mighty Mouse: the impact of rodents on advances in biomedical research. Missouri medicine 110, 207-211.

Burgos-Robles, A., Vidal-Gonzalez, I., and Quirk, G.J. (2009). Sustained conditioned responses in prelimbic prefrontal neurons are correlated with fear expression and extinction failure. The Journal of neuroscience : the official journal of the Society for Neuroscience 29, 8474-8482.

Burgos-Robles, A., Vidal-Gonzalez, I., Santini, E., and Quirk, G.J. (2007). Consolidation of fear extinction requires NMDA receptor-dependent bursting in the ventromedial prefrontal cortex. Neuron 53, 871-880.

Cai, H., Haubensak, W., Anthony, T.E., and Anderson, D.J. (2014). Central amygdala PKC-delta(+) neurons mediate the influence of multiple anorexigenic signals. Nature neuroscience 17, 1240-1248.

Callahan, L.B., Tschetter, K.E., and Ronan, P.J. (2013). Inhibition of corticotropin releasing factor expression in the central nucleus of the amygdala attenuates stress-induced behavioral and endocrine responses. Frontiers in neuroscience 7, 195.

Campeau, S., and Davis, M. (1995). Involvement of the central nucleus and basolateral complex of the amygdala in fear conditioning measured with fear-potentiated startle in rats trained concurrently with auditory and visual conditioned stimuli. The Journal of neuroscience : the official journal of the Society for Neuroscience 15, 2301-2311.

Cassell, M.D., and Wright, D.J. (1986). Topography of projections from the medial prefrontal cortex to the amygdala in the rat. Brain research bulletin 17, 321-333.

Castillo, P.E. (2012). Presynaptic LTP and LTD of excitatory and inhibitory synapses. Cold Spring Harbor perspectives in biology 4.

Chaaya, N., Battle, A.R., and Johnson, L.R. (2018). An update on contextual fear memory mechanisms: Transition between Amygdala and Hippocampus. Neuroscience and biobehavioral reviews 92, 43-54.

Chhatwal, J.P., Myers, K.M., Ressler, K.J., and Davis, M. (2005). Regulation of gephyrin and GABAA receptor binding within the amygdala after fear acquisition and extinction. The Journal of neuroscience : the official journal of the Society for Neuroscience 25, 502-506.

Chieng, B., and Christie, M.J. (2010). Somatostatin and nociceptin inhibit neurons in the central nucleus of amygdala that project to the periaqueductal grey. Neuropharmacology 59, 425-430.

Ciocchi, S., Herry, C., Grenier, F., Wolff, S.B., Letzkus, J.J., Vlachos, I., Ehrlich, I., Sprengel, R., Deisseroth, K., Stadler, M.B., *et al.* (2010). Encoding of conditioned fear in central amygdala inhibitory circuits. Nature 468, 277-282.

Cipolotti, L., and Bird, C.M. (2006). Amnesia and the hippocampus. Current opinion in neurology 19, 593-598.

Corcoran, K.A., and Maren, S. (2001). Hippocampal inactivation disrupts contextual retrieval of fear memory after extinction. The Journal of neuroscience : the official journal of the Society for Neuroscience 21, 1720-1726.

Corcoran, K.A., and Maren, S. (2004). Factors regulating the effects of hippocampal inactivation on renewal of conditional fear after extinction. Learn Mem 11, 598-603.

Corcoran, K.A., and Quirk, G.J. (2007). Activity in prelimbic cortex is necessary for the expression of learned, but not innate, fears. The Journal of neuroscience : the official journal of the Society for Neuroscience 27, 840-844.

Correia, S.S., and Goosens, K.A. (2016). Input-specific contributions to valence processing in the amygdala. Learn Mem 23, 534-543.

Cui, Y., Lv, G., Jin, S., Peng, J., Yuan, J., He, X., Gong, H., Xu, F., Xu, T., and Li, H. (2017). A Central Amygdala-Substantia Innominata Neural Circuitry Encodes Aversive Reinforcement Signals. Cell reports 21, 1770-1782.

Dalton, G.L., Wang, Y.T., Floresco, S.B., and Phillips, A.G. (2008). Disruption of AMPA receptor endocytosis impairs the extinction, but not acquisition of learned fear. Neuropsychopharmacology : official publication of the American College of Neuropsychopharmacology 33, 2416-2426.

Danguir, J. (1988). Food intake in rats is increased by intracerebroventricular infusion of the somatostatin analogue SMS 201-995 and is decreased by somatostatin antiserum. Peptides 9, 211-213.

de Kleine, R.A., Rothbaum, B.O., and van Minnen, A. (2013). Pharmacological enhancement of exposure-based treatment in PTSD: a qualitative review. European journal of psychotraumatology 4.

Dedic, N., Kuhne, C., Jakovcevski, M., Hartmann, J., Genewsky, A.J., Gomes, K.S., Anderzhanova, E., Pohlmann, M.L., Chang, S., Kolarz, A.*, et al.* (2018). Chronic CRH depletion from GABAergic, long-range projection neurons in the extended amygdala reduces dopamine release and increases anxiety. Nature neuroscience 21, 803-807.

DeMorrow, S. (2018). Role of the Hypothalamic-Pituitary-Adrenal Axis in Health and Disease. International journal of molecular sciences 19.

Do Monte, F.H., Quirk, G.J., Li, B., and Penzo, M.A. (2016). Retrieving fear memories, as time goes by. Molecular psychiatry 21, 1027-1036.

Do, V.H., Martinez, C.O., Martinez, J.L., Jr., and Derrick, B.E. (2002). Long-term potentiation in direct perforant path projections to the hippocampal CA3 region in vivo. Journal of neurophysiology 87, 669-678.

Douglass, A.M., Kucukdereli, H., Ponserre, M., Markovic, M., Grundemann, J., Strobel, C., Alcala Morales, P.L., Conzelmann, K.K., Luthi, A., and Klein, R. (2017). Central amygdala circuits modulate food consumption through a positive-valence mechanism. Nature neuroscience 20, 1384-1394.

Dragoi, G., and Tonegawa, S. (2013). Distinct preplay of multiple novel spatial experiences in the rat. Proceedings of the National Academy of Sciences of the United States of America 110, 9100-9105.

Dragoi, G., and Tonegawa, S. (2014). Selection of preconfigured cell assemblies for representation of novel spatial experiences. Philosophical transactions of the Royal Society of London Series B, Biological sciences 369, 20120522.

Dunlop, B.W., and Wong, A. (2019). The hypothalamic-pituitary-adrenal axis in PTSD: Pathophysiology and treatment interventions. Progress in neuro-psychopharmacology & biological psychiatry 89, 361-379.

Duvarci, S., and Pare, D. (2014). Amygdala microcircuits controlling learned fear. Neuron 82, 966-980.

Duvarci, S., Popa, D., and Pare, D. (2011). Central amygdala activity during fear conditioning. The Journal of neuroscience : the official journal of the Society for Neuroscience 31, 289-294.

Eichenbaum, H. (2013). What H.M. taught us. Journal of cognitive neuroscience 25, 14-21.

Etkin, A. (2010). Functional neuroanatomy of anxiety: a neural circuit perspective. Current topics in behavioral neurosciences 2, 251-277.

Evans, D.A., Stempel, A.V., Vale, R., Ruehle, S., Lefler, Y., and Branco, T. (2018). A synaptic threshold mechanism for computing escape decisions. Nature 558, 590-594.

Fadok, J.P., Krabbe, S., Markovic, M., Courtin, J., Xu, C., Massi, L., Botta, P., Bylund, K., Muller, C., Kovacevic, A.*, et al.* (2017). A competitive inhibitory circuit for selection of active and passive fear responses. Nature 542, 96-100.

Falls, W.A., Miserendino, M.J., and Davis, M. (1992). Extinction of fear-potentiated startle: blockade by infusion of an NMDA antagonist into the amygdala. The Journal of neuroscience : the official journal of the Society for Neuroscience 12, 854-863.

Fani, N., Tone, E.B., Phifer, J., Norrholm, S.D., Bradley, B., Ressler, K.J., Kamkwalala, A., and Jovanovic, T. (2012). Attention bias toward threat is associated with exaggerated fear expression and impaired extinction in PTSD. Psychological medicine 42, 533-543.

Fanselow, M.S. (1980). Conditioned and unconditional components of post-shock freezing. The Pavlovian journal of biological science 15, 177-182.

Faravelli, C., Lo Sauro, C., Lelli, L., Pietrini, F., Lazzeretti, L., Godini, L., Benni, L., Fioravanti, G., Talamba, G.A., Castellini, G., and Ricca, V. (2012). The role of life events and HPA axis in anxiety disorders: a review. Current pharmaceutical design 18, 5663-5674.

Farinelli, M., Deschaux, O., Hugues, S., Thevenet, A., and Garcia, R. (2006). Hippocampal train stimulation modulates recall of fear extinction independently of prefrontal cortex synaptic plasticity and lesions. Learn Mem 13, 329-334.

Fendt, M. (2001). Injections of the NMDA receptor antagonist aminophosphonopentanoic acid into the lateral nucleus of the amygdala block the expression of fear-potentiated startle and freezing. The Journal of neuroscience : the official journal of the Society for Neuroscience 21, 4111-4115.

Flandreau, E.I., Ressler, K.J., Owens, M.J., and Nemeroff, C.B. (2012). Chronic overexpression of corticotropin-releasing factor from the central amygdala produces HPA axis hyperactivity and behavioral anxiety associated with gene-expression changes in the hippocampus and paraventricular nucleus of the hypothalamus. Psychoneuroendocrinology 37, 27-38.

Frese, A., Summ, O., and Evers, S. (2014). Exploding head syndrome: six new cases and review of the literature. Cephalalgia : an international journal of headache 34, 823-827.

Gafford, G., Jasnow, A.M., and Ressler, K.J. (2014). Grin1 receptor deletion within CRF neurons enhances fear memory. PloS one 9, e111009.

Gafford, G.M., and Ressler, K.J. (2015). GABA and NMDA receptors in CRF neurons have opposing effects in fear acquisition and anxiety in central amygdala vs. bed nucleus of the stria terminalis. Hormones and behavior 76, 136-142.

Gale, G.D., Anagnostaras, S.G., Godsil, B.P., Mitchell, S., Nozawa, T., Sage, J.R., Wiltgen, B., and Fanselow, M.S. (2004). Role of the basolateral amygdala in the storage of fear memories across the adult lifetime of rats. The Journal of neuroscience : the official journal of the Society for Neuroscience 24, 3810-3815.

Garfinkel, S.N., Abelson, J.L., King, A.P., Sripada, R.K., Wang, X., Gaines, L.M., and Liberzon, I. (2014). Impaired contextual modulation of memories in PTSD: an fMRI and psychophysiological study of extinction retention and fear renewal. The Journal of neuroscience : the official journal of the Society for Neuroscience 34, 13435-13443.

Geddes, S.D., Assadzada, S., Lemelin, D., Sokolovski, A., Bergeron, R., Haj-Dahmane, S., and Beique, J.C. (2016). Target-specific modulation of the descending prefrontal cortex inputs to the dorsal raphe nucleus by cannabinoids. Proceedings of the National Academy of Sciences of the United States of America 113, 5429-5434.

Geracitano, R., Kaufmann, W.A., Szabo, G., Ferraguti, F., and Capogna, M. (2007). Synaptic heterogeneity between mouse paracapsular intercalated neurons of the amygdala. The Journal of physiology 585, 117-134.

Gilmartin, M.R., and Helmstetter, F.J. (2010). Trace and contextual fear conditioning require neural activity and NMDA receptor-dependent transmission in the medial prefrontal cortex. Learn Mem 17, 289-296.

Gilmartin, M.R., Kwapis, J.L., and Helmstetter, F.J. (2013a). NR2A- and NR2B-containing NMDA receptors in the prelimbic medial prefrontal cortex differentially mediate trace, delay, and contextual fear conditioning. Learn Mem 20, 290-294.

Gilmartin, M.R., Miyawaki, H., Helmstetter, F.J., and Diba, K. (2013b). Prefrontal activity links nonoverlapping events in memory. The Journal of neuroscience : the official journal of the Society for Neuroscience 33, 10910-10914.

Giustino, T.F., and Maren, S. (2015). The Role of the Medial Prefrontal Cortex in the Conditioning and Extinction of Fear. Frontiers in behavioral neuroscience 9, 298.

Gold, T., and Soter, S. (1979). Brontides: natural explosive noises. Science 204, 371-375.

Gomez, J.L., Bonaventura, J., Lesniak, W., Mathews, W.B., Sysa-Shah, P., Rodriguez, L.A., Ellis, R.J., Richie, C.T., Harvey, B.K., Dannals, R.F.*, et al.* (2017). Chemogenetics revealed: DREADD occupancy and activation via converted clozapine. Science 357, 503-507.

Goosens, K.A., and Maren, S. (2001). Contextual and auditory fear conditioning are mediated by the lateral, basal, and central amygdaloid nuclei in rats. Learn Mem 8, 148-155.

Goosens, K.A., and Maren, S. (2003). Pretraining NMDA receptor blockade in the basolateral complex, but not the central nucleus, of the amygdala prevents savings of conditional fear. Behavioral neuroscience 117, 738-750.

Gozzi, A., Jain, A., Giovannelli, A., Bertollini, C., Crestan, V., Schwarz, A.J., Tsetsenis, T., Ragozzino, D., Gross, C.T., and Bifone, A. (2010). A neural switch for active and passive fear. Neuron 67, 656-666.

Grewe, B.F., Grundemann, J., Kitch, L.J., Lecoq, J.A., Parker, J.G., Marshall, J.D., Larkin, M.C., Jercog, P.E., Grenier, F., Li, J.Z.*, et al.* (2017). Neural ensemble dynamics underlying a long-term associative memory. Nature 543, 670-675.

Griessner, J., Pasieka, M., Bohm, V., Grossl, F., Kaczanowska, J., Pliota, P., Kargl, D., Werner, B., Kaouane, N., Strobelt, S.*, et al.* (2018). Central amygdala circuit dynamics underlying the benzodiazepine anxiolytic effect. Molecular psychiatry.

Guimarais, M., Gregorio, A., Cruz, A., Guyon, N., and Moita, M.A. (2011). Time determines the neural circuit underlying associative fear learning. Frontiers in behavioral neuroscience 5, 89.

Hackett, R.A., Kivimaki, M., Kumari, M., and Steptoe, A. (2016). Diurnal Cortisol Patterns, Future Diabetes, and Impaired Glucose Metabolism in the Whitehall II Cohort Study. The Journal of clinical endocrinology and metabolism 101, 619-625.

Halladay, L.R., and Blair, H.T. (2015). Distinct ensembles of medial prefrontal cortex neurons are activated by threatening stimuli that elicit excitation vs. inhibition of movement. Journal of neurophysiology 114, 793-807.

Han, J.H., Kushner, S.A., Yiu, A.P., Cole, C.J., Matynia, A., Brown, R.A., Neve, R.L., Guzowski, J.F., Silva, A.J., and Josselyn, S.A. (2007). Neuronal competition and selection during memory formation. Science 316, 457-460.

Han, S., Soleiman, M.T., Soden, M.E., Zweifel, L.S., and Palmiter, R.D. (2015). Elucidating an Affective Pain Circuit that Creates a Threat Memory. Cell 162, 363-374.

Han, W., Tellez, L.A., Rangel, M.J., Jr., Motta, S.C., Zhang, X., Perez, I.O., Canteras, N.S., Shammah-Lagnado, S.J., van den Pol, A.N., and de Araujo, I.E. (2017). Integrated Control of Predatory Hunting by the Central Nucleus of the Amygdala. Cell 168, 311-324 e318.

Hardaway, J.A., Halladay, L.R., Mazzone, C.M., Pati, D., Bloodgood, D.W., Kim, M., Jensen, J., DiBerto, J.F., Boyt, K.M., Shiddapur, A.*, et al.* (2019). Central Amygdala Prepronociceptin-Expressing Neurons Mediate Palatable Food Consumption and Reward. Neuron 102, 1088.

Hartley, N.D., Gunduz-Cinar, O., Halladay, L., Bukalo, O., Holmes, A., and Patel, S. (2016). 2-arachidonoylglycerol signaling impairs short-term fear extinction. Translational psychiatry 6, e749.

Hassabis, D., Kumaran, D., Vann, S.D., and Maguire, E.A. (2007). Patients with hippocampal amnesia cannot imagine new experiences. Proceedings of the National Academy of Sciences of the United States of America 104, 1726-1731.

Haubensak, W., Kunwar, P.S., Cai, H., Ciocchi, S., Wall, N.R., Ponnusamy, R., Biag, J., Dong, H.W., Deisseroth, K., Callaway, E.M.*, et al.* (2010). Genetic dissection of an amygdala microcircuit that gates conditioned fear. Nature 468, 270-276.

Heldt, S.A., and Ressler, K.J. (2007). Training-induced changes in the expression of GABAA-associated genes in the amygdala after the acquisition and extinction of Pavlovian fear. The European journal of neuroscience 26, 3631-3644.

Herry, C., Ciocchi, S., Senn, V., Demmou, L., Muller, C., and Luthi, A. (2008). Switching on and off fear by distinct neuronal circuits. Nature 454, 600-606.

Herry, C., Ferraguti, F., Singewald, N., Letzkus, J.J., Ehrlich, I., and Luthi, A. (2010). Neuronal circuits of fear extinction. The European journal of neuroscience 31, 599-612.

Herry, C., and Garcia, R. (2002). Prefrontal cortex long-term potentiation, but not long-term depression, is associated with the maintenance of extinction of learned fear in mice. The Journal of neuroscience : the official journal of the Society for Neuroscience 22, 577-583.

Hobin, J.A., Ji, J., and Maren, S. (2006). Ventral hippocampal muscimol disrupts context-specific fear memory retrieval after extinction in rats. Hippocampus 16, 174-182.

Hubbard, D.T., Nakashima, B.R., Lee, I., and Takahashi, L.K. (2007). Activation of basolateral amygdala corticotropin-releasing factor 1 receptors modulates the consolidation of contextual fear. Neuroscience 150, 818-828.

Huber, D., Veinante, P., and Stoop, R. (2005). Vasopressin and oxytocin excite distinct neuronal populations in the central amygdala. Science 308, 245-248.

Hunt, S., Sun, Y., Kucukdereli, H., Klein, R., and Sah, P. (2017). Intrinsic Circuits in the Lateral Central Amygdala. eNeuro 4.

Isogawa, K., Bush, D.E., and LeDoux, J.E. (2013). Contrasting effects of pretraining, posttraining, and pretesting infusions of corticotropin-releasing factor into the lateral amygdala: attenuation of fear memory formation but facilitation of its expression. Biological psychiatry 73, 353-359.

Isosaka, T., Matsuo, T., Yamaguchi, T., Funabiki, K., Nakanishi, S., Kobayakawa, R., and Kobayakawa, K. (2015). Htr2a-Expressing Cells in the Central Amygdala Control the Hierarchy between Innate and Learned Fear. Cell 163, 1153-1164.

Jaffe, D., and Johnston, D. (1990). Induction of long-term potentiation at hippocampal mossy-fiber synapses follows a Hebbian rule. Journal of neurophysiology 64, 948-960.

Jasnow, A.M., Ehrlich, D.E., Choi, D.C., Dabrowska, J., Bowers, M.E., McCullough, K.M., Rainnie, D.G., and Ressler, K.J. (2013). Thy1-expressing neurons in the basolateral amygdala may mediate fear inhibition. The Journal of neuroscience : the official journal of the Society for Neuroscience 33, 10396-10404.

Ji, J., and Maren, S. (2008). Differential roles for hippocampal areas CA1 and CA3 in the contextual encoding and retrieval of extinguished fear. Learn Mem 15, 244-251.

Jin, J., and Maren, S. (2015). Fear renewal preferentially activates ventral hippocampal neurons projecting to both amygdala and prefrontal cortex in rats. Scientific reports 5, 8388.

Jungling, K., Seidenbecher, T., Sosulina, L., Lesting, J., Sangha, S., Clark, S.D., Okamura, N., Duangdao, D.M., Xu, Y.L., Reinscheid, R.K., and Pape, H.C. (2008). Neuropeptide S-mediated control of fear expression and extinction: role of intercalated GABAergic neurons in the amygdala. Neuron 59, 298-310.

Juruena, M.F. (2014). Early-life stress and HPA axis trigger recurrent adulthood depression. Epilepsy & behavior : E&B 38, 148-159.

Kaeser, P.S., and Regehr, W.G. (2014). Molecular mechanisms for synchronous, asynchronous, and spontaneous neurotransmitter release. Annual review of physiology 76, 333-363.

Kahl, E., and Fendt, M. (2014). Injections of the somatostatin receptor type 2 agonist L-054,264 into the amygdala block expression but not acquisition of conditioned fear in rats. Behavioural brain research 265, 49-52.

Kalisch, R., Korenfeld, E., Stephan, K.E., Weiskopf, N., Seymour, B., and Dolan, R.J. (2006). Context-dependent human extinction memory is mediated by a ventromedial prefrontal and hippocampal network. The Journal of neuroscience : the official journal of the Society for Neuroscience 26, 9503-9511.

Karam, E.G., Friedman, M.J., Hill, E.D., Kessler, R.C., McLaughlin, K.A., Petukhova, M., Sampson, L., Shahly, V., Angermeyer, M.C., Bromet, E.J., *et al.* (2014). Cumulative traumas and risk thresholds: 12-month PTSD in the World Mental Health (WMH) surveys. Depression and anxiety 31, 130-142.

Keen-Rhinehart, E., Michopoulos, V., Toufexis, D.J., Martin, E.I., Nair, H., Ressler, K.J., Davis, M., Owens, M.J., Nemeroff, C.B., and Wilson, M.E. (2009). Continuous expression of corticotropin-releasing factor in the central nucleus of the amygdala emulates the dysregulation of the stress and reproductive axes. Molecular psychiatry 14, 37-50.

Kentros, C. (2006). Hippocampal place cells: the "where" of episodic memory? Hippocampus 16, 743-754.

Kessler, R.C., Sonnega, A., Bromet, E., Hughes, M., and Nelson, C.B. (1995). Posttraumatic stress disorder in the National Comorbidity Survey. Archives of general psychiatry 52, 1048-1060.

Kikkawa, U., Matsuzaki, H., and Yamamoto, T. (2002). Protein kinase C delta (PKC delta): activation mechanisms and functions. Journal of biochemistry 132, 831-839.

Kim, J., Lee, S., Park, K., Hong, I., Song, B., Son, G., Park, H., Kim, W.R., Park, E., Choe, H.K., *et al.* (2007). Amygdala depotentiation and fear extinction. Proceedings of the National Academy of Sciences of the United States of America 104, 20955-20960.

Kim, J., Pignatelli, M., Xu, S., Itohara, S., and Tonegawa, S. (2016). Antagonistic negative and positive neurons of the basolateral amygdala. Nature neuroscience 19, 1636-1646.

Kim, J., Zhang, X., Muralidhar, S., LeBlanc, S.A., and Tonegawa, S. (2017). Basolateral to Central Amygdala Neural Circuits for Appetitive Behaviors. Neuron 93, 1464-1479 e1465.

Kitamura, T., Ogawa, S.K., Roy, D.S., Okuyama, T., Morrissey, M.D., Smith, L.M., Redondo, R.L., and Tonegawa, S. (2017). Engrams and circuits crucial for systems consolidation of a memory. Science 356, 73-78.

Kitamura, T., Pignatelli, M., Suh, J., Kohara, K., Yoshiki, A., Abe, K., and Tonegawa, S. (2014). Island cells control temporal association memory. Science 343, 896-901.

Knapska, E., and Maren, S. (2009). Reciprocal patterns of c-Fos expression in the medial prefrontal cortex and amygdala after extinction and renewal of conditioned fear. Learn Mem 16, 486-493.

Knierim, J.J. (2015). The hippocampus. Current biology : CB 25, R1116-1121.

Koenen, K.C., Stellman, S.D., Sommer, J.F., Jr., and Stellman, J.M. (2008). Persisting posttraumatic stress disorder symptoms and their relationship to functioning in Vietnam veterans: a 14-year follow-up. Journal of traumatic stress 21, 49-57.

Krashes, M.J., Koda, S., Ye, C., Rogan, S.C., Adams, A.C., Cusher, D.S., Maratos-Flier, E., Roth, B.L., and Lowell, B.B. (2011). Rapid, reversible activation of AgRP neurons drives feeding behavior in mice. J Clin Invest 121, 1424-1428.

Kwon, J.T., Nakajima, R., Kim, H.S., Jeong, Y., Augustine, G.J., and Han, J.H. (2014). Optogenetic activation of presynaptic inputs in lateral amygdala forms associative fear memory. Learn Mem 21, 627-633.

Lacagnina, A.F., Brockway, E.T., Crovetti, C.R., Shue, F., McCarty, M.J., Sattler, K.P., Lim, S.C., Santos, S.L., Denny, C.A., and Drew, M.R. (2019). Distinct hippocampal engrams control extinction and relapse of fear memory. Nature neuroscience 22, 753-761.

Laurent, V., and Westbrook, R.F. (2009). Inactivation of the infralimbic but not the prelimbic cortex impairs consolidation and retrieval of fear extinction. Learn Mem 16, 520-529.

Leal, S.L., and Yassa, M.A. (2015). Neurocognitive Aging and the Hippocampus across Species. Trends in neurosciences 38, 800-812.

LeDoux, J. (1996). Emotional networks and motor control: a fearful view. Progress in brain research 107, 437-446.

LeDoux, J.E. (2000). Emotion circuits in the brain. Annual review of neuroscience 23, 155-184.

LeDoux, J.E., Iwata, J., Cicchetti, P., and Reis, D.J. (1988). Different projections of the central amygdaloid nucleus mediate autonomic and behavioral correlates of conditioned fear. The Journal of neuroscience : the official journal of the Society for Neuroscience 8, 2517-2529.

Ledoux, J.E., and Muller, J. (1997). Emotional memory and psychopathology. Philosophical transactions of the Royal Society of London Series B, Biological sciences 352, 1719-1726.

Lee, H., and Kim, J.J. (1998). Amygdalar NMDA receptors are critical for new fear learning in previously fear-conditioned rats. The Journal of neuroscience : the official journal of the Society for Neuroscience 18, 8444-8454.

Lee, Y., Walker, D., and Davis, M. (1996). Lack of a temporal gradient of retrograde amnesia following NMDA-induced lesions of the basolateral amygdala assessed with the fear-potentiated startle paradigm. Behavioral neuroscience 110, 836-839.

Lemos, J.C., Wanat, M.J., Smith, J.S., Reyes, B.A., Hollon, N.G., Van Bockstaele, E.J., Chavkin, C., and Phillips, P.E. (2012). Severe stress switches CRF action in the nucleus accumbens from appetitive to aversive. Nature 490, 402-406.

Lesting, J., Daldrup, T., Narayanan, V., Himpe, C., Seidenbecher, T., and Pape, H.C. (2013). Directional theta coherence in prefrontal cortical to amygdalo-hippocampal pathways signals fear extinction. PloS one 8, e77707.

Lesting, J., Narayanan, R.T., Kluge, C., Sangha, S., Seidenbecher, T., and Pape, H.C. (2011). Patterns of coupled theta activity in amygdala-hippocampal-prefrontal cortical circuits during fear extinction. PloS one 6, e21714.

Li, H., Penzo, M.A., Taniguchi, H., Kopec, C.D., Huang, Z.J., and Li, B. (2013). Experience-dependent modification of a central amygdala fear circuit. Nature neuroscience 16, 332-339.

Likhtik, E., Popa, D., Apergis-Schoute, J., Fidacaro, G.A., and Pare, D. (2008). Amygdala intercalated neurons are required for expression of fear extinction. Nature 454, 642-645.

Likhtik, E., Stujenske, J.M., Topiwala, M.A., Harris, A.Z., and Gordon, J.A. (2014). Prefrontal entrainment of amygdala activity signals safety in learned fear and innate anxiety. Nature neuroscience 17, 106-113.

Lin, C.H., Lee, C.C., and Gean, P.W. (2003). Involvement of a calcineurin cascade in amygdala depotentiation and quenching of fear memory. Molecular pharmacology 63, 44-52.

Lin, D., Boyle, M.P., Dollar, P., Lee, H., Lein, E.S., Perona, P., and Anderson, D.J. (2011). Functional identification of an aggression locus in the mouse hypothalamus. Nature 470, 221-226.

Lin, M.T., Lujan, R., Watanabe, M., Adelman, J.P., and Maylie, J. (2008). SK2 channel plasticity contributes to LTP at Schaffer collateral-CA1 synapses. Nature neuroscience 11, 170-177.

Lindquist, D.H., and Brown, T.H. (2004). Amygdalar NMDA receptors control the expression of associative reflex facilitation and three other conditional responses. Behavioral neuroscience 118, 36-52.

Lissek, S., and van Meurs, B. (2015). Learning models of PTSD: Theoretical accounts and psychobiological evidence. International journal of psychophysiology : official journal of the International Organization of Psychophysiology 98, 594-605.

Liu, X., Ramirez, S., Pang, P.T., Puryear, C.B., Govindarajan, A., Deisseroth, K., and Tonegawa, S. (2012). Optogenetic stimulation of a hippocampal engram activates fear memory recall. Nature 484, 381-385.

Liu, X., Ramirez, S., and Tonegawa, S. (2014). Inception of a false memory by optogenetic manipulation of a hippocampal memory engram. Philosophical transactions of the Royal Society of London Series B, Biological sciences 369, 20130142.

Lomo, T. (2018). Discovering long-term potentiation (LTP) - recollections and reflections on what came after. Acta Physiol (Oxf) 222.

MacAskill, A.F., Cassel, J.M., and Carter, A.G. (2014). Cocaine exposure reorganizes cell type- and input-specific connectivity in the nucleus accumbens. Nature neuroscience 17, 1198-1207.

Madisen, L., Garner, A.R., Shimaoka, D., Chuong, A.S., Klapoetke, N.C., Li, L., van der Bourg, A., Niino, Y., Egolf, L., Monetti, C.*, et al.* (2015). Transgenic mice for intersectional targeting of neural sensors and effectors with high specificity and performance. Neuron 85, 942-958.

Mahanty, N.K., and Sah, P. (1998). Calcium-permeable AMPA receptors mediate long-term potentiation in interneurons in the amygdala. Nature 394, 683-687.

Mao, S.C., Hsiao, Y.H., and Gean, P.W. (2006). Extinction training in conjunction with a partial agonist of the glycine site on the NMDA receptor erases memory trace. The Journal of neuroscience : the official journal of the Society for Neuroscience 26, 8892-8899.

Marcinkiewcz, C.A., Mazzone, C.M., D'Agostino, G., Halladay, L.R., Hardaway, J.A., DiBerto, J.F., Navarro, M., Burnham, N., Cristiano, C., Dorrier, C.E.*, et al.* (2016). Serotonin engages an anxiety and fear-promoting circuit in the extended amygdala. Nature 537, 97-101.

Maren, S. (1999). Neurotoxic basolateral amygdala lesions impair learning and memory but not the performance of conditional fear in rats. The Journal of neuroscience : the official journal of the Society for Neuroscience 19, 8696-8703.

Maren, S. (2000). Auditory fear conditioning increases CS-elicited spike firing in lateral amygdala neurons even after extensive overtraining. The European journal of neuroscience 12, 4047-4054.

Maren, S. (2001). Neurobiology of Pavlovian fear conditioning. Annual review of neuroscience 24, 897-931.

Maren, S. (2005). Building and burying fear memories in the brain. The Neuroscientist : a review journal bringing neurobiology, neurology and psychiatry 11, 89-99.

Maren, S., Aharonov, G., and Fanselow, M.S. (1996a). Retrograde abolition of conditional fear after excitotoxic lesions in the basolateral amygdala of rats: absence of a temporal gradient. Behavioral neuroscience 110, 718-726.

Maren, S., Aharonov, G., Stote, D.L., and Fanselow, M.S. (1996b). N-methyl-D-aspartate receptors in the basolateral amygdala are required for both acquisition and expression of conditional fear in rats. Behavioral neuroscience 110, 1365-1374.

Maren, S., and Fanselow, M.S. (1995). Synaptic plasticity in the basolateral amygdala induced by hippocampal formation stimulation in vivo. The Journal of neuroscience : the official journal of the Society for Neuroscience 15, 7548-7564.

Maren, S., and Hobin, J.A. (2007). Hippocampal regulation of context-dependent neuronal activity in the lateral amygdala. Learn Mem 14, 318-324.

McCall, J.G., Al-Hasani, R., Siuda, E.R., Hong, D.Y., Norris, A.J., Ford, C.P., and Bruchas, M.R. (2015). CRH Engagement of the Locus Coeruleus Noradrenergic System Mediates Stress-Induced Anxiety. Neuron 87, 605-620.

McCullough, K.M., Choi, D., Guo, J., Zimmerman, K., Walton, J., Rainnie, D.G., and Ressler, K.J. (2016). Molecular characterization of Thy1 expressing fear-inhibiting neurons within the basolateral amygdala. Nature communications 7, 13149.

McDonald, A.J., and Augustine, J.R. (1993). Localization of GABA-like immunoreactivity in the monkey amygdala. Neuroscience 52, 281-294.

McDonald, A.J., Mascagni, F., and Guo, L. (1996). Projections of the medial and lateral prefrontal cortices to the amygdala: a Phaseolus vulgaris leucoagglutinin study in the rat. Neuroscience 71, 55-75.

McGarry, L.M., and Carter, A.G. (2017). Prefrontal Cortex Drives Distinct Projection Neurons in the Basolateral Amygdala. Cell reports 21, 1426-1433.

McHenry, J.A., Otis, J.M., Rossi, M.A., Robinson, J.E., Kosyk, O., Miller, N.W., McElligott, Z.A., Budygin, E.A., Rubinow, D.R., and Stuber, G.D. (2017). Hormonal gain control of a medial preoptic area social reward circuit. Nature neuroscience 20, 449-458.

McHugh, S.B., Deacon, R.M., Rawlins, J.N., and Bannerman, D.M. (2004). Amygdala and ventral hippocampus contribute differentially to mechanisms of fear and anxiety. Behavioral neuroscience 118, 63-78.

Milad, M.R., and Quirk, G.J. (2002). Neurons in medial prefrontal cortex signal memory for fear extinction. Nature 420, 70-74.

Milad, M.R., Wright, C.I., Orr, S.P., Pitman, R.K., Quirk, G.J., and Rauch, S.L. (2007). Recall of fear extinction in humans activates the ventromedial prefrontal cortex and hippocampus in concert. Biological psychiatry 62, 446-454.

Miserendino, M.J., Sananes, C.B., Melia, K.R., and Davis, M. (1990). Blocking of acquisition but not expression of conditioned fear-potentiated startle by NMDA antagonists in the amygdala. Nature 345, 716-718.

Mitchell, A.S., and Chakraborty, S. (2013). What does the mediodorsal thalamus do? Frontiers in systems neuroscience 7, 37.

Mizumori, S.J.Y., and Baker, P.M. (2017). The Lateral Habenula and Adaptive Behaviors. Trends in neurosciences 40, 481-493.

Myers, K.M., Ressler, K.J., and Davis, M. (2006). Different mechanisms of fear extinction dependent on length of time since fear acquisition. Learn Mem 13, 216-223.

Namburi, P., Beyeler, A., Yorozu, S., Calhoon, G.G., Halbert, S.A., Wichmann, R., Holden, S.S., Mertens, K.L., Anahtar, M., Felix-Ortiz, A.C*., et al.* (2015). A circuit mechanism for differentiating positive and negative associations. Nature 520, 675-678.

Narayanan, R.T., Seidenbecher, T., Kluge, C., Bergado, J., Stork, O., and Pape, H.C. (2007). Dissociated theta phase synchronization in amygdalo- hippocampal circuits during various stages of fear memory. The European journal of neuroscience 25, 1823-1831.

Nicoll, R.A. (2017). A Brief History of Long-Term Potentiation. Neuron 93, 281-290.

Nieuwenhuys, R. (2012). The insular cortex: a review. Progress in brain research 195, 123-163.

Nijsen, M.J., Croiset, G., Diamant, M., De Wied, D., and Wiegant, V.M. (2001). CRH signalling in the bed nucleus of the stria terminalis is involved in stress-induced cardiac vagal activation in

conscious rats. Neuropsychopharmacology : official publication of the American College of Neuropsychopharmacology 24, 1-10.

Orsini, C.A., Kim, J.H., Knapska, E., and Maren, S. (2011). Hippocampal and prefrontal projections to the basal amygdala mediate contextual regulation of fear after extinction. The Journal of neuroscience : the official journal of the Society for Neuroscience 31, 17269-17277.

Packard, P.A., Rodriguez-Fornells, A., Stein, L.M., Nicolas, B., and Fuentemilla, L. (2014). Tracking explicit and implicit long-lasting traces of fearful memories in humans. Neurobiology of learning and memory 116, 96-104.

Pape, H.C., Narayanan, R.T., Smid, J., Stork, O., and Seidenbecher, T. (2005). Theta activity in neurons and networks of the amygdala related to long-term fear memory. Hippocampus 15, 874-880.

Pare, D., and Collins, D.R. (2000). Neuronal correlates of fear in the lateral amygdala: multiple extracellular recordings in conscious cats. The Journal of neuroscience : the official journal of the Society for Neuroscience 20, 2701-2710.

Pare, D., and Smith, Y. (1993a). Distribution of GABA immunoreactivity in the amygdaloid complex of the cat. Neuroscience 57, 1061-1076.

Pare, D., and Smith, Y. (1993b). The intercalated cell masses project to the central and medial nuclei of the amygdala in cats. Neuroscience 57, 1077-1090.

Parsons, R.G., and Ressler, K.J. (2013). Implications of memory modulation for post-traumatic stress and fear disorders. Nature neuroscience 16, 146-153.

Pastalkova, E., Serrano, P., Pinkhasova, D., Wallace, E., Fenton, A.A., and Sacktor, T.C. (2006). Storage of spatial information by the maintenance mechanism of LTP. Science 313, 1141-1144.

Pattwell, S.S., and Bath, K.G. (2017). Emotional learning, stress, and development: An ever-changing landscape shaped by early-life experience. Neurobiology of learning and memory 143, 36-48.

Penzo, M.A., Robert, V., Tucciarone, J., De Bundel, D., Wang, M., Van Aelst, L., Darvas, M., Parada, L.F., Palmiter, R.D., He, M.*, et al.* (2015). The paraventricular thalamus controls a central amygdala fear circuit. Nature 519, 455-459.

Pereira, A.G., and Moita, M.A. (2016). Is there anybody out there? Neural circuits of threat detection in vertebrates. Current opinion in neurobiology 41, 179-187.

Perlman, R.L. (2016). Mouse models of human disease: An evolutionary perspective. Evolution, medicine, and public health 2016, 170-176.

Phelps, E.A., and LeDoux, J.E. (2005). Contributions of the amygdala to emotion processing: from animal models to human behavior. Neuron 48, 175-187.

Pitman, R.K., Rasmusson, A.M., Koenen, K.C., Shin, L.M., Orr, S.P., Gilbertson, M.W., Milad, M.R., and Liberzon, I. (2012). Biological studies of post-traumatic stress disorder. Nature reviews Neuroscience 13, 769-787.

Pitts, M.W., and Takahashi, L.K. (2011). The central amygdala nucleus via corticotropin-releasing factor is necessary for time-limited consolidation processing but not storage of contextual fear memory. Neurobiology of learning and memory 95, 86-91.

Pitts, M.W., Todorovic, C., Blank, T., and Takahashi, L.K. (2009). The central nucleus of the amygdala and corticotropin-releasing factor: insights into contextual fear memory. The Journal of neuroscience : the official journal of the Society for Neuroscience 29, 7379-7388.

Pliota, P., Bohm, V., Grossl, F., Griessner, J., Valenti, O., Kraitsy, K., Kaczanowska, J., Pasieka, M., Lendl, T., Deussing, J.M., and Haubensak, W. (2018). Stress peptides sensitize fear circuitry to promote passive coping. Molecular psychiatry.

Pomrenze, M.B., Tovar-Diaz, J., Blasio, A., Maiya, R., Giovanetti, S.M., Lei, K., Morikawa, H., Hopf, F.W., and Messing, R.O. (2019). A Corticotropin Releasing Factor Network in the Extended Amygdala for Anxiety. The Journal of neuroscience : the official journal of the Society for Neuroscience 39, 1030-1043.

Popa, D., Duvarci, S., Popescu, A.T., Lena, C., and Pare, D. (2010). Coherent amygdalocortical theta promotes fear memory consolidation during paradoxical sleep. Proceedings of the National Academy of Sciences of the United States of America 107, 6516-6519.

Quirk, G.J., Repa, C., and LeDoux, J.E. (1995). Fear conditioning enhances short-latency auditory responses of lateral amygdala neurons: parallel recordings in the freely behaving rat. Neuron 15, 1029-1039.

Quirk, G.J., Russo, G.K., Barron, J.L., and Lebron, K. (2000). The role of ventromedial prefrontal cortex in the recovery of extinguished fear. The Journal of neuroscience : the official journal of the Society for Neuroscience 20, 6225-6231.

Ramchand, R., Schell, T.L., Karney, B.R., Osilla, K.C., Burns, R.M., and Caldarone, L.B. (2010). Disparate prevalence estimates of PTSD among service members who served in Iraq and Afghanistan: possible explanations. Journal of traumatic stress 23, 59-68.

Ramirez, S., Liu, X., Lin, P.A., Suh, J., Pignatelli, M., Redondo, R.L., Ryan, T.J., and Tonegawa, S. (2013a). Creating a false memory in the hippocampus. Science 341, 387-391.

Ramirez, S., Tonegawa, S., and Liu, X. (2013b). Identification and optogenetic manipulation of memory engrams in the hippocampus. Frontiers in behavioral neuroscience 7, 226.

Rauch, S.L., Shin, L.M., and Phelps, E.A. (2006). Neurocircuitry models of posttraumatic stress disorder and extinction: human neuroimaging research--past, present, and future. Biological psychiatry 60, 376-382.

Repa, J.C., Muller, J., Apergis, J., Desrochers, T.M., Zhou, Y., and LeDoux, J.E. (2001). Two different lateral amygdala cell populations contribute to the initiation and storage of memory. Nature neuroscience 4, 724-731.

Roberto, M., Spierling, S.R., Kirson, D., and Zorrilla, E.P. (2017). Corticotropin-Releasing Factor (CRF) and Addictive Behaviors. International review of neurobiology 136, 5-51.

Roozendaal, B., Brunson, K.L., Holloway, B.L., McGaugh, J.L., and Baram, T.Z. (2002). Involvement of stress-released corticotropin-releasing hormone in the basolateral amygdala in regulating memory consolidation. Proceedings of the National Academy of Sciences of the United States of America 99, 13908-13913.

Rosenkranz, J.A. (2011). Neuronal activity causes rapid changes of lateral amygdala neuronal membrane properties and reduction of synaptic integration and synaptic plasticity in vivo. The Journal of neuroscience : the official journal of the Society for Neuroscience 31, 6108-6120.

Roy, D.S., Kitamura, T., Okuyama, T., Ogawa, S.K., Sun, C., Obata, Y., Yoshiki, A., and Tonegawa, S. (2017a). Distinct Neural Circuits for the Formation and Retrieval of Episodic Memories. Cell 170, 1000-1012 e1019.

Roy, D.S., Muralidhar, S., Smith, L.M., and Tonegawa, S. (2017b). Silent memory engrams as the basis for retrograde amnesia. Proceedings of the National Academy of Sciences of the United States of America 114, E9972-E9979.

Royer, S., Martina, M., and Pare, D. (1999). An inhibitory interface gates impulse traffic between the input and output stations of the amygdala. The Journal of neuroscience : the official journal of the Society for Neuroscience 19, 10575-10583.

Royer, S., Martina, M., and Pare, D. (2000). Polarized synaptic interactions between intercalated neurons of the amygdala. Journal of neurophysiology 83, 3509-3518.

Royer, S., and Pare, D. (2002). Bidirectional synaptic plasticity in intercalated amygdala neurons and the extinction of conditioned fear responses. Neuroscience 115, 455-462.

Royer, S., and Pare, D. (2003). Conservation of total synaptic weight through balanced synaptic depression and potentiation. Nature 422, 518-522.

Runyan, J.D., Moore, A.N., and Dash, P.K. (2004). A role for prefrontal cortex in memory storage for trace fear conditioning. The Journal of neuroscience : the official journal of the Society for Neuroscience 24, 1288-1295.

Russell, F.A., King, R., Smillie, S.J., Kodji, X., and Brain, S.D. (2014). Calcitonin gene-related peptide: physiology and pathophysiology. Physiological reviews 94, 1099-1142.

Ryan, T.J., Roy, D.S., Pignatelli, M., Arons, A., and Tonegawa, S. (2015). Memory. Engram cells retain memory under retrograde amnesia. Science 348, 1007-1013.

Samson, R.D., Dumont, E.C., and Pare, D. (2003). Feedback inhibition defines transverse processing modules in the lateral amygdala. The Journal of neuroscience : the official journal of the Society for Neuroscience 23, 1966-1973.

Samson, R.D., and Pare, D. (2006). A spatially structured network of inhibitory and excitatory connections directs impulse traffic within the lateral amygdala. Neuroscience 141, 1599-1609.

Sanford, C.A., Soden, M.E., Baird, M.A., Miller, S.M., Schulkin, J., Palmiter, R.D., Clark, M., and Zweifel, L.S. (2017). A Central Amygdala CRF Circuit Facilitates Learning about Weak Threats. Neuron 93, 164-178.

Scheich, B., Gaszner, B., Kormos, V., Laszlo, K., Adori, C., Borbely, E., Hajna, Z., Tekus, V., Bolcskei, K., Abraham, I.*, et al.* (2016). Somatostatin receptor subtype 4 activation is involved in anxiety and depression-like behavior in mouse models. Neuropharmacology 101, 204-215.

Schnall, P.L., Landsbergis, P.A., and Baker, D. (1994). Job strain and cardiovascular disease. Annual review of public health 15, 381-411.

Schwartzbaum, J.S., Thompson, J.B., and Kellicutt, M.H. (1964). Auditory Frequency Discrimination and Generalization Following Lesions of the Amygdaloid Area in Rats. Journal of comparative and physiological psychology 57, 257-266.

Scoville, W.B., and Milner, B. (2000). Loss of recent memory after bilateral hippocampal lesions. 1957. The Journal of neuropsychiatry and clinical neurosciences 12, 103-113.

Senn, V., Wolff, S.B., Herry, C., Grenier, F., Ehrlich, I., Grundemann, J., Fadok, J.P., Muller, C., Letzkus, J.J., and Luthi, A. (2014). Long-range connectivity defines behavioral specificity of amygdala neurons. Neuron 81, 428-437.

Sierra-Mercado, D., Jr., Corcoran, K.A., Lebron-Milad, K., and Quirk, G.J. (2006). Inactivation of the ventromedial prefrontal cortex reduces expression of conditioned fear and impairs subsequent recall of extinction. The European journal of neuroscience 24, 1751-1758.

Smith, S.M., and Vale, W.W. (2006). The role of the hypothalamic-pituitary-adrenal axis in neuroendocrine responses to stress. Dialogues in clinical neuroscience 8, 383-395.

Soden, M.E., Miller, S.M., Burgeno, L.M., Phillips, P.E.M., Hnasko, T.S., and Zweifel, L.S. (2016). Genetic Isolation of Hypothalamic Neurons that Regulate Context-Specific Male Social Behavior. Cell reports 16, 304-313.

Sotres-Bayon, F., Bush, D.E., and LeDoux, J.E. (2007). Acquisition of fear extinction requires activation of NR2B-containing NMDA receptors in the lateral amygdala. Neuropsychopharmacology : official publication of the American College of Neuropsychopharmacology 32, 1929-1940.

Sotres-Bayon, F., Sierra-Mercado, D., Pardilla-Delgado, E., and Quirk, G.J. (2012). Gating of fear in prelimbic cortex by hippocampal and amygdala inputs. Neuron 76, 804-812.

Spampanato, J., Polepalli, J., and Sah, P. (2011). Interneurons in the basolateral amygdala. Neuropharmacology 60, 765-773.

Steenkamp, M.M., Litz, B.T., Hoge, C.W., and Marmar, C.R. (2015). Psychotherapy for Military-Related PTSD: A Review of Randomized Clinical Trials. Jama 314, 489-500.

Stengel, A., and Tache, Y. (2019). Central somatostatin signaling and regulation of food intake. Annals of the New York Academy of Sciences.

Stujenske, J.M., Likhtik, E., Topiwala, M.A., and Gordon, J.A. (2014). Fear and safety engage competing patterns of theta-gamma coupling in the basolateral amygdala. Neuron 83, 919-933.

Suh, J., Rivest, A.J., Nakashiba, T., Tominaga, T., and Tonegawa, S. (2011). Entorhinal cortex layer III input to the hippocampus is crucial for temporal association memory. Science 334, 1415-1420.

Sun, C., Kitamura, T., Yamamoto, J., Martin, J., Pignatelli, M., Kitch, L.J., Schnitzer, M.J., and Tonegawa, S. (2015). Distinct speed dependence of entorhinal island and ocean cells, including respective grid cells. Proceedings of the National Academy of Sciences of the United States of America 112, 9466-9471.

Swiergiel, A.H., Takahashi, L.K., and Kalin, N.H. (1993). Attenuation of stress-induced behavior by antagonism of corticotropin-releasing factor receptors in the central amygdala in the rat. Brain research 623, 229-234.

Tervo, D.G., Hwang, B.Y., Viswanathan, S., Gaj, T., Lavzin, M., Ritola, K.D., Lindo, S., Michael, S., Kuleshova, E., Ojala, D*., et al.* (2016). A Designer AAV Variant Permits Efficient Retrograde Access to Projection Neurons. Neuron 92, 372-382.

Thau, L., and Sharma, S. (2019). Physiology, Cortisol. In StatPearls (Treasure Island (FL)).

Thoeringer, C.K., Henes, K., Eder, M., Dahlhoff, M., Wurst, W., Holsboer, F., Deussing, J.M., Moosmang, S., and Wotjak, C.T. (2012). Consolidation of remote fear memories involves Corticotropin-Releasing Hormone (CRH) receptor type 1-mediated enhancement of AMPA receptor GluR1 signaling in the dentate gyrus. Neuropsychopharmacology : official publication of the American College of Neuropsychopharmacology 37, 787-796.

Tipps, M., Marron Fernandez de Velasco, E., Schaeffer, A., and Wickman, K. (2018). Inhibition of Pyramidal Neurons in the Basal Amygdala Promotes Fear Learning. eNeuro 5.

Tovote, P., Esposito, M.S., Botta, P., Chaudun, F., Fadok, J.P., Markovic, M., Wolff, S.B., Ramakrishnan, C., Fenno, L., Deisseroth, K.*, et al.* (2016). Midbrain circuits for defensive behaviour. Nature 534, 206-212.

Treit, D., and Menard, J. (1997). Dissociations among the anxiolytic effects of septal, hippocampal, and amygdaloid lesions. Behavioral neuroscience 111, 653-658.

Tye, K.M. (2018). Neural Circuit Motifs in Valence Processing. Neuron 100, 436-452.

Tye, K.M., Prakash, R., Kim, S.Y., Fenno, L.E., Grosenick, L., Zarabi, H., Thompson, K.R., Gradinaru, V., Ramakrishnan, C., and Deisseroth, K. (2011). Amygdala circuitry mediating reversible and bidirectional control of anxiety. Nature 471, 358-362.

van de Weyer, P.S., Praetorius, M., and Tisch, M. (2011). [Update: blast and explosion trauma]. Hno 59, 811-818.

van den Pol, A.N. (2012). Neuropeptide transmission in brain circuits. Neuron 76, 98-115.

Van Wimersma Greidanus, T.B., Maigret, C., and Krechting, B. (1987). Excessive grooming induced by somatostatin or its analog SMS 201-995. European journal of pharmacology 144, 277-285.

VanElzakker, M.B., Dahlgren, M.K., Davis, F.C., Dubois, S., and Shin, L.M. (2014). From Pavlov to PTSD: the extinction of conditioned fear in rodents, humans, and anxiety disorders. Neurobiology of learning and memory 113, 3-18.

Vecsei, L., Pavo, I., Zsigo, J., Penke, B., and Widerlov, E. (1989). Comparative studies of somatostatin-14 and some of its fragments on passive avoidance behavior, open field activity and on barrel rotation phenomenon in rats. Peptides 10, 1153-1157.

Vecsei, L., and Widerlov, E. (1990). Effects of somatostatin-28 and some of its fragments and analogs on open-field behavior, barrel rotation, and shuttle box learning in rats. Psychoneuroendocrinology 15, 139-145.

Vidal-Gonzalez, I., Vidal-Gonzalez, B., Rauch, S.L., and Quirk, G.J. (2006). Microstimulation reveals opposing influences of prelimbic and infralimbic cortex on the expression of conditioned fear. Learn Mem 13, 728-733.

Viosca, J., Lopez de Armentia, M., Jancic, D., and Barco, A. (2009). Enhanced CREB-dependent gene expression increases the excitability of neurons in the basal amygdala and primes the consolidation of contextual and cued fear memory. Learn Mem 16, 193-197.

Viviani, D., Charlet, A., van den Burg, E., Robinet, C., Hurni, N., Abatis, M., Magara, F., and Stoop, R. (2011). Oxytocin selectively gates fear responses through distinct outputs from the central amygdala. Science 333, 104-107.

Vuilleumier, P. (2005). How brains beware: neural mechanisms of emotional attention. Trends in cognitive sciences 9, 585-594.

Wallace, K.J., and Rosen, J.B. (2001). Neurotoxic lesions of the lateral nucleus of the amygdala decrease conditioned fear but not unconditioned fear of a predator odor: comparison with electrolytic lesions. The Journal of neuroscience : the official journal of the Society for Neuroscience 21, 3619-3627.

Waterston, R.H., Lindblad-Toh, K., Birney, E., Rogers, J., Abril, J.F., Agarwal, P., Agarwala, R., Ainscough, R., Alexandersson, M., An, P.*, et al.* (2002). Initial sequencing and comparative analysis of the mouse genome. Nature 420, 520-562.

Whitworth, J.A., Williamson, P.M., Mangos, G., and Kelly, J.J. (2005). Cardiovascular consequences of cortisol excess. Vascular health and risk management 1, 291-299.

Wiersma, A., Baauw, A.D., Bohus, B., and Koolhaas, J.M. (1995). Behavioural activation produced by CRH but not alpha-helical CRH (CRH-receptor antagonist) when microinfused into the central nucleus of the amygdala under stress-free conditions. Psychoneuroendocrinology 20, 423-432.

Wiersma, A., Knollema, S., Konsman, J.P., Bohus, B., and Koolhaas, J.M. (1997). Corticotropin-releasing hormone modulation of a conditioned stress response in the central amygdala of Roman high (RHA/Verh)-avoidance and low (RLA/Verh)-avoidance rats. Behavior genetics 27, 547-555.

Wiersma, A., Konsman, J.P., Knollema, S., Bohus, B., and Koolhaas, J.M. (1998). Differential effects of CRH infusion into the central nucleus of the amygdala in the Roman high-avoidance and low-avoidance rats. Psychoneuroendocrinology 23, 261-274.

Windle, R.J., Shanks, N., Lightman, S.L., and Ingram, C.D. (1997). Central oxytocin administration reduces stress-induced corticosterone release and anxiety behavior in rats. Endocrinology 138, 2829-2834.

Yeung, M., Engin, E., and Treit, D. (2011). Anxiolytic-like effects of somatostatin isoforms SST 14 and SST 28 in two animal models (Rattus norvegicus) after intra-amygdalar and intra-septal microinfusions. Psychopharmacology 216, 557-567.

Yeung, M., and Treit, D. (2012). The anxiolytic effects of somatostatin following intra-septal and intra-amygdalar microinfusions are reversed by the selective sst2 antagonist PRL2903. Pharmacology, biochemistry, and behavior 101, 88-92.

Yoshii, T., Hosokawa, H., and Matsuo, N. (2017). Pharmacogenetic reactivation of the original engram evokes an extinguished fear memory. Neuropharmacology 113, 1-9.

Yu, K., Ahrens, S., Zhang, X., Schiff, H., Ramakrishnan, C., Fenno, L., Deisseroth, K., Zhao, F., Luo, M.H., Gong, L., *et al.* (2017). The central amygdala controls learning in the lateral amygdala. Nature neuroscience 20, 1680-1685.

Yu, K., Garcia da Silva, P., Albeanu, D.F., and Li, B. (2016). Central Amygdala Somatostatin Neurons Gate Passive and Active Defensive Behaviors. The Journal of neuroscience : the official journal of the Society for Neuroscience 36, 6488-6496.

Yue, J., Shi, L., Lin, X., Khan, M.Z., Shi, J., and Lu, L. (2018). Behavioral interventions to eliminate fear responses. Science China Life sciences 61, 625-632.

Zemla, R., and Basu, J. (2017). Hippocampal function in rodents. Current opinion in neurobiology 43, 187-197.

Zhang, X., and Li, B. (2018). Population coding of valence in the basolateral amygdala. Nature communications 9, 5195.

Zhou, Y., Won, J., Karlsson, M.G., Zhou, M., Rogerson, T., Balaji, J., Neve, R., Poirazi, P., and Silva, A.J. (2009). CREB regulates excitability and the allocation of memory to subsets of neurons in the amygdala. Nature neuroscience 12, 1438-1443.

Zilleruelo, G., and Beca, J.P. (1975). [A guide line for the evaluation of medical interns (author's transl]. Revista medica de Chile 103, 138-142.

Zuj, D.V., and Norrholm, S.D. (2019). The clinical applications and practical relevance of human conditioning paradigms for posttraumatic stress disorder. Progress in neuro-psychopharmacology & biological psychiatry 88, 339-351.